

**BUILDING THERMAL STORAGE**

by

**Mark David Ruud**

**A thesis submitted in partial fulfillment  
of the requirements for the degree of**

**Master of Science  
(Mechanical Engineering)**

at the  
**UNIVERSITY OF WISCONSIN—MADISON**  
1990

---

## ABSTRACT

---

The use of ice and chilled water storage systems to reduce peak energy demands is well established. However, relatively few experimental results have been published on the use of building thermal mass to offset peak energy demand. The use of off peak cooling to extract heat from a buildings thermal store may increase energy use while reducing peak cooling loads and cooling costs.

This paper describes a project sponsored by ASHRAE TC 4.6 on building thermal storage. The purpose of this research project was to evaluate the effect of building thermal energy storage on the peak cooling load. Two experiments were performed on the Independent Life Insurance building located in Jacksonville Florida. This building is 37 stories high with one million square feet of floor area. The objective of the experiments was to pre-cool the building at night and during the weekend to reduce daytime cooling loads. Measurements of airflow and temperature on a story with pre-cooling and a story without pre-cooling were used to calculate the energy supplied to each story. Additional measurements of temperature and heat flux at the concrete floor surface were made on the pre-cooled story

Results from the experiment show the reduction in cooling load due to pre-cooling. Temperature and heat flux measurements at the concrete floor surface reveal the extent of charging and discharging of the thermal mass. Results from the experiments were compared to diurnal heat capacity calculations. Diurnal heat capacity is a frequency method which can be used to calculate the potential for energy storage in a building.

---

## ACKNOWLEDGEMENTS

---

It was another dark and gloomy night at the laboratory. Graduate students huddled in front of computers, their eyes transfixed by the effervescent glow of the monitor. The screen illuminated their pale faces as they struggled to meet impossible deadlines. Yet somehow I am sad that it is now all over.

I am sincerely grateful to have been able to complete my masters degree at the best graduate program in the nation - the University of Wisconsin Solar Energy Laboratory (UWSEL). I have gained much from my experiences at the UWSEL and I hope in some small way I have given something back. I will have many fond memories of the my time spent in Madison.

This project was sponsored by ASHRAE Committee TC 4.6 Building Operation Dynamics. Experiments performed at the Independent Life Insurance Building would not have been possible without the support and assistance of Ed Cavin, Fred Wheeler, Dan Frey, and the many helpful building operators. The financial support of the ASHRAE Grant in Aid program is greatly appreciated.

I would like to sincerely thank those who made this research possible. To Professor Duffie for having the foresight to found the UWSEL. To Professor Beckman, its current director, for carrying on the important work of the laboratory. To my advisors Professor Klein and Professor Mitchell for their help, insights, and suggestions.

Special thanks to Maria for her unending love, devotion, support, and for helping me write this acknowledgement. Thanks for putting up with me through all this. To Honey for listening to my complaints and for the reassuring wag of her tail. To my family for

their support and encouragement. And finally to all the graduate students in the UWSEL including the class of 89-90:



---

# CONTENTS

---

<b>Tables .....</b>	<b>ix</b>
<b>Figures.....</b>	<b>x</b>
<b>Symbols .....</b>	<b>xiii</b>
<b>1 INTRODUCTION.....</b>	<b>1</b>
1.1 Building Description.....	1
1.2 HVAC System.....	3
1.3 Control.....	4
1.3.1 Core System.....	4
1.3.2 Perimeter System.....	5
1.4 Summary.....	6
<b>2 EXPERIMENTS.....</b>	<b>7</b>
2.1 Experiment Design.....	7
2.1.1 Measurements.....	7
2.1.2 Calibration.....	9
2.2 First Experiment: June 16 to June 23.....	13
2.2.1 Local Measurements .....	14
2.2.2 Corrections.....	16
2.3 Second Experiment: September 8 to September 15.....	17
2.3.1 Local Measurements .....	17
2.3.2 Corrections.....	18
2.4 Summary .....	19
<b>REFERENCES 2.....</b>	<b>20</b>

<b>3 DATA ANALYSIS .....</b>	<b>21</b>
3.1 Thermal Comfort.....	21
3.1.1 First Experiment.....	21
3.1.2 Second Experiment .....	25
3.2 Heat Flux.....	28
3.2.1 First Experiment.....	30
3.2.1 Second Experiment .....	32
3.3 cooling Energy .....	35
3.3.1 Charging vs. Discharging.....	35
3.3.2 Load Reduction .....	39
3.3.3 Peak Reduction Strategy .....	42
3.4 Summary .....	44
REFERENCES 3.....	45
 <b>FREQUENCY ANALYSIS .....</b>	 <b>46</b>
4.1 Fourier Transform.....	48
4.2 Thermal Admittance.....	49
4.3 X Y Z Admittance.....	51
4.4 Superposition.....	59
4.5 Admittance Calculations.....	61
4.5.1 Boundary Conditions.....	63
4.5.2 Lumped Capacitance.....	66
4.6 Admittance of Layered Walls .....	68
4.6.1 Resistive Layer.....	68
4.6.2 X and Z admittance .....	70
4.6.3 Y admittance .....	74

4.6.4 Symmetric Interior Wall.....	75
4.7 Calculated Admittance vs Measured Floor Heat Flux.....	78
4.7.1 Discrete Fourier Transform.....	79
4.7.2 Heat Flux.....	79
4.8 Diurnal heat capacity.....	83
4.9 Effectiveness.....	88
4.10 Chapter summary.....	91
REFERENCES 4.....	92
<b>5 VENTILATION COOLING.....</b>	<b>93</b>
5.1 Simulation.....	93
5.2 Building Description.....	95
5.3 Simulation Results.....	97
5.4 Summary.....	102
REFERENCES 5.....	103
<b>6 CONCLUSIONS.....</b>	<b>104</b>
6.1 Results.....	104
Thermal Comfort.....	104
Heat Flux.....	105
Energy Use.....	105
Diurnal Heat Capacity.....	106
Ventilation Cooling.....	107
Pre-cooling Guidelines.....	107

**Bibliography .....108**

**Appendix .....111**

**A Sensors - Product Information.....112**

**B Finite Difference Program.....113**

**C Admittance Program .....119**

**D Component Material Properties .....127**

**E Discrete Fourier Transform Program.....128**

**F TRNSYS Simulation Deck.....132**

**G TRNSYS Building Input Description .....137**

---

## TABLES

---

Table	Page
2.1	Duct Area & Traverse Correction Factors .....13
3.1	Weekday Temperatures - First Experiment .....26
3.2	Weekday Temperatures - Second Experiment.....27
3.3	Carpet Resistance and Surface Resistance - First Experiment .....32
3.4	Carpet Resistance and Surface Resistance - Second Experiment.....34
3.5	Energy Parameters - First & Second Experiment .....38
3.6	Summer Peak Period.....42
4.1	Frequency & Period .....48
4.2	Time and Frequency Domain.....52
4.3	X and Z Admittance Values.....74
4.4	X Admittance Values .....77
4.5	ILIB Admittance Values .....78
4.6	Diurnal Heat Capacity.....85
4.8	Temperature Difference and Thermal Storage.....88
4.9	Thermal Effectiveness.....90
5.1	Internal Loads & Schedules .....97
5.2	Simulation Summary.....101
6.1	Carpet and Surface Resistance .....105
6.2	Energy Parameters - First & Second Experiment .....106

---

## FIGURES

---

Figure		Page
1.1	Thermal Mass.....	2
1.2	HVAC Layout.....	3
1.3	Supply Damper & Duct.....	4
1.4	VAV Diffuser Cross Section.....	5
2.1	Independent Life Insurance Building.....	8
2.2	Instrumentation.....	10
2.3	Pitot Calibration .....	11
2.4	9th & 15th Story Temperature & Humidity.....	15
2.5	Return vs. Average Zone Temperature.....	16
2.6	15th Story Supply Air Temperatures - Second Experiment.....	18
2.7	15th Story Supply Air Temperatures - First Experiment.....	19
3.1	Outdoor Temperature & Humidity - First Experiment.....	22
3.2	9th Story Average Zone Temperature.....	23
3.3	Globe & Room Air Temperature .....	24
3.4	Outdoor Temperature and Humidity - Second Experiment.....	26
3.5	Outdoor and Zone Temperature vs. Temperature Rate.....	27
3.6	Finite Difference Model.....	29
3.7	Temperature and Heat Flux.....	31
3.8	Heat Flux - Sensor and Finite Difference Method.....	33
3.9	Energy Supplied 9 & 15.....	36
3.10	Energy Supplied 9 - 15.....	37

Figure	Page
3.11	Average Zone Temperature.....40
3.12	E <sub>9</sub> - E <sub>15</sub> Hourly Distribution..... 41
3.13	Pre-cooling Strategy.....43
4.1	Sine Waves and Temperature.....47
4.2	A B C Vector Diagram.....50
4.3	Heat Flux & Temperature .....51
4.4	X, Y, & Z Admittance.....53
4.5	X Admittance Phase Lead.....54
4.6	X Admittance .....55
4.7	Y Admittance .....56
4.8	Z admittance.....56
4.9	Nyquist Diagram.....57
4.10	Superposition.....60
4.11	Surface 1&2.....62
4.12	Symmetric Wall.....64
4.13	Admittance vs. Thickness .....65
4.14	Resistive Layer.....69
4.15	9th Floor Admittance .....71
4.16	Symmetric Internal Wall.....75
4.17	DFT Temperature and Heat Flux.....80
4.18	Calculated Heat Flux vs. the DFT of the Heat Flux.....81
4.19	Calculated Heat Flux vs. the DFT of the Heat Flux.....82
4.20	Diurnal Heat Capacity.....83

<b>Figure</b>		<b>Page</b>
5.1	Building Zone Model.....	95
5.2	Hours Below Temperature.....	96
5.3	Total Sensible and Latent Loads.....	98
5.4	Latent Loads.....	99

---

## SYMBOLS

---

### ROMAN

a	.....	$\sqrt{\omega\rho ck}$ .....	Btu/hr-ft <sup>2</sup> -F
A	.....	area .....	ft <sup>2</sup>
A <sub>n</sub> , B <sub>n</sub> , C <sub>n</sub>	.....	Fourier series coefficients	
Bi	.....	Biot number .....	(hl/k)
c	.....	specific heat .....	Btu/lb-F
C	.....	correction factor	
d	.....	derivative	
dhc	.....	diurnal heat capacity.....	Btu/ft <sup>2</sup> -F
DHC	.....	diurnal heat capacity.....	Btu/F
$\dot{E}$	.....	energy rate.....	Btu/hr
E	.....	energy.....	Btu
Fo	.....	Fourier number .....	(2 $\alpha$ / $\omega L^2$ )
g	.....	$e^{i\pi/4}$	
h	.....	convection coefficient .....	Btu/hr-ft <sup>2</sup> -F
i	.....	complex number .....	$\sqrt{-1}$
k	.....	thermal conductivity .....	Btu/hr-ft-F
L	.....	wall thickness.....	ft
$\dot{m}$	.....	mass flow rate.....	lb/hr
m	.....	elements of transfer matrix	
M	.....	transfer matrix	
P	.....	period.....	hr
Q	.....	thermal energy.....	Btu
R	.....	resistance.....	hr-ft <sup>2</sup> -F/Btu

## ROMAN (Continued)

S.....	dimensionless admittance
s.....	sample standard deviation
q.....	heat flux.....Btu/hr-ft <sup>2</sup>
Q.....	quantity of heat.....Btu/ft <sup>2</sup>
t.....	time.....hr
thc.....	total heat capacity.....Btu/ft <sup>2</sup> -F
T.....	temperature.....F
U.....	U value.....Btu/hr-ft <sup>2</sup> -F
V.....	velocity.....ft/min
X, Y, Z.....	thermal admittance.....Btu/hr-ft <sup>2</sup> -F
x.....	distance.....ft

## GREEK

$\alpha$ .....	thermal diffusivity (k/ $\rho c$ )..... ft <sup>2</sup> /hr
$\partial$ .....	partial derivative
$\emptyset$ .....	phase.....radians, degrees
$\gamma$ .....	$(1 + i) \sqrt{\frac{\pi \rho c}{Pk}}$
$\eta$ .....	thermal effectiveness
$\rho$ .....	density.....lb/ft <sup>3</sup>
$\tau$ .....	dimensionless thickness
$\omega$ .....	frequency $\omega = \frac{2\pi}{P}$ .....radians/hr

## SUBSCRIPTS

a.....	air
b.....	boundary
c.....	carpet

**SUBSCRIPTS (Continued)**

d..... diurnal frequency (24 hour period)  
f..... floor  
fp..... fireproofing  
i..... inside  
o..... outside  
r..... room  
ra..... return air  
s ..... steady state (zero frequency)  
sa..... supply air  
w ..... wall  
z ..... zero  
 $\infty$ ..... ambient



## *CHAPTER 1*

---

# INTRODUCTION

---

The use of ice and chilled water storage systems to reduce peak energy demands is well established. However, relatively few experimental results have been published on the use of building thermal mass to offset peak energy demand. The use of off peak cooling to extract heat from a building's thermal store may increase the total energy use while reducing peak cooling loads and cooling costs.

This thesis describes a research project sponsored by ASHRAE TC 4.6 on building thermal storage. The purpose of the research was to evaluate the effect of building thermal energy storage on peak cooling loads. To study the effect of a building's thermal mass on peak cooling loads, two experiments were performed on the Independent Life Insurance building located in Jacksonville, Florida. The objective of these experiments was to measure the building's response to pre-cooling. Pre-cooling is defined as the cooling of a building during unoccupied night-time and/or weekend periods. To measure the building response, the energy supplied to a story with pre-cooling was compared to the energy supplied to a story without pre-cooling. Pre-cooling was provided by mechanical refrigeration.

### **1.1 BUILDING DESCRIPTION**

The Independent Life Insurance Building (ILIB) is located in Jacksonville Florida. The building is 37 stories high and has one million square feet of floor area. The building is used primarily for office space.

The ILIB is not particularly massive but it is typical of most modern office buildings. The exterior consists of a glass curtain wall. Structural steel supports the building. The interior includes a carpeted concrete floor, gypsum walls, partitions, and a concrete block core. A suspended ceiling also serves as the return air plenum.

The thermal capacitance was calculated for the components of a typical story of the ILIB. The main source of thermal mass is the concrete under the floor and above the ceiling as shown in Figure 1.1.

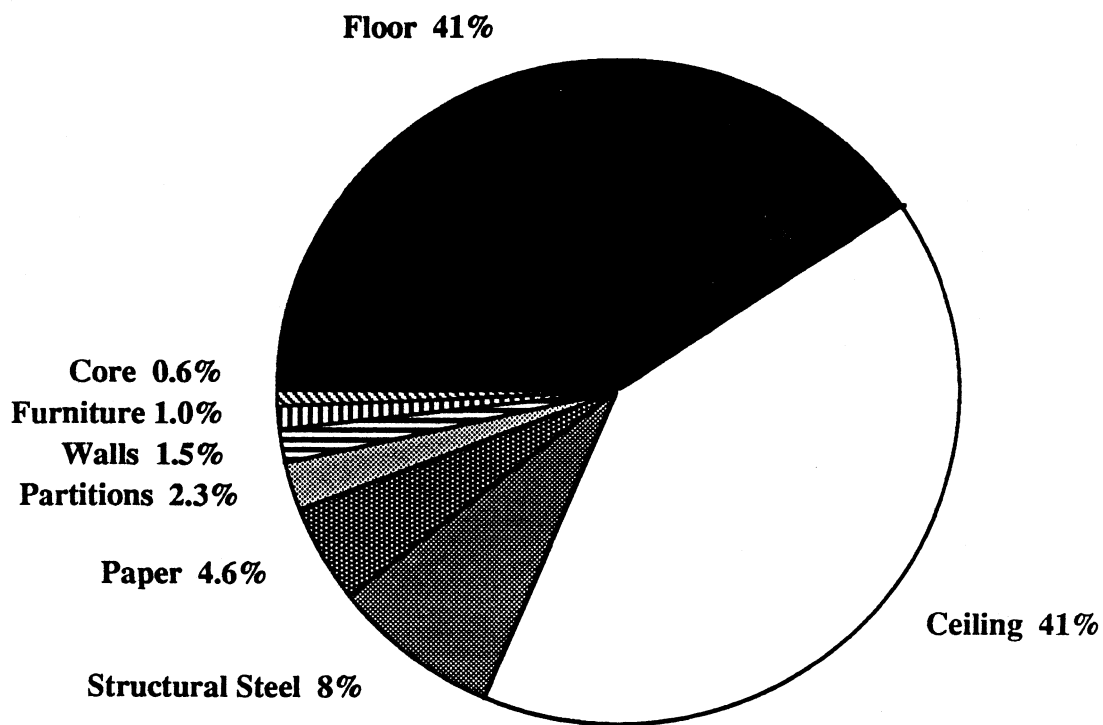


Figure 1.1 Thermal Mass

## 1.2 HVAC SYSTEM

Air conditioning is supplied by three 1,233 ton chillers, and two 180 ton chillers for reduced loads. Hot water for heating is provided by electric water heaters. Figure 1.2 shows how the air handling units are divided into core and perimeter systems. The core and perimeter systems are divided into northeast and southwest zones.

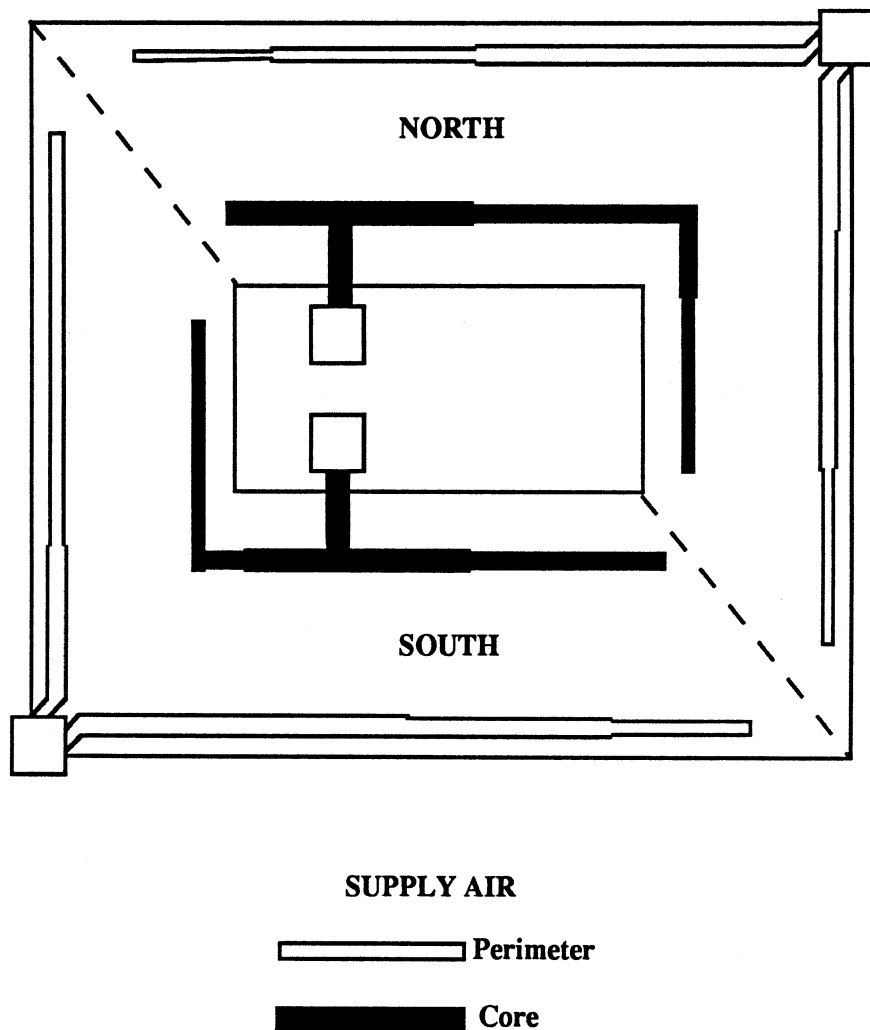


Figure 1.2 HVAC Layout

The perimeter system delivers heating or cooling at a constant flow rate. This is known as a constant air volume (CAV) system. The perimeter system is used to reduce thermal gradients near the windows. Heating is provided by hot water terminal reheat coils. The core system supplies cooling at a variable flow rate. This is known as a variable air volume (VAV) system. The core system is the main source of cooling for each zone.

### 1.3 CONTROL

The ILIB has a supervisory energy management and control system (EMCS) for the building heating ventilation and air conditioning (HVAC) system. The EMCS supervisory functions include scheduling of equipment, outdoor air enthalpy control, optimum start stop, and zone damper control.

#### 1.3.1 Core System

Each story has a separate supply air damper for each zone located at the main supply air duct. The damper is open when the zone temperature is above 73°F and closed when the zone temperature is below 73°F. Figure 1.3 is a schematic of the supply air damper.

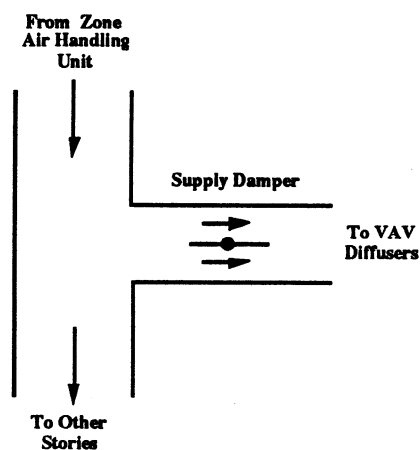


Figure 1.3 Supply Damper & Duct

The duct from the supply air damper branches to several VAV slot diffusers in the suspended ceiling. Figure 1.4 illustrates a cross sectional view of the VAV diffuser. Each diffuser is controlled locally using an adjustable temperature set point. When the temperature exceeds the set point the pneumatic diaphragm inflates which reduces airflow. When the temperature is below the set point the diaphragm deflates which allows for more airflow.

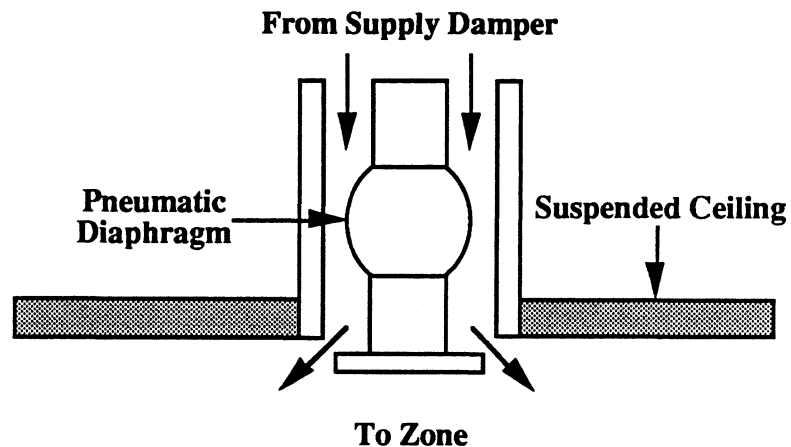


Figure 1.4 VAV Diffuser Cross Section

The variable speed fans respond to changes in system static pressure. If for example, a zone damper closed, or if the VAV diffusers start to restrict airflow, the system static pressure would rise and the speed of the supply fan would be reduced.

### 1.3.2 Perimeter System

The perimeter system is controlled by an outdoor "solar" sensor which consists of a temperature sensor inside a metal box. When the solar sensor reaches its set-point

(approximately 140°F) the perimeter cooling is turned on. The perimeter system then delivers cooling at a constant flow rate until the temperature of the solar sensor drops below its set-point. The northeast and southwest zones are controlled individually by separate solar sensors.

#### **1.4 SUMMARY**

This chapter provides an introduction to the HVAC systems at the ILIB. In the chapters that follow, the interaction of the HVAC system with the building's thermal mass is investigated. Chapter 2 describes the experiments performed at the ILIB. The experimental design is delineated. Chapter 3 is an analysis of the data received from these experiments. The results show the effect of pre-cooling on thermal comfort, heat flux, and energy use. Chapter 4 describes the use of frequency methods to predict heat flux and energy storage. Results from the experiments are compared to frequency method calculations. Chapter 5 is an investigation into the use of cool outdoor air as a source of cooling. Results are drawn from a simulation model based on the ILIB.

## *CHAPTER 2*

---

# **EXPERIMENTS**

---

Two experiments were performed to evaluate the effect of pre-cooling on day-time cooling loads. The first experiment examined the effect of maximum pre-cooling. In the second experiment the amount of pre-cooling during the weekend was reduced. Experience gained from the first experiment helped to refine the plan for the second experiment.

### **2.1 EXPERIMENT DESIGN**

Two stories of the ILIB were used for the experiments. The 15th story was the control story with no pre-cooling. The 9th story was the test story with pre-cooling. Stories 8 and 10 were also pre-cooled to reduce heat transfer between these stories and the 9th story.

Stories 9 and 15 are similar in use and configuration. External loads (solar and outdoor temperature) and internal gains (people, lights, and equipment) are assumed to be similar for both stories. Since these stories are not adjacent, interactions between the test story and the control story were avoided.

#### **2.1.1 Measurements**

Measurements of airflow and temperature were used to calculate the energy supplied to each story. Differences between the energy supplied to the story with pre-cooling (9th story) and the energy supplied to the story without pre-cooling (15th story) were used to measure the response to pre-cooling. Measurements of floor heat flux were taken on the 9th story to reveal the extent of charging and discharging of the thermal mass.

**Independent Life Insurance  
Building**

37 Stories , 537 Feet Tall

1,000,000 Square Feet

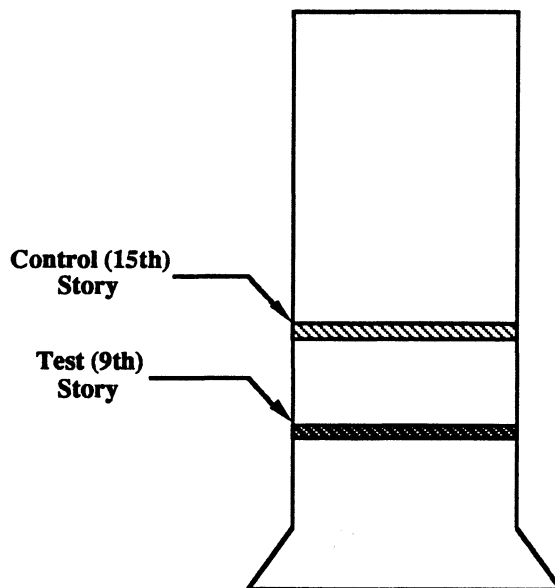


**Figure 2.1 Independent Life Insurance Building**

The EMCS was used to record:

- o Supply air temperature
- o Supply air velocity
- o Return air temperature
- o Return air velocity
- o Room air temperature
- o Outside air temperature and humidity

Measurements of air velocity and temperature were made on each story. Air velocity was measured by a hot wire anemometer which was installed near the supply air damper for

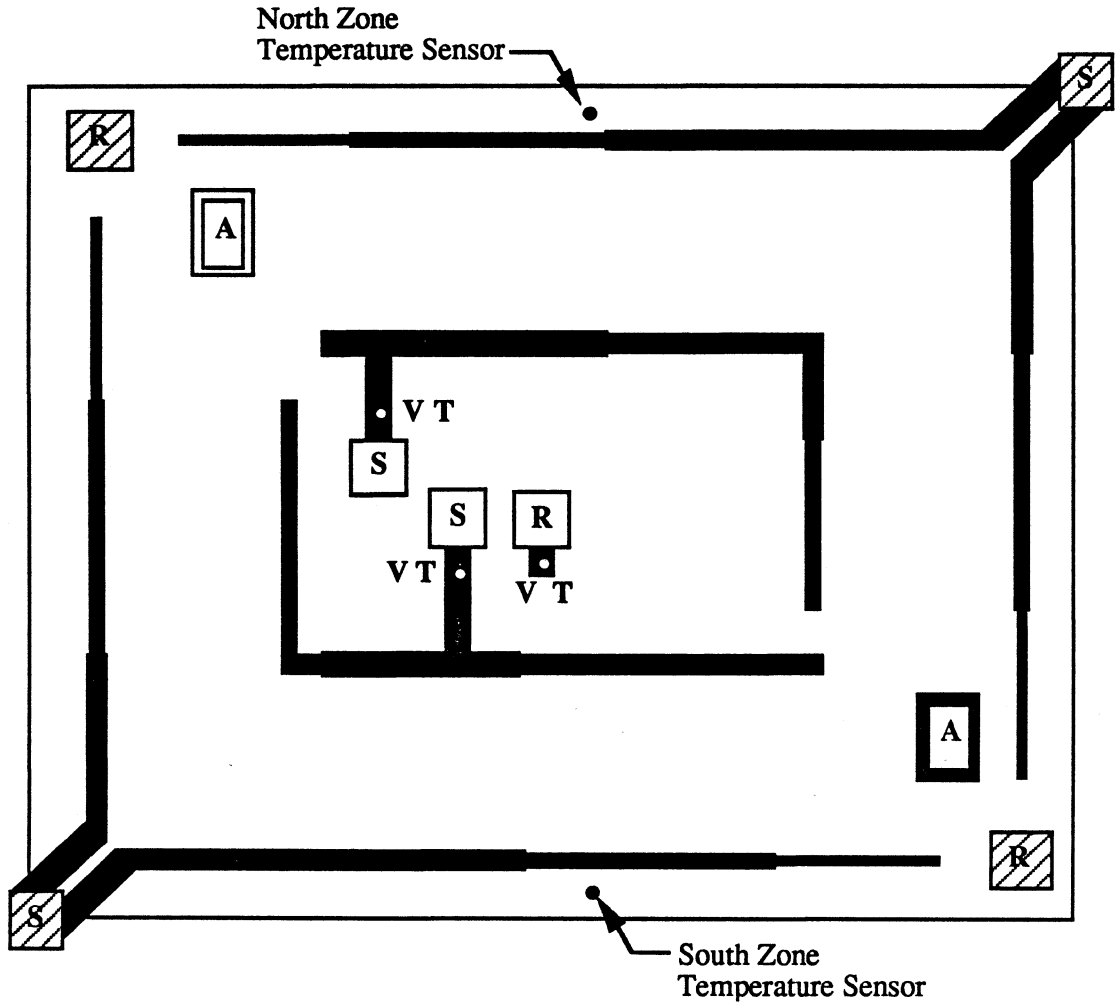
each zone. A temperature sensor was installed next to the velocity sensor to measure the supply air temperature. Velocity and temperature sensors were also installed in the core return air duct on each story. Measurements of zone temperatures on each story were made by existing north and south zone temperature sensors. No measurements of the perimeter system were taken since the perimeter system was to be locked out during the experiment.

A computer monitoring station was placed on the 9th story. This computer was setup to record 8 analog inputs. Measurements of the floor temperature at the floor surface (on top of the carpet) and at the concrete surface (under the carpet) were recorded by the computer. The location of the computer monitoring station and the EMCS sensors is shown in Figure 2.2. Local measurements of temperature, relative humidity, and velocity were taken with a hand held meter.

### **2.1.2 Calibration**

All the EMCS temperature sensors used in the experiments were calibrated using a hand held meter with a temperature probe. The temperature probe was calibrated against a mercury thermometer. Temperature sensors were calibrated to an accuracy of within 1.0 °F. Humidity measurements with the hand held meter were calibrated using a sling psychrometer.

Flow measurements were calibrated using a hand held meter with a velocity probe. The probe measured velocity by using a hot wire anemometer. The velocity probe was calibrated against a Pitot tube in a wind tunnel. Figure 2.3 gives the relationship between the Pitot tube and hand held sensor.



- |   |                   |   |                     |
|---|-------------------|---|---------------------|
| <b><u>SENSORS</u></b>   |                   | <b><u>COMPUTER</u></b>  |                     |
| T-  | Temperature       |  | 1st Experiment      |
| V-  | Velocity          |  | 2nd Experiment      |
| <b><u>CORE</u></b>  |                   | <b><u>PERIMETER</u></b>   |                     |
|  | Supply Air - Open |  | Supply Air - Closed |
|  | Return Air - Open |  | Return Air - Closed |

Figure 2.2 Instrumentation

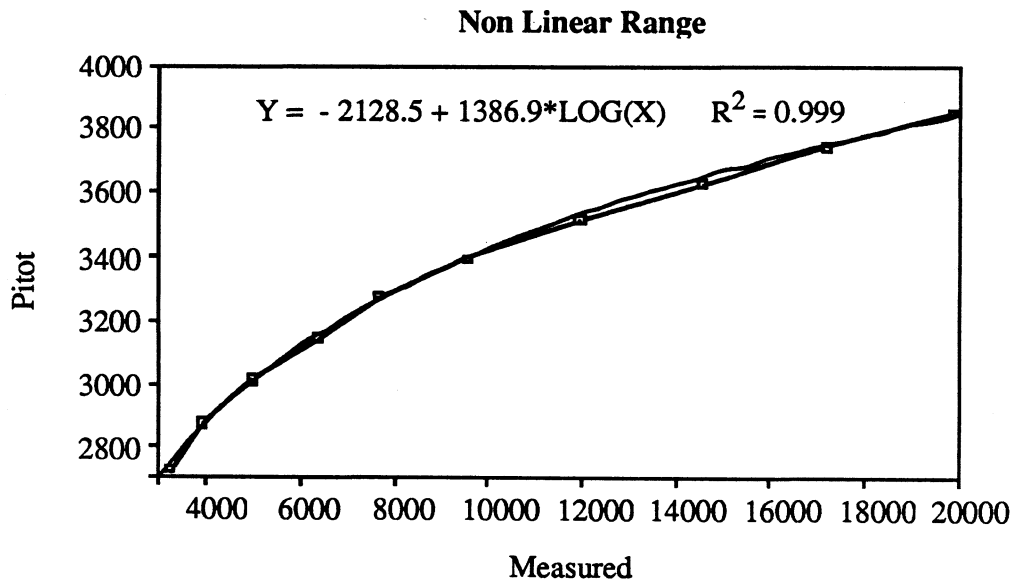
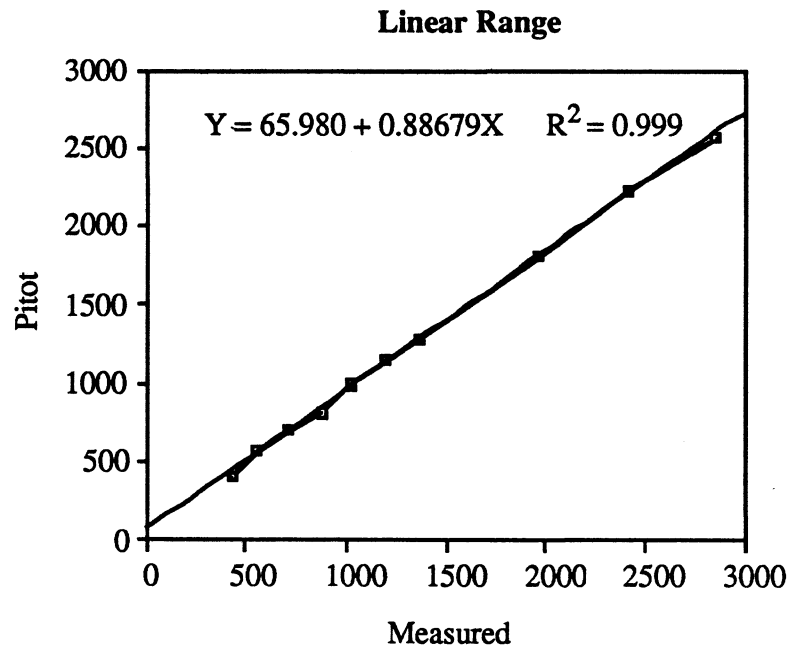


Figure 2.3 Pitot Calibration

A total of 6 velocity sensors were calibrated, one sensor in each of the four supply air ducts, and one sensor in each of the two return air ducts. All of the velocity sensors were connected to the EMCS. Each supply air velocity sensor was calibrated by taking a traverse along the vertical axis of each supply air duct. Readings were taken at measured intervals across the supply air duct. The velocity probe was inserted through a hole drilled in an access door near the velocity sensor. Access was not possible for a horizontal traverse. Return air velocity sensors were calibrated by taking a traverse at the opening to the return air duct. Readings were taken at equally spaced intervals along the horizontal and vertical axis of the return air duct. A reading from the EMCS of velocity sensor was taken at the same time as the traverse. From these readings a correction factor (C) was calculated

$$C = \frac{\text{Average of the Traverse Readings}}{\text{EMCS Velocity Sensor Reading}} \quad (2.1)$$

The EMCS velocity sensor measures velocity at a single point in the duct. The correction factor accounts for the velocity distribution across the duct. The product of the velocity sensor reading and the correction factor gives an estimate of the average velocity across the duct.

Measurements of the duct cross sectional area were taken at each sensor location. The air flow-rate could then be calculated by

$$\text{Airflow (cfm)} = V * C * A \quad (2.2)$$

where

V = measured air velocity (fpm)

C = correction factor for velocity profile

A = duct area (ft<sup>2</sup>)

The accuracy of the calculated airflow is approximately 10% to 20% [1]. The duct areas and traverse correction factors are given in Table 2.1. Product information on the sensors installed at the ILIB and the hand held meter is given in the Appendix.

Supply Air Duct	Duct Area (ft <sup>2</sup> )	Traverse Correction Factor (C)	
		Damper Open	Damper Closed
9 South	5.074	0.986	0.972
9 North	3.792	1.131	0.590
15 South	4.174	1.020	0.481
15 North	4.076	0.806	0.760

**Table 2.1 Duct Area & Traverse Correction Factors**

## **2.2 FIRST EXPERIMENT: JUNE 16 TO JUNE 23**

The first experiment began by cooling the 9th story starting at 5pm Friday and continuing until 5am Monday morning. During the weekend the 9th story supply air damper was locked open and the 9th story VAV diffusers were set to allow maximum cooling. During the week (Monday thru Friday) the 9th story was cooled at night beginning at 5 pm and continuing until 5 am. Normal occupancy is from 7am to 4pm. The 9th story VAV diffusers were set to their normal position on Monday morning and for the remainder of the week. No control changes were made for the 15th story. The 15th story received no cooling at night or during the weekend. The supply air temperature for both stories was set at 50°F.

### 2.2.1 Local Measurements

On the 9th story the computer with analog inputs was used to record:

- o Globe temperature
- o Wall surface temperatures
- o Floor temperature - on and under the carpet
- o Room air temperature
- o Return air temperature in the plenum
- o Supply air temperature at the VAV diffuser.

Temperatures were taken at the floor surface (on top of the carpet) and at the concrete surface (under the carpet). The carpet consisted of tiles which could be removed to provide access for the sensors. The globe temperature sensor was located approximately 5 feet above the floor surface. The globe sensor consisted of a thermocouple in a copper sphere which was painted black. Temperatures were measured with type J thermocouples. The computer monitoring station was located in the northwest corner near the core of the building.

Readings of temperature and humidity were taken with the hand held instrument every hour. Measurements were taken at the location of the EMCS north and south zone temperature sensors on the 9th and 15th story. Figure 2.4 shows the average of the north and south indoor humidity readings. Humidity readings fluctuated around the 40 percent level during the week for both the 9th and 15th stories.

Temperature readings from the hand held instrument were inconsistent. Therefore, zone temperature measurements were taken from the EMCS north and south zone temperature sensors.

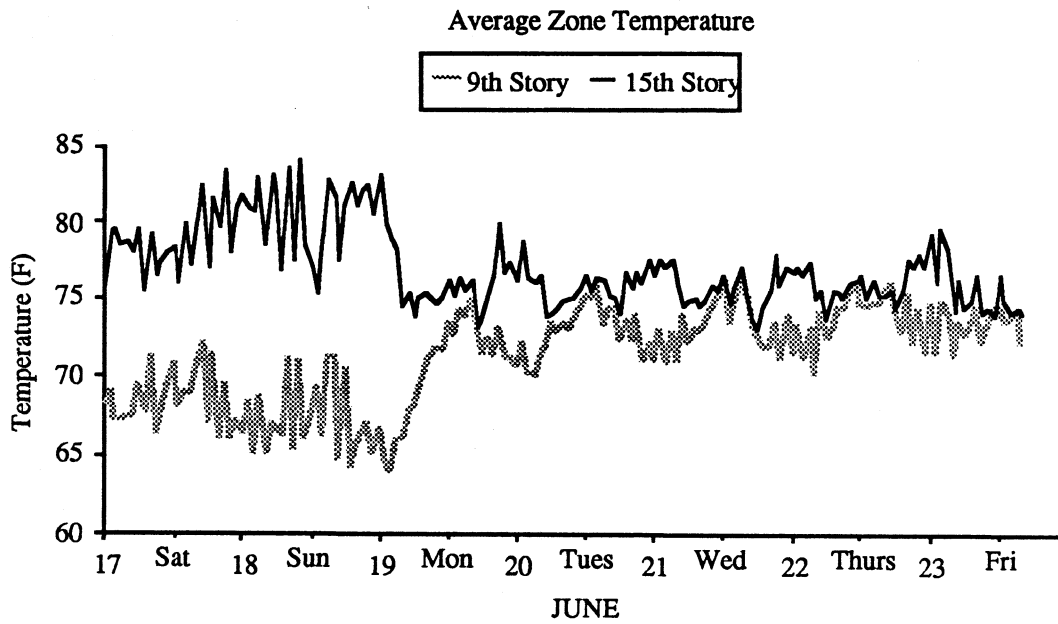
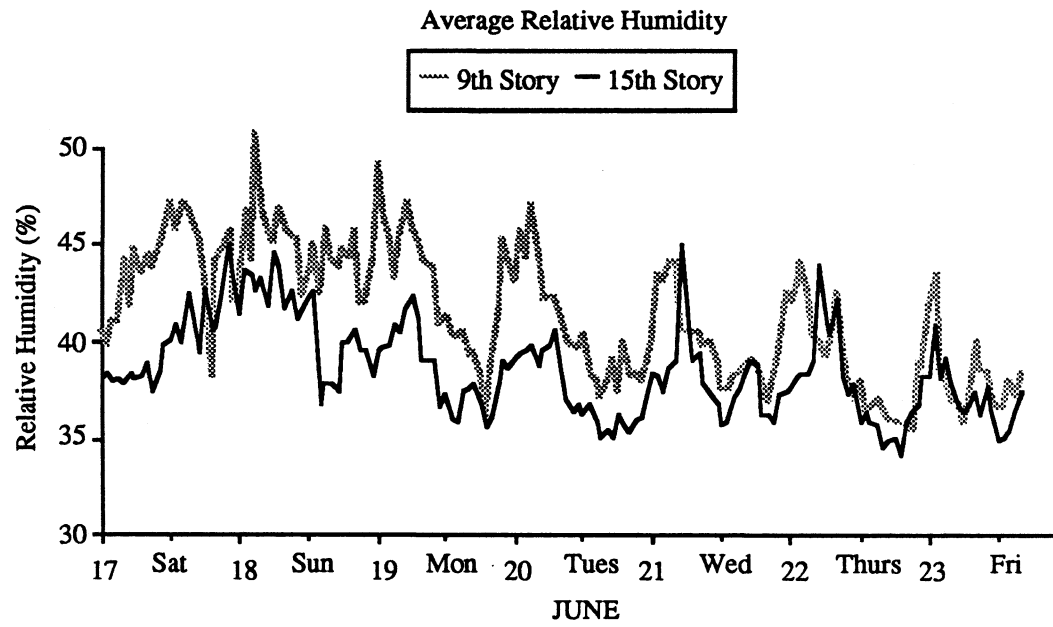


Figure 2.4 9th & 15th Story Temperature & Humidity

### 2.2.2 Corrections

On Monday the perimeter system was turned on. Inspection of the perimeter dampers revealed that the 9th story dampers were open while the 15th story dampers were closed. This event provided additional unmeasured cooling to the 9th story on Monday. On Tuesday the 9th story supply air dampers in the perimeter system were locked in the closed position.

Attempts to calibrate the 9th story return air (RA) temperature sensor indicated that this sensor was faulty. A replacement sensor was not installed until 4:00 pm Wednesday. Comparisons were made between the RA temperature readings with the good sensor and the average of the EMCS north and south zone temperature sensors. Figure 2.5 shows that the average EMCS zone temperature is a good approximation for the RA temperature. This approximation was used to replace the data from the faulty RA sensor readings.

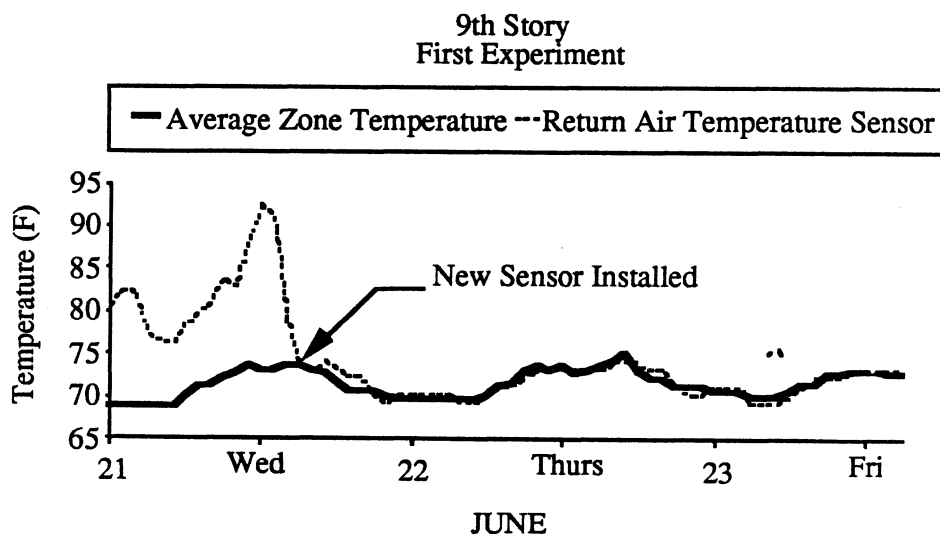


Figure 2.5 Return vs. Average Zone Temperature

The computer monitoring system was setup to record 8 temperatures at 15 minute intervals. Originally it was thought that the data disk could record up to 5 days of data at this rate. On Tuesday the data disk was removed for backup. It was then discovered that the data from 4am Sunday to 10am Tuesday were missing. This left about a two day gap in the temperature record. The disks were backed up daily for the remainder of the week.

### **2.3 SECOND EXPERIMENT: SEPTEMBER 8 TO SEPTEMBER 15**

The second experiment was similar in design to the first experiment. However, less weekend pre-cooling was applied in the second experiment. Results from the first experiment (discussed in chapter 3) indicated that large amounts of weekend pre-cooling may not be effective. To limit the amount of weekend pre-cooling applied to 9th story, the average zone temperature was not allowed to fall below 66°F, and the VAV diffusers were left in their normal positions. The 9th story weekend pre-cooling period started at 7pm Friday and continued until 5am Monday morning.

#### **2.3.1 Local Measurements**

On the 9th story the computer with analog temperature inputs was used to record:

- o Floor heat flux
- o Floor temperature - on and under the carpet
- o Room air temperature
- o Return air temperature in the plenum
- o Supply air temperature at the diffuser.

Measurements of globe and surface temperature, taken in the first experiment, were eliminated to allow additional heat flux measurements. A heat flux sensor was added to allow direct measurement of the floor heat flux. The heat flux sensor has a rated accuracy of 1%. The heat flux sensor was placed on the concrete surface (under the carpet). Two

sets of temperature measurements, on and under the carpet, were taken near the heat flux sensor. The computer monitoring system was setup to read 7 thermocouples and 1 heat flux sensor at 1 hour intervals. The computer monitoring station was located in the southeast corner near between the core and perimeter of the building.

### 2.3.2 Corrections

Figure 2.6 shows the north and south supply air temperatures. Trends in the 15th story supply air (SA) temperatures indicated that the south SA temperature sensor was faulty. Figure 2.7 shows the 15th story SA temperatures from the first experiment. Comparison of the SA temperatures in Figure 2.7 show that the north and south SA temperatures are reasonably close. Also, north and south supply air temperatures were set to 50°F in both experiments. Since these temperatures are approximately the same, temperature readings from the north sensor were used to replace data from the faulty south sensor.

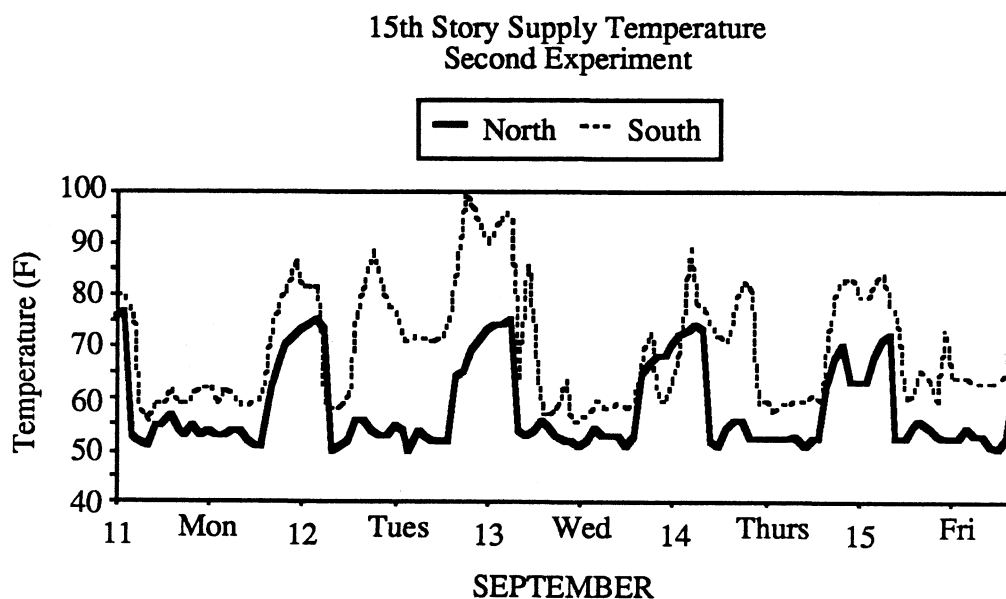
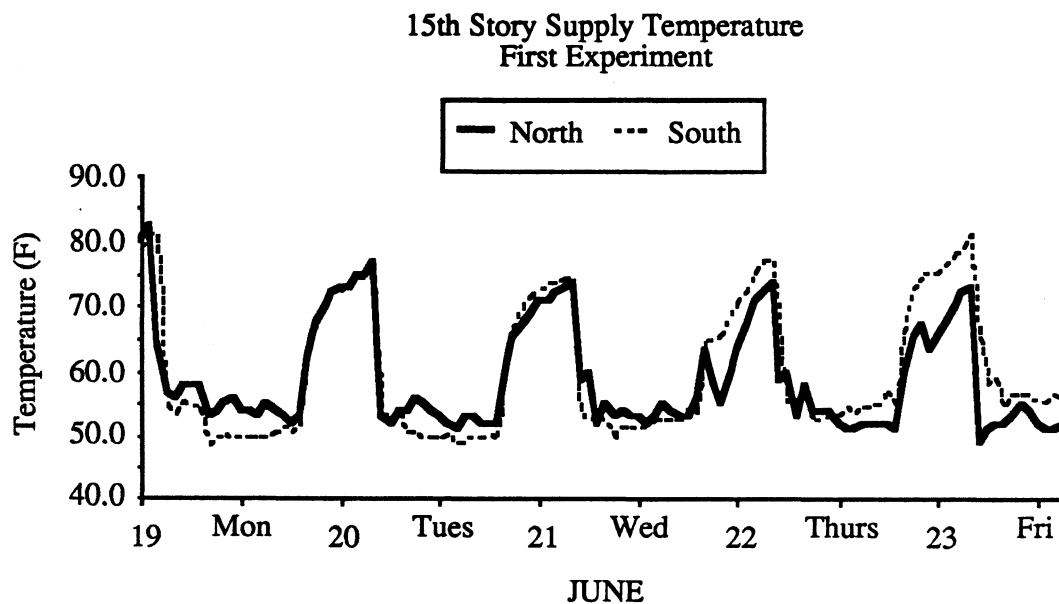


Figure 2.6 15th Story Supply Air Temperatures - Second Experiment



**Figure 2.7 15th Story Supply Air Temperatures - First Experiment**

## 2.4 SUMMARY

Two experiments were performed on the ILIB. The first experiment maximized the amount of weekend pre-cooling. In the second experiment the amount of weekend pre-cooling was reduced. Two stories were used for the experiments. The 9th story was the test story with pre-cooling and the 15th story was the control story without pre-cooling. Measurements were made of the energy supplied to the 9th and 15th stories. Heat flux measurements at the concrete floor surface were taken on the 9th story. All temperature and velocity measurements were calibrated. Approximations using reliable sensors were used to replace data from faulty sensors.

---

## REFERENCES 2

---

1. *ASHRAE Handbook, Fundamentals Volume*, American Society of Heating, Refrigerating, and Air Conditioning Engineers, Atlanta, Georgia, 1989.

## **CHAPTER 3**

---

# **DATA ANALYSIS**

---

Since data from the EMCS were only available on printouts, over 9000 data points were manually transferred from EMCS printouts to a computer spreadsheet. Each data entry recorded by the computer monitoring station had to be manually reformatted and transformed into spreadsheet form. Data from the spreadsheets were then used to produce plots of all measured variables. Plots of the measured variables were analyzed for errors and trends. The results of this analysis show the effect of pre-cooling on thermal comfort, heat flux, and energy use.

### **3.1 THERMAL COMFORT**

Pre-cooling can have a significant effect on the thermal comfort of the building occupants. Pre-cooling could cause the zone temperature to be uncomfortably cold at the beginning of occupancy. A pre-cooling strategy must include a warm-up period to allow the building temperature to reach comfort levels. The warm-up period should be accomplished without auxiliary heating since auxiliary heating would increase the cost and reduce the effectiveness of pre-cooling.

#### **3.1.1 First Experiment**

Numerous complaints were received from occupants on the 8, 9, and 10th stories on Monday morning. An overcast, cool morning coupled with the large amount of weekend pre-cooling caused the zone temperature to remain uncomfortably cold throughout the morning. Figure 3.1 shows the outdoor temperature and humidity measured by the EMCS. Note the drop in temperature on Monday morning.

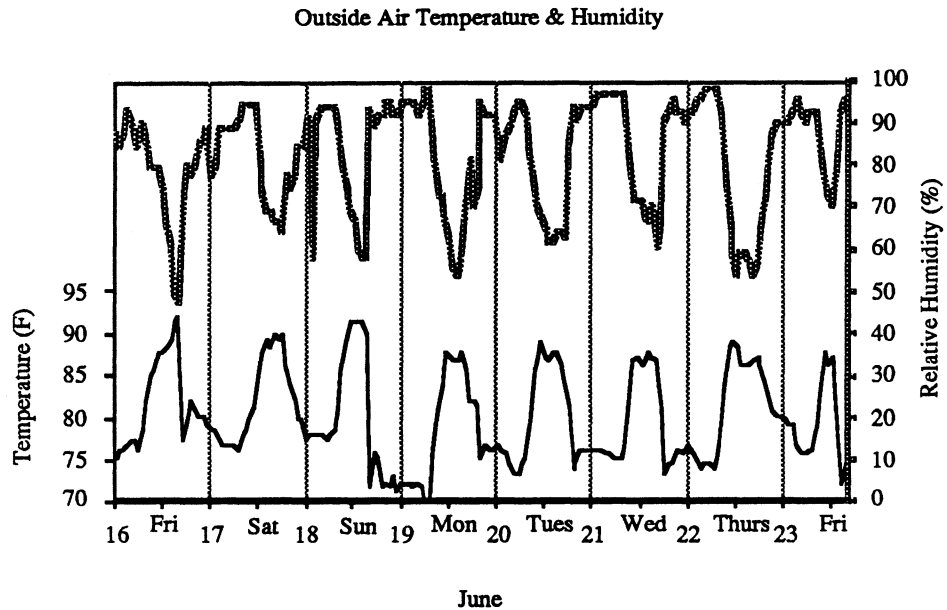


**Figure 3.1 Outdoor Temperature & Humidity - First Experiment**

Weekend pre-cooling was turned off at 5am Monday to allow the zone temperature to increase before occupants arrived. Occupancy normally starts at 7am. At 5am the average (north and south) zone temperature was 63°F. By 8am the temperature rose to 66°F. By noon the temperature reached 70°F. Figure 3.2 shows the change in temperature from 5am to 10am for each day of the week.

A linear regression gives the slope and intercept for a straight line approximation of the data in Figure 3.2. The slope is the change in temperature per hour ( $\Delta T/\Delta t$ ). The rate at which the zone temperature increases without auxiliary heating ( $\Delta T/\Delta t$ ) is defined as the temperature rate. The increase in zone temperature is caused by energy gains from internal (lights, people, and equipment), and external (solar and outdoor temperature) sources. Table 3.1 lists the temperature rate, the average zone temperature at 5am, and the outdoor temperature at 5am for each day of the week.

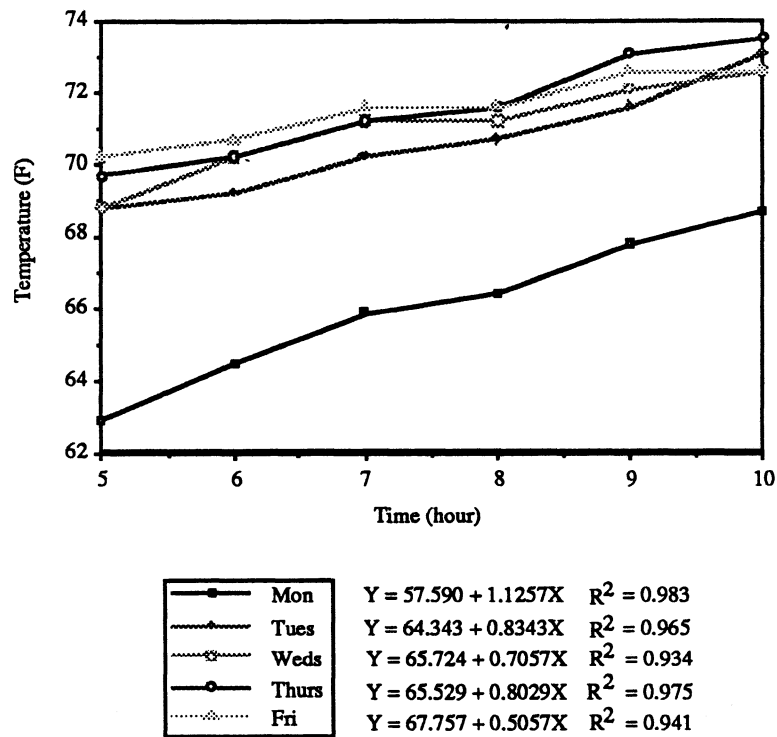


Figure 3.2 9th Story Average Zone Temperature

	Temperature Rate (°F/hr)	Zone Temperature @ 5am	Outdoor Temperature @ 5am
Monday	1.13	62.9°F	71.7°F
Tuesday	0.83	68.8°F	73.4°F
Wednesday	0.71	68.8°F	75.2°F
Thursday	0.80	69.7°F	74.6°F
Friday	0.51	70.2°F	75.7°F
Average	0.80	68.1°F	74.1°F

Table 3.1 Weekday Temperatures - First Experiment

The temperature rates are similar except on Monday and Friday. Monday morning the temperature rate is higher, while the zone temperature and outdoor temperature were below average. On Friday the temperature rate is lower, while the zone temperature and outdoor temperature were above average. This suggests that the temperature rate may be effected by the zone temperature and/or outdoor air temperature.

Measurements of globe temperature and room air temperature were recorded by the computer monitoring station. Globe temperature measures the combined effect of radiation and convection [1] and is an indicator of thermal comfort. Figure 3.3 shows that the globe temperature did not vary significantly from the room air temperature.

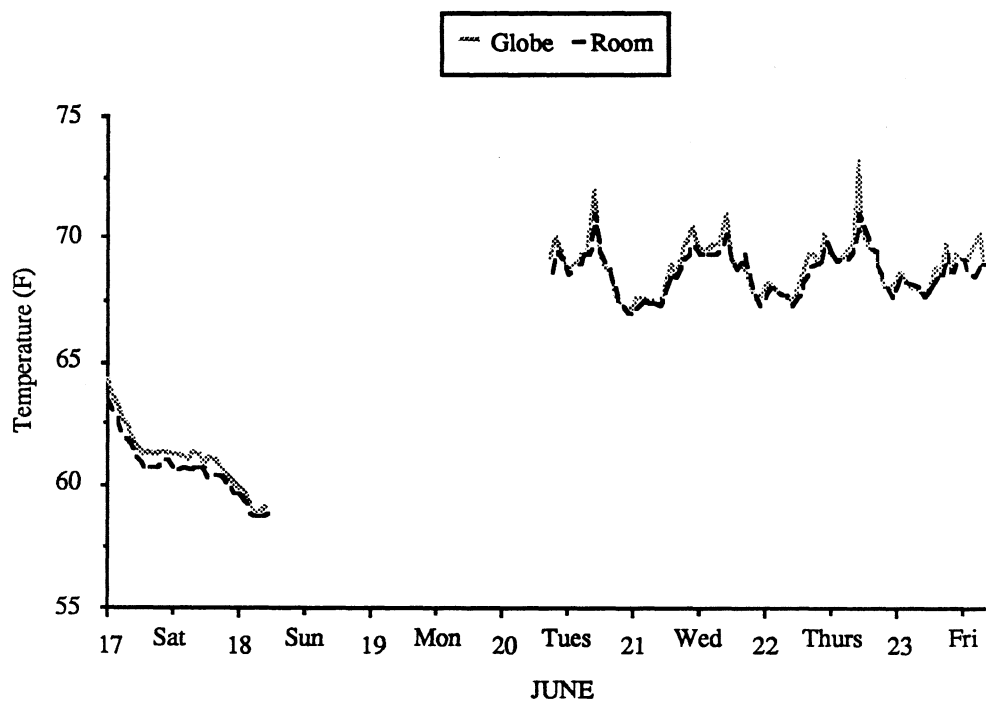


Figure 3.3 Globe & Room Air Temperature

Lower globe temperatures would have occurred if the pre-cooling caused building surfaces to remain significantly cooler than the room air. Radiation from occupants to cool building surfaces could cause thermal discomfort. Differences between humidity readings for the the 9th and 15th stories, shown previously in Figure 2.4, were not significant during the day-time. Therefore, pre-cooling did not significantly effect the room humidity ratio or globe temperature during occupancy.

### 3.1.2 Second Experiment

The 9th story zone temperatures were monitored Monday morning to ensure that there was enough warm-up time before occupancy. Estimates of warm-up time were based on the average temperature rate in Table 3.1. Warm-up time was calculated according to

$$\text{Warm-up Time (hours)} = \frac{(\text{Zone Temperature} - \text{Target Temperature})}{\text{Temperature Rate}} \quad (3.1)$$

where

$$\text{Target Temperature} = 70.0 \text{ } ^\circ\text{F}$$

$$\text{Temperature Rate} = 0.80 \text{ } ^\circ\text{F/hr}$$

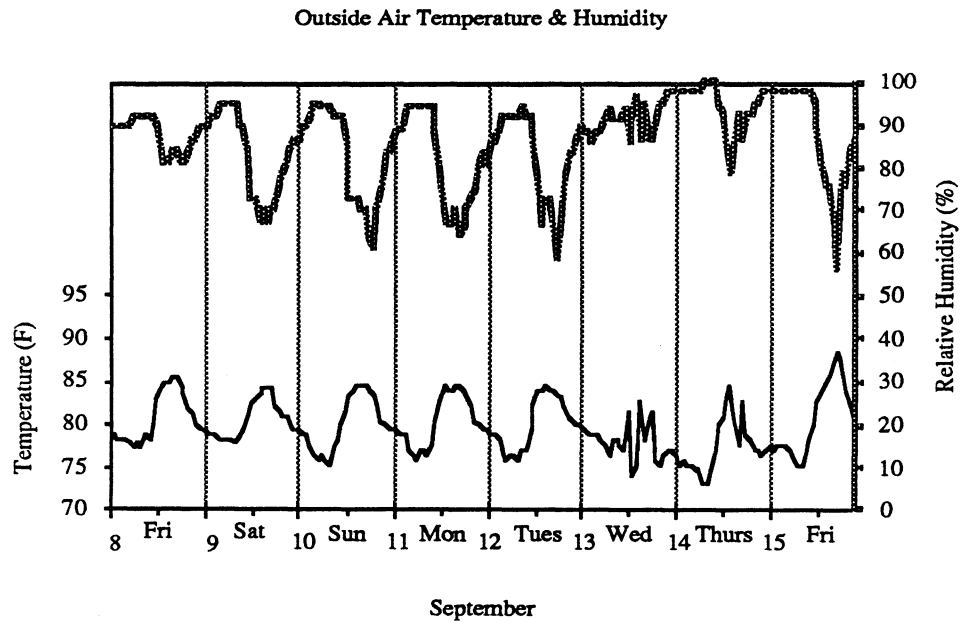
The target temperature is the desired temperature at the beginning of occupancy. This method is similar to the way optimum start and stop times are calculated by the EMCS. No complaints were received from occupants on the 8th, 9th, and 10th stories on Monday morning or during the rest of the week.

Table 3.2 lists the calculated temperature rate ( $\Delta T/\Delta t$ ), the average zone temperature at 5am, and the outdoor temperature at 5am, for each day of the week. The average temperature rate in Table 3.2 is less than the average temperature rate in the first experiment.

Weather conditions for the second experiment were milder. Figure 3.4 shows the outdoor air temperature and humidity during the second experiment.

	Temperature Rate (°F/hr)	Zone Temperature @ 5am	Outdoor Temperature @ 5am
Monday	0.70	68.3°F	75.9°F
Tuesday	0.48	69.7°F	76.5°F
Wednesday	0.53	70.2°F	77.7°F
Thursday	0.74	69.5°F	74.9°F
Friday	0.62	70.0°F	75.9°F
Average	0.61	68.1°F	74.1°F

**Table 3.2 Weekday Temperatures - Second Experiment**



**Figure 3.4 Outdoor Temperature and Humidity - Second Experiment**

Although the average outdoor temperature for both experiments is about the same, (80.4°F in the first experiment and 79.8°F in the second experiment) variations in temperature were less extreme in the second experiment. The readings of high humidity ratios and uneven temperatures on Wednesday and Thursday could be due to rain storms [2].

Figure 3.5 shows the temperature rate, from Tables 3.1 and 3.2, plotted against outdoor air temperature at 5am and zone air temperature at 5am.

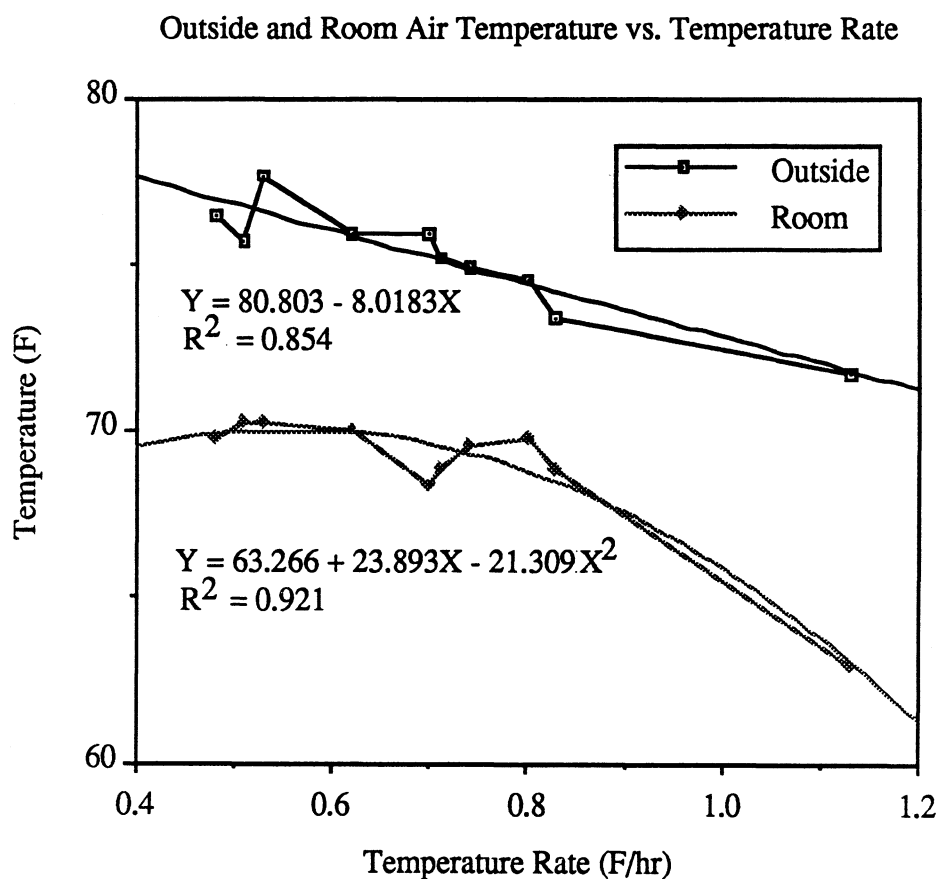


**Figure 3.5 Outdoor and Zone Temperature vs. Temperature Rate**

Temperature rate seems to have a linear correlation with outdoor temperature and a quadratic relation with zone temperature. Further experimental data could help to validate these correlations. An adaptive control scheme could be used to update the correlation coefficients [3]. The updated correlation could provide a better prediction of the temperature rate.

These correlations are consistent with findings by [3] in a paper which evaluated different algorithms for predicting recovery time. Recovery time is the time interval required for the auxiliary heating or cooling to recover from night setback to daytime comfort levels. In this study estimates using indoor temperature and outdoor temperature were found to be best predictor when heating was required for recovery. When cooling was required for recovery, an estimate using only the indoor temperature provided the best prediction.

### 3.2 HEAT FLUX

A finite difference model (Figure 3.6) was constructed to calculate the floor heat flux from temperatures measured at the concrete surface (under the carpet). Underneath the floor a convective boundary is defined using temperatures in the return air plenum. The model is adapted from a finite difference program listed in [4]. A listing of the adapted finite difference program is given in the Appendix. Heat flux into the floor is defined as positive.

The floor is supported by a metal deck covered with fireproofing. The resistance at the convective boundary ( $R_b$ ) is the sum of the resistance of the fireproofing ( $R_{fp}$ ) and the surface convective resistance ( $R_o$ ).

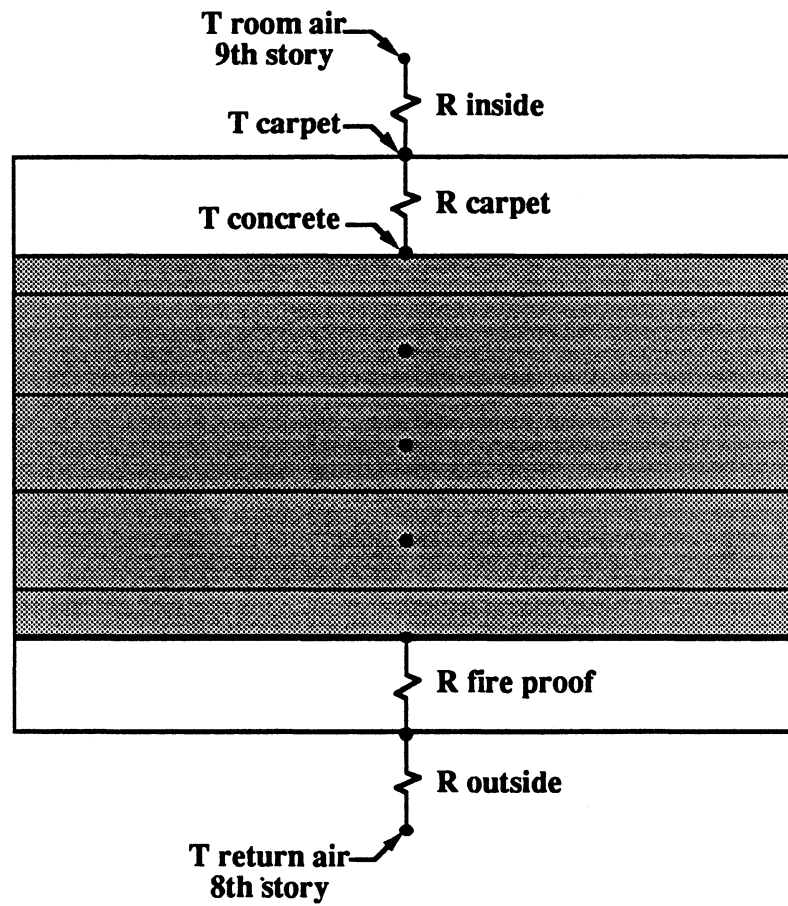


Figure 3.6 Finite Difference Model

$$R_b = R_{fp} + R_o = 2.50 + 0.77 = 3.27 \left[ \frac{\text{hr ft}^2 \text{ F}}{\text{Btu}} \right] \quad (3.2)$$

where

$$R_{fp} = \frac{L}{k} = \frac{0.75}{0.30} = 2.50 \left[ \frac{\text{hr ft}^2 \text{ F}}{\text{Btu}} \right] \quad (3.3)$$

$$R_o = \frac{1}{2} (0.61 + 0.92) = 0.77 \left[ \frac{\text{hr ft}^2 \text{ F}}{\text{Btu}} \right] \quad (3.4)$$

The average thickness of the fireproofing is assumed to be 3/4 inches. The direction of the heat transfer at the boundary changes as the floor charges and discharges. Therefore, the average surface convective resistance is the average of the values given by ASHRAE [1] for heat flow upward and heat flow downward.

Material properties for the concrete floor are given by [5]

$$c = \frac{1}{3.934 + 0.006\rho} \left[ \frac{\text{Btu}}{\text{lb F}} \right] \quad (3.5)$$

$$k = 0.05 e^{0.02\rho} \left[ \frac{\text{Btu}}{\text{hr ft F}} \right] \quad (3.6)$$

For the 9th floor concrete

$$L = 4.75 \text{ inches} = 0.396 \text{ ft} \quad (3.7)$$

$$\rho = 110 \left[ \frac{\text{lb}}{\text{ft}^3} \right] \quad (3.8)$$

$$c = 0.22 \left[ \frac{\text{Btu}}{\text{lb F}} \right] \quad (3.9)$$

$$k = 0.45 \left[ \frac{\text{Btu}}{\text{hr ft F}} \right] \quad (3.10)$$

### 3.2.1 First Experiment

In the first experiment temperatures on the 9th story were recorded by the computer monitoring station at 15 minute intervals. The 8th story return air plenum is underneath the 9th floor and is modeled as a convective boundary. Temperatures measured in the 9th story return air plenum were assumed to be representative of temperatures in the 8th story return air plenum.

The finite difference model (FDM) provides a means for estimating heat flow from the measured temperatures. The results in Figure 3.7 show the periodic behavior of the temperature and heat flux.

Using the calculated heat flux, and measured temperatures, experimental values for the carpet resistance and the floor surface convection resistance can be calculated

$$R_{\text{carpet}} = \frac{T_{\text{carpet}} - T_{\text{concrete}}}{q_{\text{floor}}} \quad (3.11)$$

$$R_{\text{surface}} = \frac{T_{\text{air}} - T_{\text{carpet}}}{q_{\text{floor}}} \quad (3.12)$$

Temperatures for the air and carpet were taken from values recorded in 15 minute time steps by the computer monitoring system. Values of resistance were calculated at each time step when the temperature difference was  $\geq 0.5^{\circ}\text{F}$ . A temperature difference of  $0.5^{\circ}\text{F}$  was chosen since the accuracy of the temperature sensors is about  $\pm 0.5^{\circ}\text{F}$ . Also, a zero temperature difference would result in an zero resistance. Table 3.3 lists the average R values, their sample standard deviation (s), and the number of calculations (N).

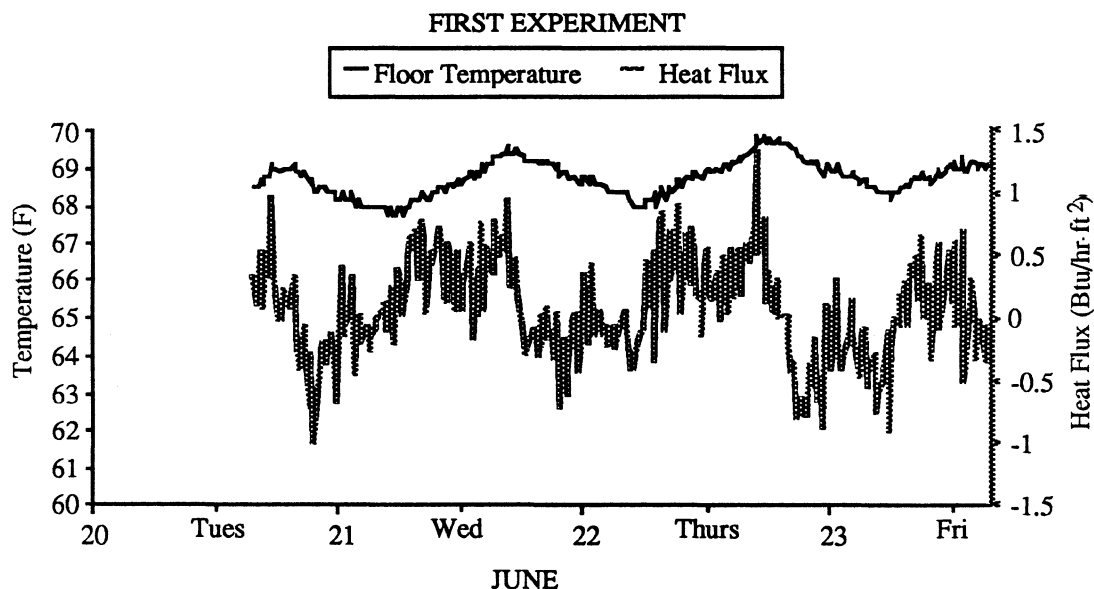


Figure 3.7 Temperature and Heat Flux

Carpet Resistance $\left[ \frac{\text{hr-ft}^2\text{-F}}{\text{Btu}} \right]$	Surface Resistance $\left[ \frac{\text{hr-ft}^2\text{-F}}{\text{Btu}} \right]$
R = 1.02	R = 1.02
s = 0.27	s = 0.47
N = 72	N = 48

**Table 3.3 Carpet Resistance and Surface Resistance - First Experiment**

The resistance values in Table 3.3 are close to values given by ASHRAE [1]. ASHRAE lists a R value of 1.23 (hr-ft<sup>2</sup>-F/Btu) for carpet. However, the actual resistance is probably less since the carpet consisted of thin (5/16 inch) tiles of nylon with a rubber backing. The surface resistances given by ASHRAE are 0.92 (Btu/hr-ft<sup>2</sup>-F) for positive heat flux, and 0.61 (Btu/hr-ft<sup>2</sup>-F) for negative heat flux. Comparison of the FDM values to the ASHRAE values provides a means of checking if the finite difference results are reasonable.

### 3.2.1 Second Experiment

In the second experiment a heat flux sensor was available. The heat flux sensor provided a direct measurement of the floor heat flux. Readings from the heat flux sensor and the temperature sensors were recorded at hourly intervals. The hourly intervals coincided with readings from the EMCS and reduced the amount of data that had to be backed up and transformed.

In the first experiment, temperatures measured in the 9th story return air plenum were used to approximate temperatures in the 8th story return air plenum. Instead of using the 9th story return air temperatures, temperatures in the 8th story return air plenum were estimated by using the average 8th story zone temperature. In section 2.2.2 it was shown that the average zone temperature is a good approximation for the return air temperature. Hourly values of the north and south zone temperature on the 8th story were available from EMCS printouts. Figure 3.8 shows that the finite difference results, with the average 8th story zone temperature, are consistent with the heat flux sensor readings.

Calculations using the 9th story return air temperature did not compare as favorably to the heat flux sensor readings. Fifteen minute values of the 8th story zone temperature were not available for the first experiment.

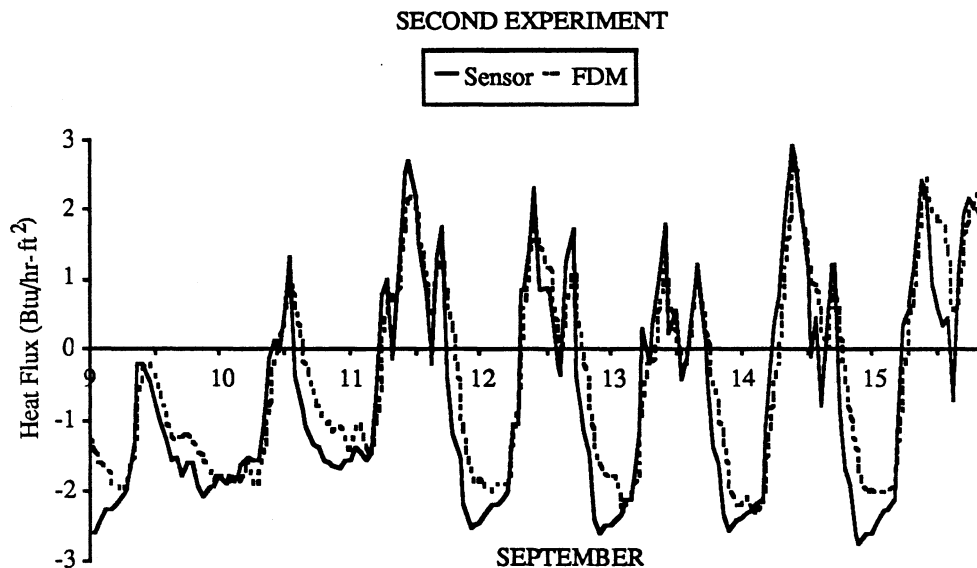


Figure 3.8 Heat Flux - Sensor and Finite Difference Method

The calculated values of carpet resistance and floor surface resistance are shown in Table 3.4. Since the finite difference results from the second experiment were verified

Carpet Resistance $\left[\frac{\text{hr-ft}^2\text{-F}}{\text{Btu}}\right]$	Surface Resistance $\left[\frac{\text{hr-ft}^2\text{-F}}{\text{Btu}}\right]$
R = 0.77	R = 1.59
s = 0.33	s = 0.93
N = 105	N = 115

**Table 3.4 Carpet Resistance and Surface Resistance - Second Experiment**

against the heat flux sensor, and since the first experiment is missing some of the weekly data, the results in Table 3.4 should be more accurate than those in Table 3.3. Table 3.5 shows that the sum of the calculated surface and carpet resistances for the first and second experiment are similar.

Resistance $\left[\frac{\text{hr-ft}^2\text{-F}}{\text{Btu}}\right]$	First Experiment	Second Experiment
Carpet	1.02	0.77
Surface	1.02	1.59
Total	2.04	2.36

**Table 3.5 Carpet and Surface Resistance - First and Second Experiment**

### 3.3 COOLING ENERGY

The energy supplied to both stories was calculated from supply air velocities and supply and return temperatures. The calculated airflow through the core return air duct was less than half of the supply airflow. Surveys during the experiments with the hand held velocity sensor located sources of leakage through the perimeter return air dampers, elevators, stairwells, toilet exhausts, and a mail conveyor. All the air entering the room at the supply air temperature ( $T_{sa}$ ) is assumed to leave the room at the return air temperature ( $T_{ra}$ ). The sensible energy supplied ( $\dot{E}_{sens}$ ) is then

$$\dot{E}_{sens} = 1.10 * V * C * A * (T_{ra} - T_{sa}) \text{ [Btu/hr]} \quad (3.13)$$

where

V = air velocity (fpm)

C = velocity profile correction factor from Table 2.1

A = duct area (ft<sup>2</sup>) from Table 2.1

Figure 3.9 shows the energy supplied to the 9th and 15th stories for both experiments. These energy values were calculated from instantaneous readings taken every hour. Figure 3.9 shows the large energy input to 9th story during the weekend of the first experiment. Some cooling was supplied to the 15th story for tenants who came in during the weekend. Spikes in the energy supplied to the 9th story, can be attributed to the opening and closing of supply dampers on other stories, supplied by the same air handling unit. When the 9th story supply dampers are open, the opening or closing of supply dampers on other floors will cause the flow to surge.

#### 3.3.1 Charging vs. Discharging

A comparison between stories 9 and 15 is shown in Figure 3.10 where the energy supplied to the 9th story is subtracted from the energy supplied to the 15th story.

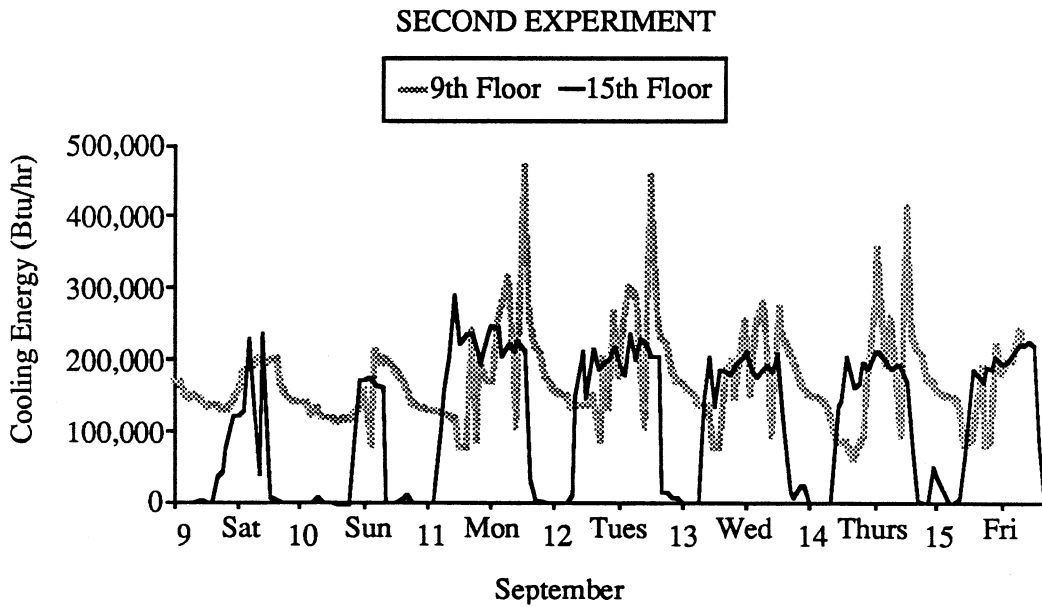
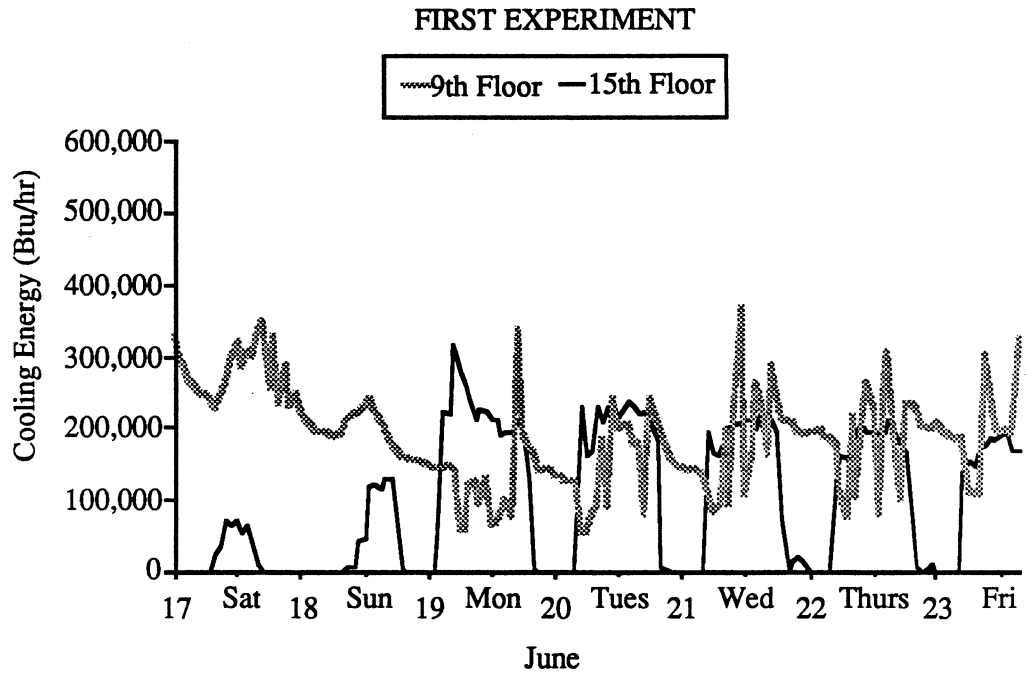


Figure 3.9 Energy Supplied 9 & 15

Positive values indicate that more energy was supplied to the 9th story. This is defined as charging since the additional energy supplied to the 9th story is assumed to be cooling the thermal mass. Negative values indicate that less energy was supplied to the 9th story. This is defined as discharging since the energy reduction is assumed to occur due to warming of the thermal mass.

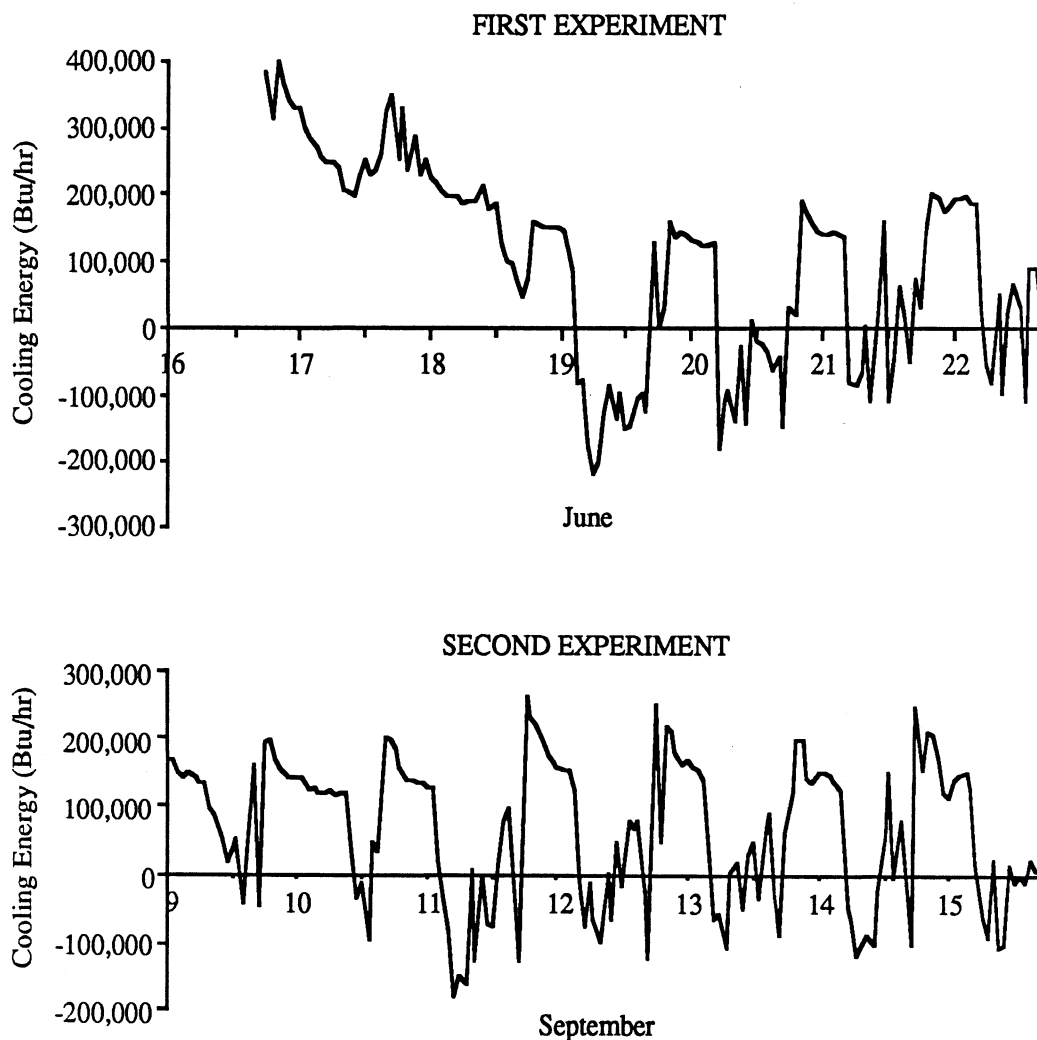


Figure 3.10 Energy Supplied 9 - 15

The total energy supplied to the 9th story during the first experiment was about twice the amount supplied to the 15th story. During the week (not including the weekend) the energy supplied to the 9th story was about 1.4 times the energy supplied to the 15th story. The ratio of discharge ( $E_9 - E_{15}$  negative) to charge ( $E_9 - E_{15}$  positive) for the first experiment was 19%. The ratio of discharge to charge energy for the week days only was 42%. Table 3.6 lists these parameters for the first and second experiment.

First Experiment	Week - 5 Days Monday to Friday	Experiment - 7 Days Friday to Friday
9 Energy / 15 Energy	1.36	2.04
Discharge / Charge	42%	19%

Second Experiment	Week - 5 Days Monday to Friday	Experiment - 7 Days Friday to Friday
9 Energy / 15 Energy	1.34	1.61
Discharge / Charge	40%	26%

**Table 3.6 Energy Parameters - First & Second Experiment**

Note that the parameters for the week days are similar for the first and second experiment. This seems to indicate that the greater amount of weekend cooling in the first experiment had little effect in reducing the weekday cooling loads. The ratio of charge to discharge during the experiment is less than 100% since some of energy supplied for charging is "lost" through the building envelope.

### 3.3.2 Load Reduction

During the night, cooling is applied to the 9th story while the 15th story receives no cooling. Therefore, night-time temperatures on the 9th story are lower than on the 15th story. Since ambient temperatures are higher than the 9th story zone temperatures, envelope losses ( $Q_{env}$ ) on the 9th story are greater than on the 15th story. Also, since the 9th story is ventilated, exfiltration energy losses ( $Q_{inf}$ ) on the 9th story will be greater than on the 15th story. Some of the energy ( $Q_{store}$ ) supplied to the 9th story will lower the temperature of (charge) the thermal mass. Therefore, during the night charging period, energy use for the 9th story is greater than the 15th story. The difference in energy use between the 9th and 15th story is then:

$$E_9 - E_{15} = (Q_{env9} - Q_{env15}) + (Q_{inf9} - Q_{inf15}) + (Q_{store9} - Q_{store15}) \quad (3.14)$$

During the day both stories are ventilated and controlled to maintain a zone temperature of not more than 73°F. If the zone temperature on both stories is approximately the same, and infiltration is assumed to be the same for both stories, then the energy difference can be attributed to the thermal energy storage:

$$E_9 - E_{15} = Q_{store9} - Q_{store15} \quad (3.15)$$

Figure 3.11 shows that the 9th and 15th story temperatures are reasonably close during the daytime (non pre-cooling) period.

Figure 3.12 shows the sum of  $E_9 - E_{15}$  for each hour of the week. For example, the value at 1am is the sum of  $(E_9 - E_{15})$  at 1am on Monday, Tuesday, Wednesday, Thursday, and Friday. Figure 3.12 shows that cooling reductions on the 9th story occur mainly in the morning from 5 am to 12 noon. Some reduction in afternoon cooling occurred in the first experiment. The reduction at 17:00 hours (5 pm) in the second

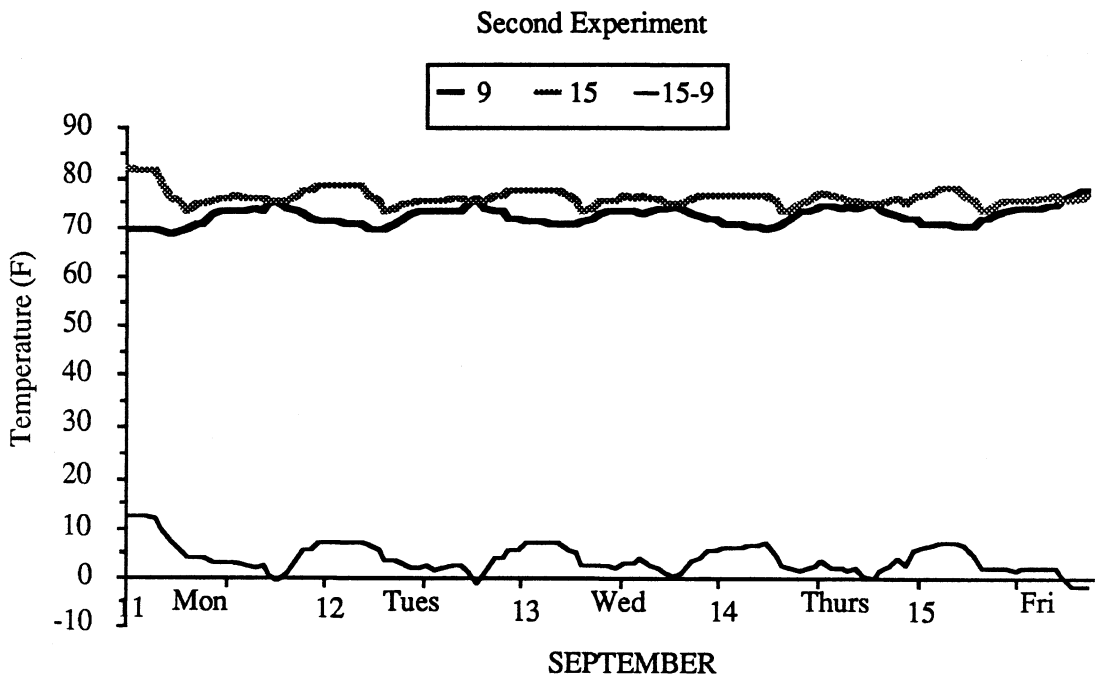
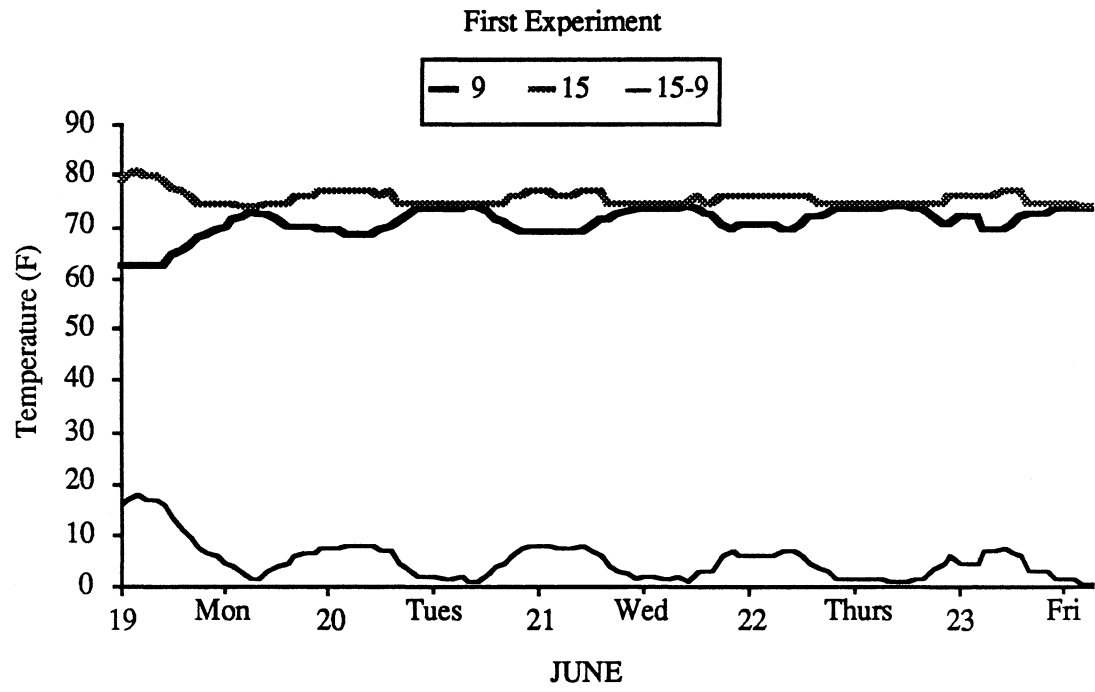
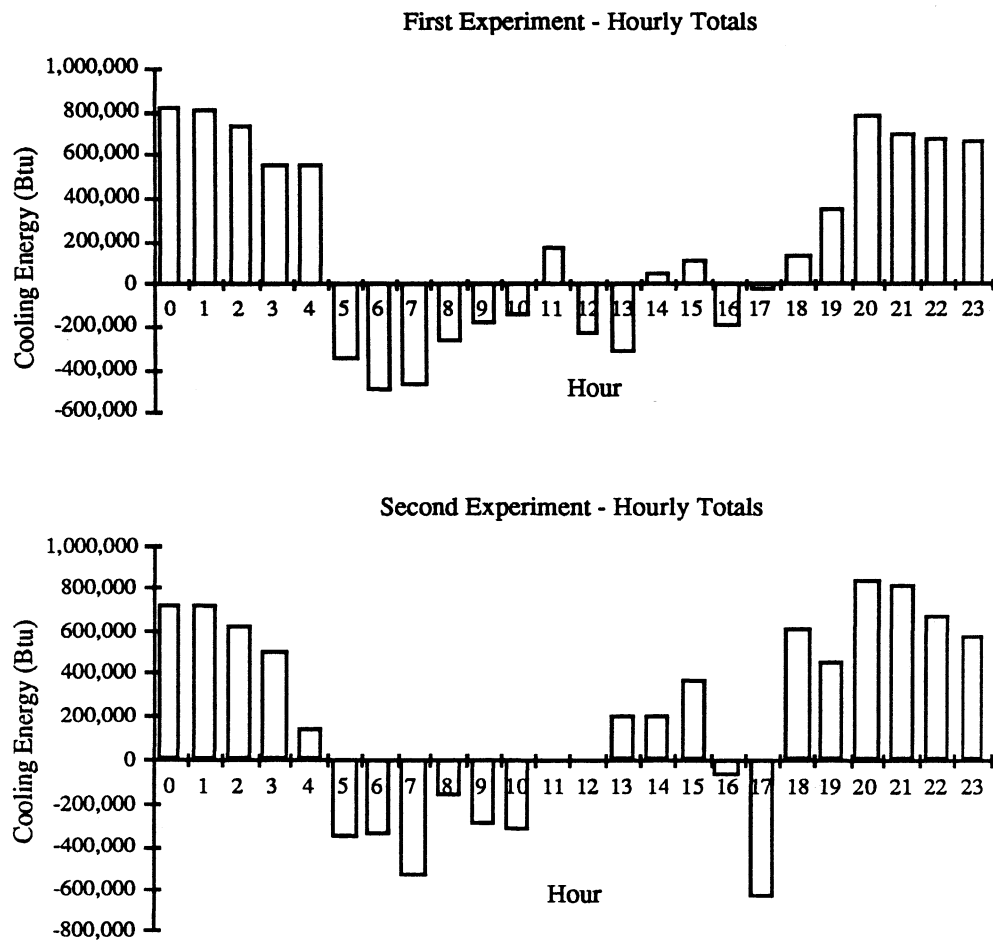


Figure 3.11 Average Zone Temperature

experiment occurred because the cooling on the 9th story was off while the 15th story cooling was still on. Most of the cooling reduction occurred shortly after the pre-cooling period ended. The effect of pre-cooling for this building appears to last for only short periods (less than 8 hours). This is probably due to the limited amount of thermal mass in the building.



**Figure 3.12 E<sub>9</sub> - E<sub>15</sub> Hourly Distribution**

### 3.3.3 Peak Reduction Strategy

A pre-cooling strategy should consider peak periods, comfort requirements, and minimum zone temperatures. Peak periods are defined in electric rate schedules. The cost of electricity increases during the peak period. The time of use rate schedule applicable to the ILIB [6] has the summer peak period listed in Table 3.7. The ILIB is not currently on a time of use rate schedule.

Summer	Peak Period
April thru October	Monday thru Friday - 12 noon to 9 pm

Table 3.7 Summer Peak Period

Since the cooling load reduction occurs shortly after the pre-cooling period ends, the temperature of the thermal mass should remain as low as possible before the start of the peak period. However, temperatures during occupied periods must remain within an acceptable comfort region. ASHRAE [1] defines a comfort region which covers a temperature range ( $\Delta T$ ) of about 7°F for a given humidity ratio. During occupied off-peak periods the zone temperature should be regulated to temperatures in the low end of a comfort region. During peak periods the temperature should be allowed to rise to, but not to exceed, the high end of the comfort range. Figure 3.13 illustrates the constraints on a pre-cooling strategy.

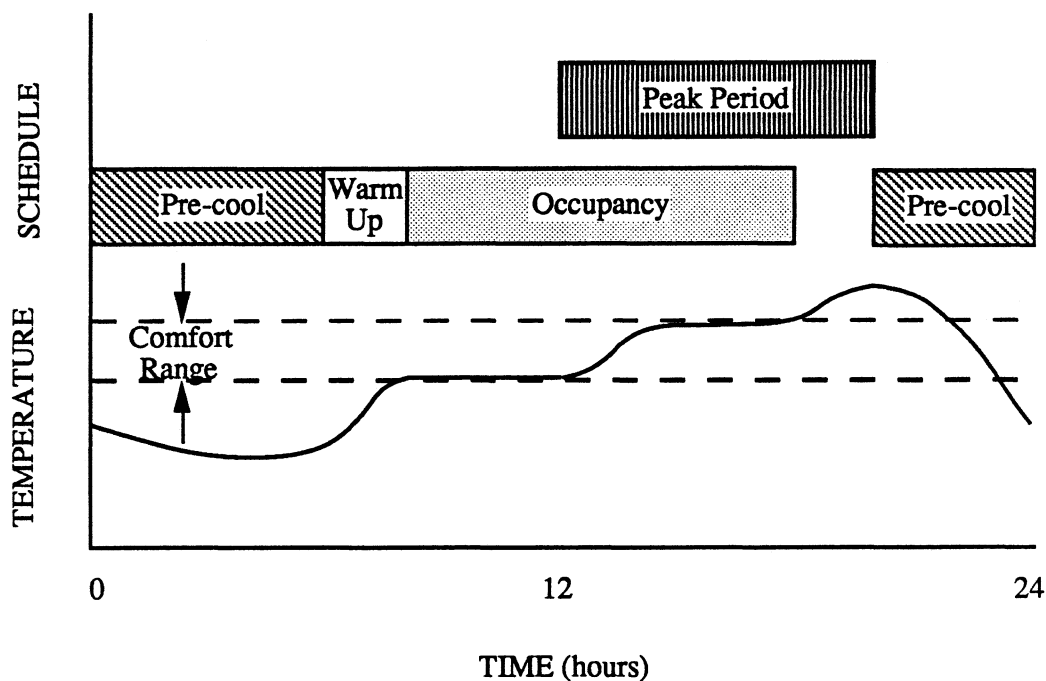


Figure 3.13 Pre-cooling Strategy

Within these constraints, effective pre-cooling becomes an optimization problem. Pre-cooling may be applied through the use of mechanical refrigeration, or by ventilation with cool outdoor air. For mechanical refrigeration, supply air temperature and flow rate can be adjusted to obtain maximum peak reductions at minimum cooling cost. For ventilation, the enthalpy of the outdoor air and the flow-rate effect the benefit and cost of pre-cooling. Effects of moisture storage [7] may increase latent loads when ventilating with outdoor air. The duration of the pre-cooling (charging) period is also a factor. Experiments on the ILIB indicate that longer term (weekend) pre-cooling was not effective for this building.

### 3.4 SUMMARY

Pre-cooling can lower building temperatures to uncomfortable levels during occupancy. To insure the thermal comfort of the building occupants, a warm-up period is required. The time required to reach a comfortable temperature can be calculated using estimates of the temperature rate.

Since the concrete floor is the main source of thermal mass in the ILIB, the temperature and heat flux were monitored at the floor surface. Results using the finite difference calculations and readings from the heat flux sensor revealed the charging and discharging of the thermal mass. These results show the effect of pre-cooling on the building thermal mass.

Longer (weekend) charging periods proved to be an ineffective pre-cooling strategy. Results from the experiments also show that the maximum cooling load reduction occurred shortly after the pre-cooling (charging) period ended. An effective pre-cooling strategy should have shorter charging periods, and should keep zone temperatures as low as possible before the start of the peak period.

---

## REFERENCES 3

---

1. *ASHRAE Handbook, Fundamentals Volume*, American Society of Heating, Refrigerating, and Air Conditioning Engineers, Atlanta, Georgia, 1989.
2. Fred Wheeler, Independent Life, Personal Communication, December 1989.
3. Seem, J. E., Armstrong, P. R., and C. E. Hancock, "Algorithms for Predicting Recovery Time from Night Setback," *ASHRAE Transactions*, Part 2, Volume 96, 1989.
4. Myers, G. E., Class Notes for ME 764, Department of Mechanical Engineering, University of Wisconsin-Madison, 1988.
5. Balcomb, J. D., *Heat Storage and Distribution Inside Passive Solar Buildings*, Report LA-9694-MS, Los Alamos National Laboratory, 1983.
6. Plicque, J. A., Jacksonville Electric Authority, Personal Communication, March 1989.
7. Halabi, O. A. F., "Moisture Storage in Buildings," M.S. Thesis, University of Wisconsin-Madison, 1990.

## CHAPTER 4

---

# FREQUENCY ANALYSIS

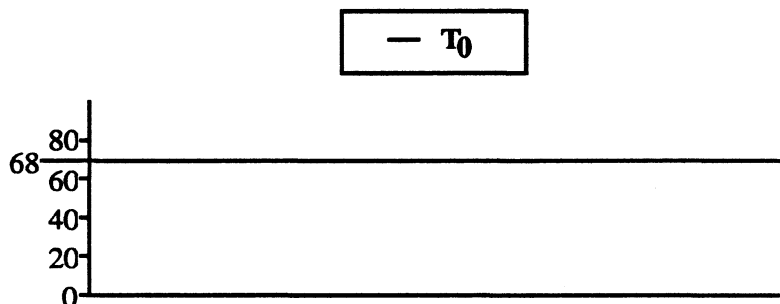
---

Most important driving forces in building heat transfer are periodic. Solar gains, outdoor air temperature, and internal loads all have cyclic patterns. However, steady state methods are commonly used for building heat transfer calculations. Steady state methods ignore the dynamic effect of thermal energy storage. Steady state methods may be adequate for buildings with little thermal mass. However, thermal energy storage can be a significant factor in the dynamic performance of commercial buildings. Frequency methods provide a convenient way to extend steady state methods to the dynamic performance of buildings.

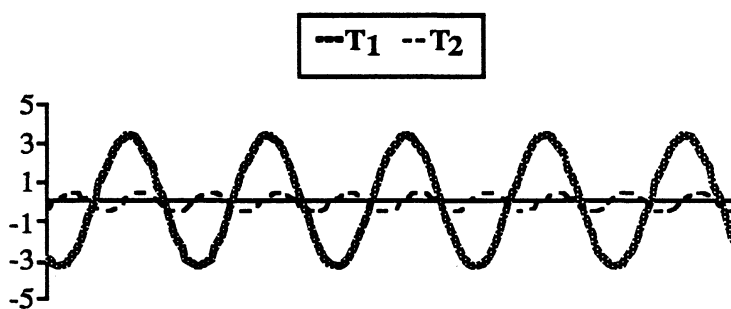
In this chapter calculations of heat flux and thermal energy storage using frequency methods will be developed. These calculations will then be compared to the experimental results. Frequency methods were used since they provide a simplified and intuitive method that can evaluate the transient effects of thermal storage. More complex calculations based on finite difference methods or transfer function methods are less intuitive and better suited for computer simulations.

The frequency method is based on the application of electrical and control theory to building heat transfer. Periodic temperatures and heat gains are approximated by sine waves at various frequencies. Figure 4.1 demonstrates how temperature can be approximated by sine waves. The measured air temperature is from the 9th story computer monitoring station. The sum of the average temperature  $T_0$ , and two sine waves  $T_1$  and  $T_2$ , approximates the measured air temperature.

### Average Temperature



### Sine Waves



### 9th Story Temperature - Experiment 2

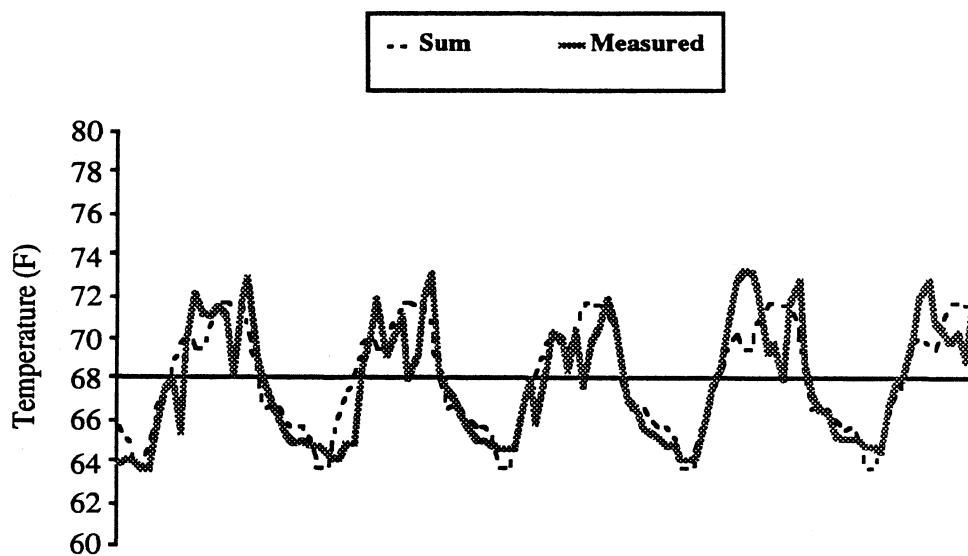


Figure 4.1 Sine Waves and Temperature

$$T_{\text{sum}} = T_0 + T_1 + T_2 \quad (4.1)$$

As shown in Figure 4.1 and Table 4.1, each sine wave has a different frequency ( $\omega$ ). Closer approximations could be made by adding more sine waves at different frequencies.

Temperature (T)	Frequency ( $\omega$ )	Period (P)
$T_0 = 68^\circ\text{F}$	$\omega_0 = 0$	$P_1 = \infty$
$T_1 = 3.4 \sin(\omega_1 t)$	$\omega_1 = \frac{2\pi}{P_1}$	$P_1 = 24 \text{ hours}$
$T_2 = 1.0 \sin(\omega_2 t)$	$\omega_2 = \frac{2\pi}{P_2}$	$P_2 = 8 \text{ hours}$

Table 4.1 Frequency & Period

An excellent introduction to frequency methods is given by [1, 2, & 3]. Thermal admittance and diurnal heat capacity are frequency methods that will be compared to results from the experiments.

#### 4.1 FOURIER TRANSFORM

A Fourier series can be used to describe a function by a series of sine waves at different frequencies [4 & 5]. Figure 4.1 illustrates how temperature can be approximated by a Fourier series with three terms ( $T_0$ ,  $T_1$ , and  $T_2$ ). A Fourier transform can be used to determine the coefficients of the Fourier series. Each coefficient is the amplitude of a the sine wave at a certain frequency. In terms of control theory, the Fourier transform takes

values in the time domain and transforms them into the frequency domain. An example of a discrete Fourier series expansion for temperature is

$$T(t) = A_0 + \sum_{n=1}^N B_n \cos(n\omega t) + C_n \sin(n\omega t) \quad (4.2)$$

$$= A_0 + \sum_{n=1}^N A_n \sin(n\omega t + \varnothing_n) \quad (4.3)$$

where

$$A_0 = \frac{1}{M} \sum_{m=1}^M T_m \quad (4.4)$$

$$A_n = \sqrt{B_n^2 + C_n^2} \quad (4.5)$$

$$\varnothing_n = \tan^{-1} \left[ \frac{B_n}{C_n} \right] \quad (4.6)$$

N = number of frequencies

M = number of data points

The data points are temperatures measured at discrete intervals.  $A_0$  is the average or steady state temperature. Coefficients  $A_n$  and  $B_n$  are obtained from a Fourier transform. Figure 4.2 shows the relation between  $A_n$ ,  $B_n$ , and  $C_n$ . This figure is a geometric representation of the identity

$$A \sin(\omega t + \varnothing) = B \cos(\omega t) + C \sin(\omega t) \quad (4.7)$$

## 4.2 THERMAL ADMITTANCE

Thermal admittance is the ratio of heat flux to temperature at a wall surface. Thermal admittance is a function of material properties and frequency. Each frequency has a unique admittance value.

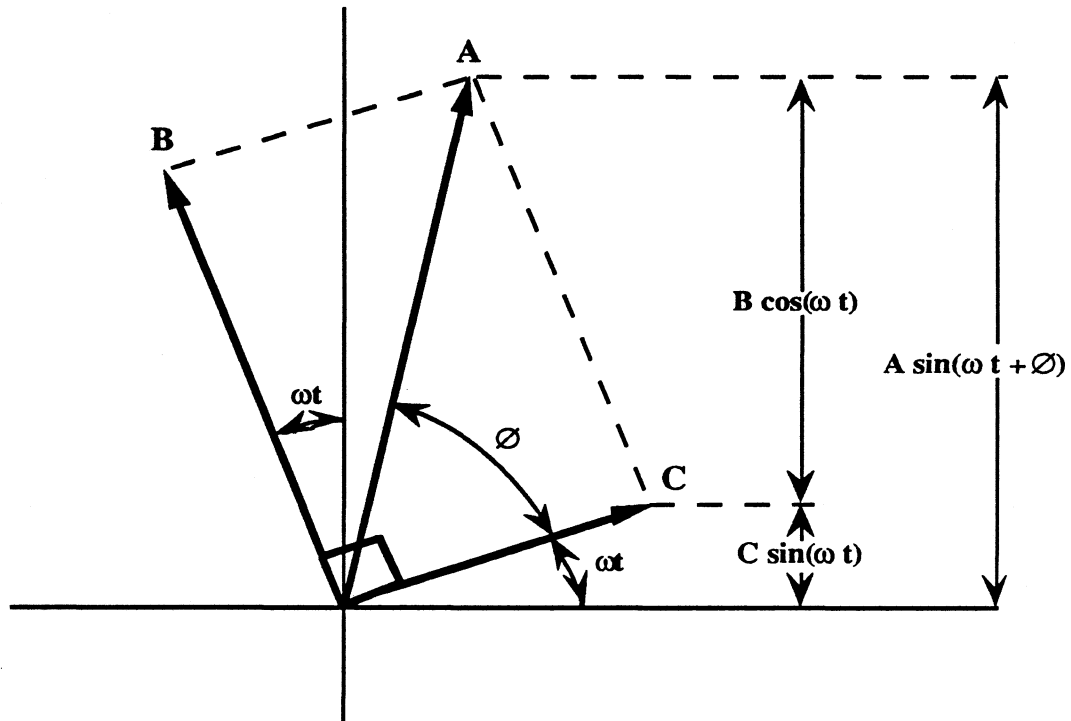


Figure 4.2 A B C Vector Diagram

Buildings typically have prominent diurnal (24 hour period) and zero (steady state) frequencies. Figure 4.1 and Table 4.1 show that the diurnal ( $T_1$ ), and steady state ( $T_0$ ) frequencies are the most significant components of the temperature approximation. To simplify the following frequency analysis, only these two dominant frequencies will be used.

The basis for the admittance method is given by [6]. The admittance concept is further developed by [7] in a graphical method for predicting swings in indoor air temperature. In this chapter the admittance method will be used to predict heat flux for a given temperature difference. From this heat flux, the effects of thermal mass on peak energy use can be identified.

### 4.3 X Y Z ADMITTANCE

Sine waves are the time domain representation of periodic temperature and heat flux.

Figure 4.3 and Table 4.1 depict the temperature and heat flux sine waves.

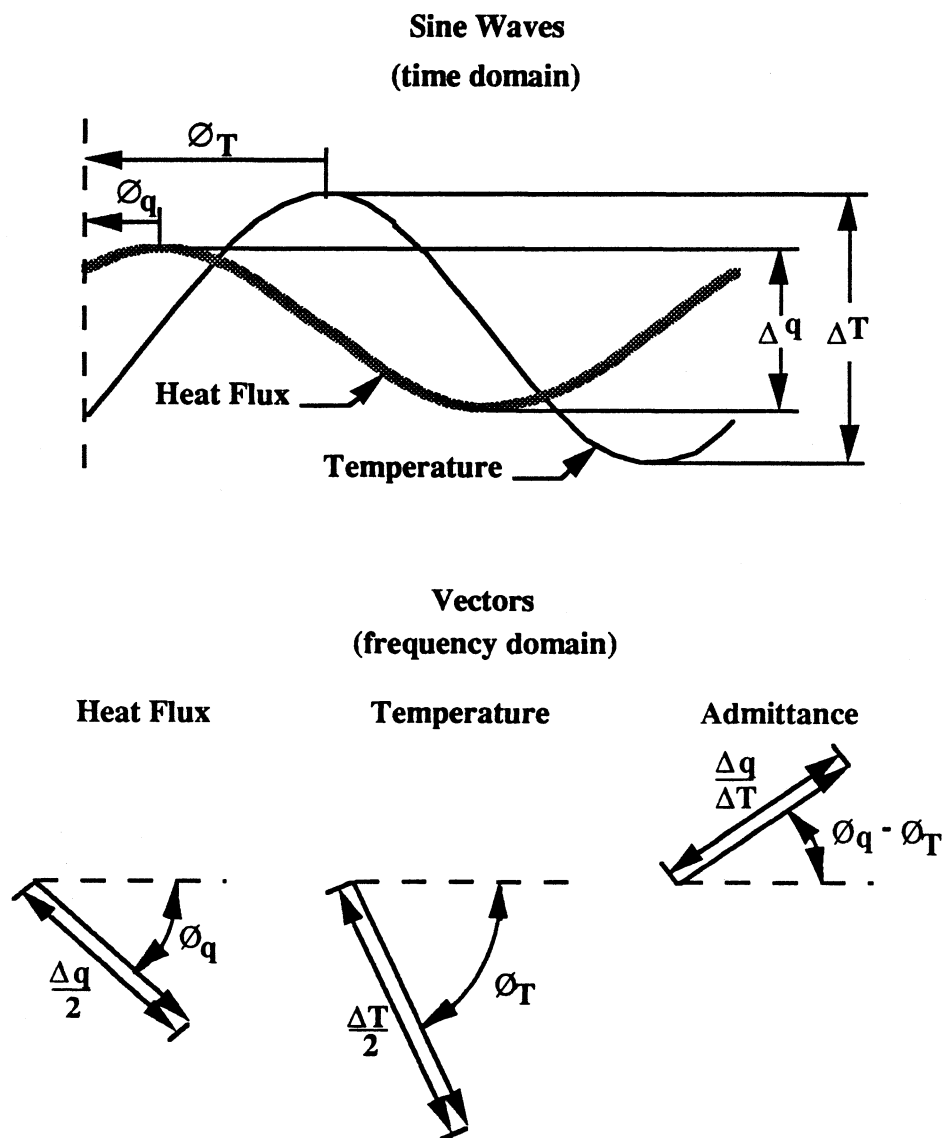


Figure 4.3 Heat Flux & Temperature

Both sine waves have the same frequency. These sine waves can be represented by vectors. Vectors are the frequency domain representation of the temperature and heat flux. The magnitude of the vector is equal to the amplitude of the sine wave. The admittance vector is the ratio of the heat flux vector to the temperature vector. The magnitude of the admittance vector is the ratio of the heat flux amplitude to the temperature amplitude. The angle of the admittance vector is the difference in phase between the heat flux and temperature sine waves. A positive phase indicates that the heat flux leads the temperature. A negative phase indicates that the heat flux lags the temperature.

	Time Domain	Frequency Domain
Heat Flux	$\frac{\Delta q}{2} \sin(\omega t + \phi_q)$	$\frac{\Delta q}{2} \angle \phi_q$
Temperature	$\frac{\Delta T}{2} \sin(\omega t + \phi_T)$	$\frac{\Delta T}{2} \angle \phi_T$
Admittance	$\frac{\Delta q}{\Delta T} \sin(\omega t + \phi_q - \phi_T)$	$\frac{\Delta q}{\Delta T} \angle (\phi_q - \phi_T)$

**Table 4.2 Time and Frequency Domain**

Three admittance values (X, Y, and Z) shown in Figure 4.4 characterize periodic heat transfer in a wall. X admittance is the ratio of the change in heat flux to change in temperature at the inside surface of the wall.

$$X = \frac{\Delta q \text{ inside}}{\Delta T \text{ inside}} \quad (4.8)$$

X admittance is known as driving point admittance because the temperature "driving point" is on the same side as the heat flux.

Y admittance is the ratio of the change in heat flux on one surface of the wall to the change in temperature on the opposite surface

$$Y = \frac{\Delta q \text{ inside}}{\Delta T \text{ outside}} = \frac{\Delta q \text{ outside}}{\Delta T \text{ inside}} \quad (4.9)$$

Y admittance is known as the transfer admittance since the heat flux and temperature are at opposite sides of the wall. Z admittance is similar to X admittance except that the heat flux and temperature are at the outside surface of the wall

$$Z = \frac{\Delta q \text{ outside}}{\Delta T \text{ outside}} \quad (4.10)$$

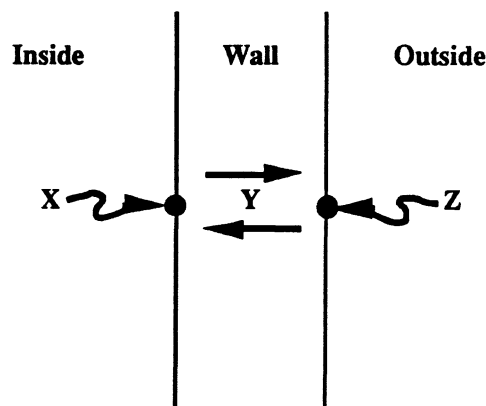


Figure 4.4 X, Y, & Z Admittance

The  $X$  admittance vector has a positive phase since heat flux will lead temperature at the inside surface. This phase lead is illustrated in Figure 4.5. The surface temperature will lag the ambient air temperature. The amount of lag depends on the material properties of the wall and the surface convective-radiative resistance. Heat flux is

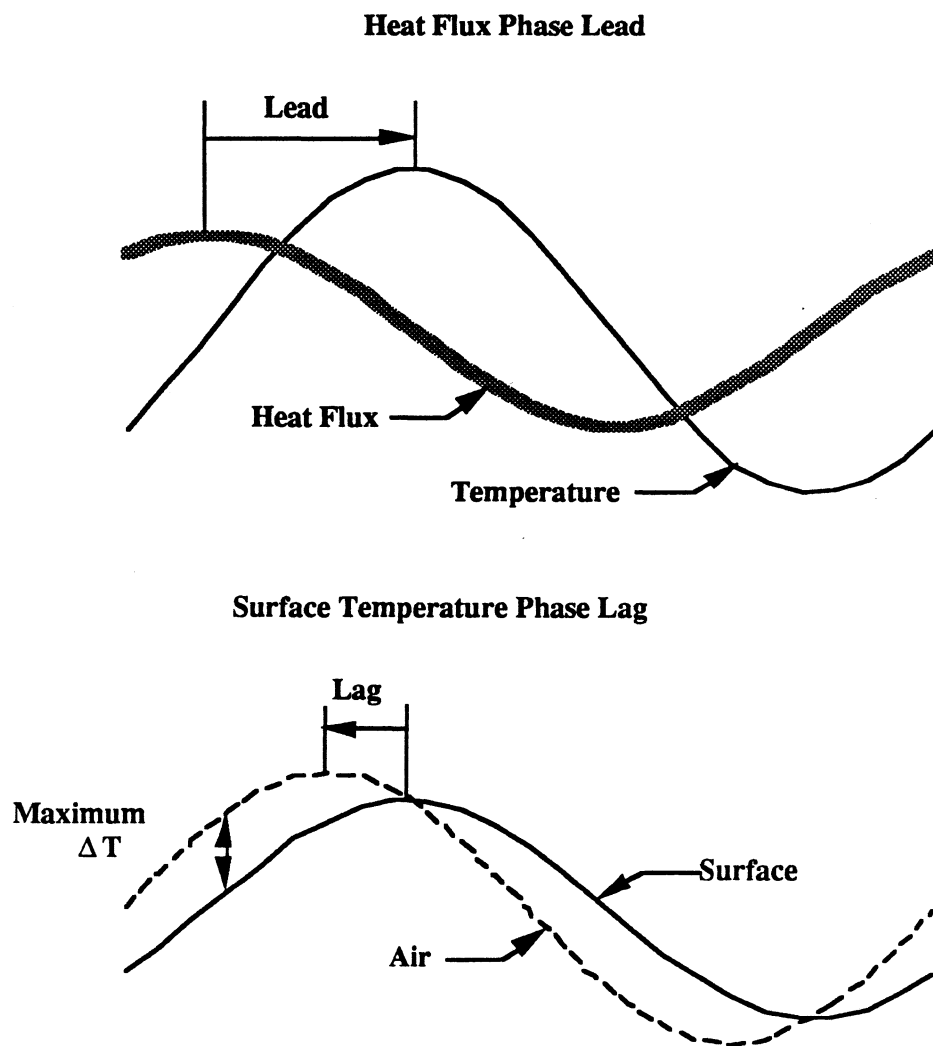


Figure 4.5 X Admittance Phase Lead

proportional to the difference between the surface and ambient temperatures. Maximum heat flux will occur at the maximum temperature difference. Since the surface temperature lags the ambient temperature, the maximum flux occurs before the maximum surface temperature. X admittance is illustrated in Figure 4.6

The Y admittance vector has a negative phase angle. Y admittance exhibits the thermal damping and lag characteristic of massive walls. Figure 4.7 shows that the heat flux at the inside surface lags the temperature at the outside surface. This lag allows passive solar homes to store excess gains during the day and then release these gains later at night [8]. Whether the temperature is at the outside surface and heat flux is at the inside surface or vice versa, the Y admittance vector will be the same for a given frequency.

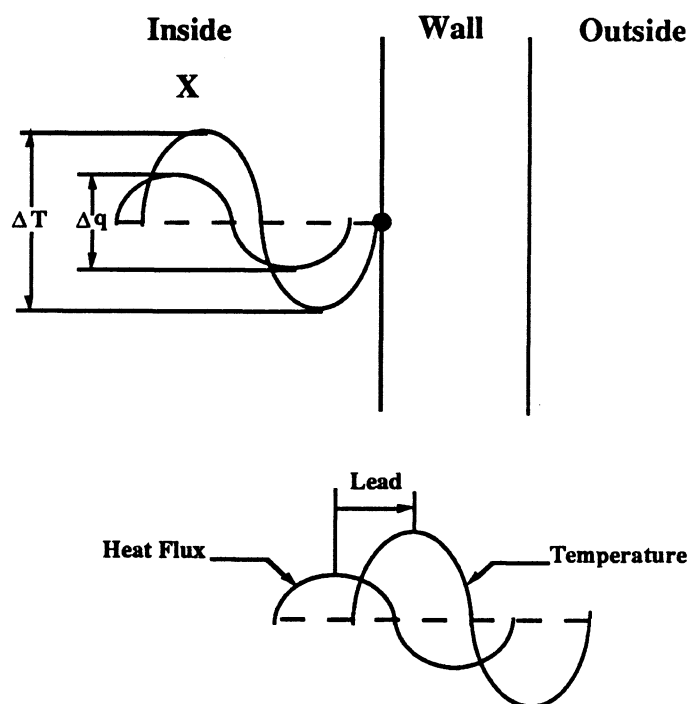


Figure 4.6 X Admittance

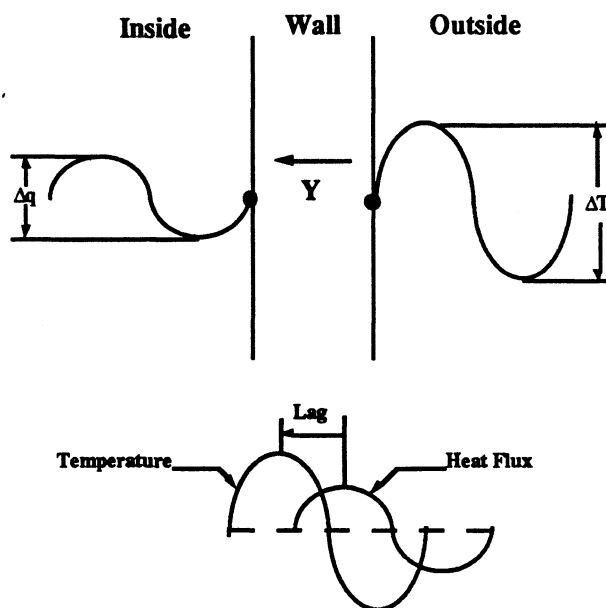


Figure 4.7 Y Admittance

The Z admittance (Figure 4.8) will exhibit a positive phase for the same reasons as the X admittance phase lead. However, the Z admittance vector is not the same as the X admittance vector unless the wall is symmetric.

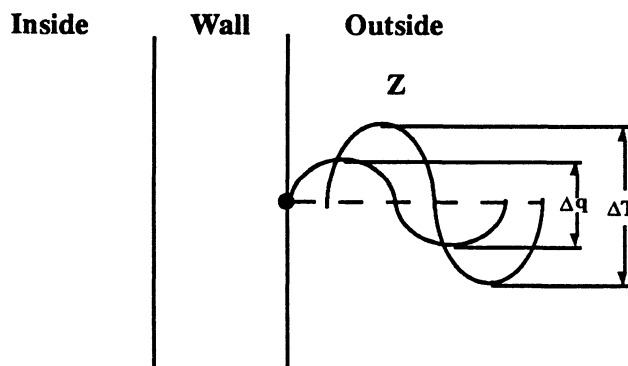
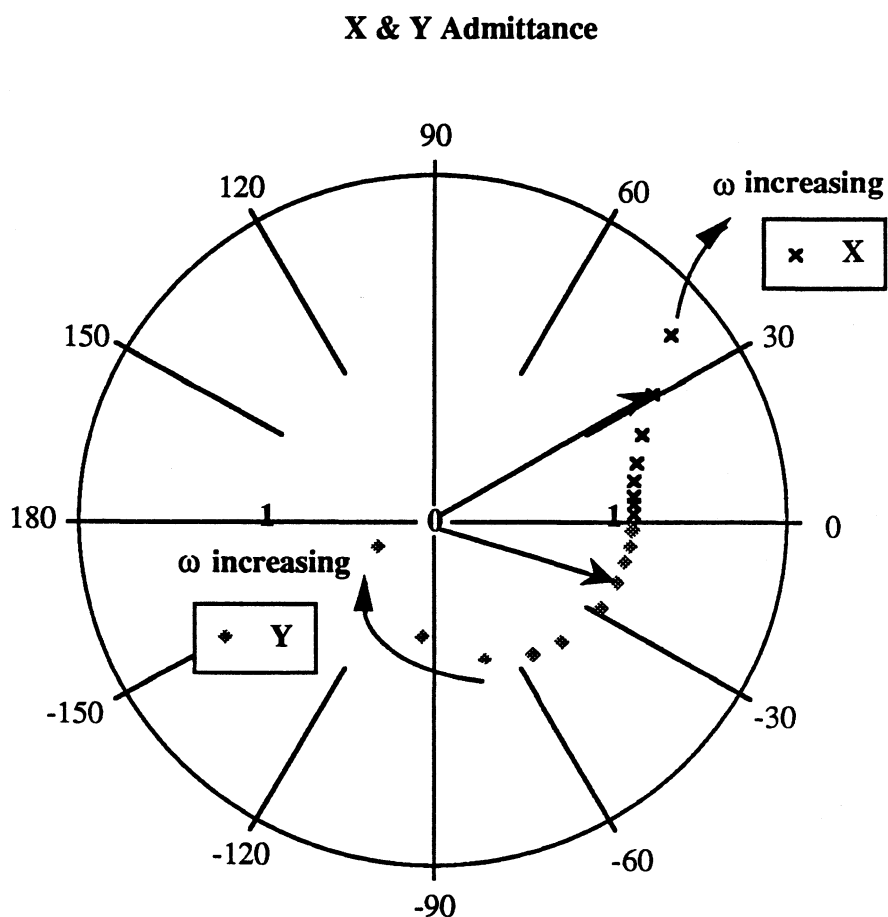


Figure 4.8 Z Admittance

The relationship between X and Y admittances can be seen if their values are plotted for various frequencies. Figure 4.9 is a polar plot also known as a Nyquist diagram [4 & 7] in control theory. Each point on the Nyquist diagram is part of a continuous line which defines the admittance over a range of frequencies. Values of the X and Y admittance shown were calculated for a 4-3/4 inch thick concrete slab which is a part of the ILIB floor.



**Figure 4.9 Nyquist Diagram**

Each point defines an admittance value calculated at a certain frequency. The distance from the origin to a point is the magnitude of the admittance. The angle between a line drawn from the origin to a point, and the real (horizontal) axis, is the phase of the admittance. Admittances for the diurnal frequency (24 hour period) are shown by arrows. The diurnal X admittance has a magnitude of 1.4 Btu/hr-ft<sup>2</sup>-F and a phase of + 31 degrees. The diurnal Y admittance has a magnitude of 1.1 Btu/hr-ft<sup>2</sup>-F and a phase of -19 degrees.

When the frequency is zero the X and Y admittance lie on the real axis. As the frequency increases (moves away from the real axis) the magnitude (distance from the origin) of the X admittance increases, while the magnitude of the Y admittance decreases. The decrease in Y admittance as the frequency increases is a characteristic known as thermal damping. Thermal damping is the the ability of the wall to reduce the magnitude of or "dampen" the heat flux response to a sinusoidal temperature. Since the magnitude of admittance is the ratio of heat flux to temperature, a decreasing magnitude will give a decreased heat flux ( $\Delta q$ ) for a given temperature difference ( $\Delta T$ ).

At the real axis, the frequency is zero and the X value is equal to the Y value. This is the expected steady state result since for heat flux at the inside surface

$$q = XT_i - YT_o \quad (4.11)$$

where heat flux is defined positive into the inside surface. Then at zero frequency

$$X = Y = U \quad (4.12)$$

and Equation 4.11 becomes

$$q = U(T_i - T_o) \quad (4.13)$$

Where  $U$  is the overall conductance based on steady state calculations. This demonstrates that thermal admittance is a more general form of the steady state  $U$  value.

#### 4.4 SUPERPOSITION

$X$ ,  $Y$ , and  $Z$  admittances can be applied to building heat transfer problems using the principle of superposition. Superposition allows a complex linear function to be represented by the sum of simpler functions. Consider the wall shown in Figure 4.10. The inside temperature can be represented by the sum of the steady state temperature ( $T_{si}$ ) and a diurnal temperature sine wave ( $T_{di}$ )

$$T_i = T_{si} + T_{di} \quad (4.14)$$

Likewise, the outside temperature is

$$T_o = T_{so} + T_{do} \quad (4.15)$$

By superposition, heat flux at the wall surface can be found from the sum of three separate solutions. The first is the steady state or zero frequency solution

$$q_s = U(T_{si} - T_{so}) \quad (4.16)$$

Next at the inside surface the diurnal heat flux is given by

$$q_{di} = XT_{di} - YT_{do} \quad (4.17)$$

Likewise, the diurnal heat flux at the outside surface is

$$q_{do} = YT_{di} - ZT_{do} \quad (4.18)$$

Since the heat flux is as positive into the inside surface, the total heat flux at the inside surface is then

$$q_i = q_s + q_{di} \quad (4.19)$$

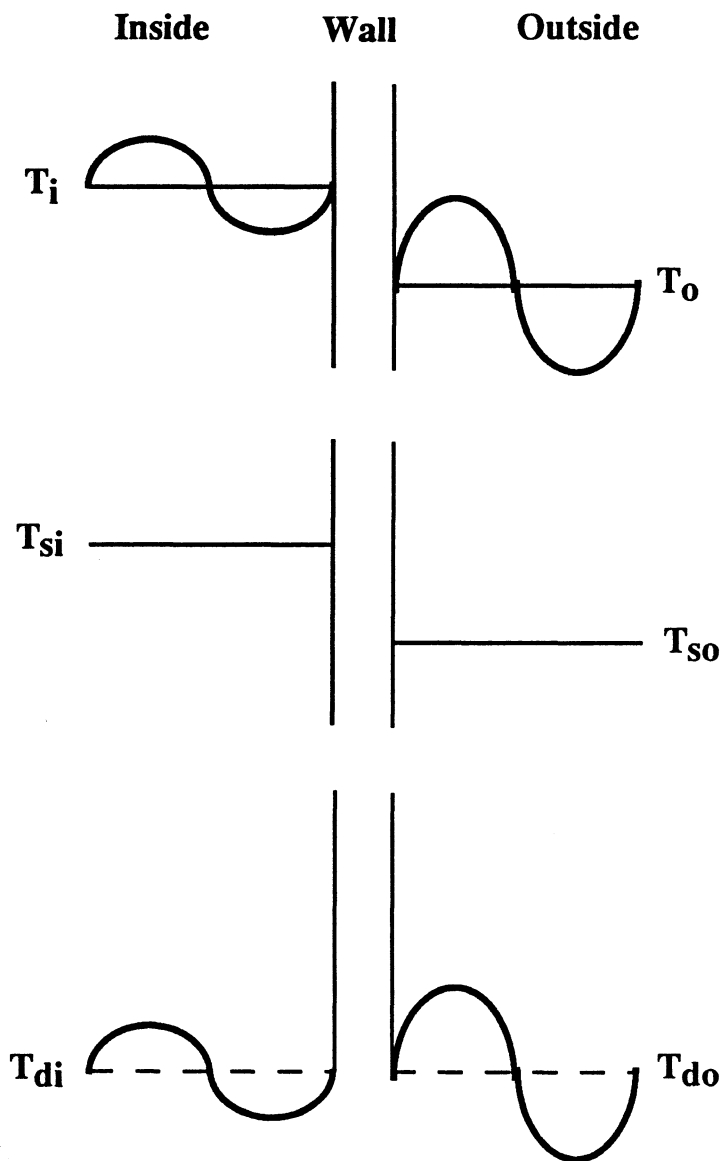


Figure 4.10 Superposition

Heat flux out of the outside surface is also positive so the total heat flux at the outside surface is

$$q_o = q_{do} - q_s \quad (4.20)$$

#### 4.5 ADMITTANCE CALCULATIONS

There is no commonly accepted notation for admittance. The notation used here is a compilation of the symbols used by [6, 7, & 9].

Thermal admittance is derived by solving the heat conduction Equation (4.21) for a wall driven by a sinusoidal surface temperature. A derivation of thermal admittance is given by [6].

$$\frac{\partial^2 T}{\partial x^2} = \frac{\rho c}{k} \frac{\partial T}{\partial t} \quad (4.21)$$

The result is a transfer matrix ( $\mathbf{M}$ ) which relates heat flux and temperature at surface 1 to heat flux and temperature at surface 2.

$$\begin{bmatrix} q_1 \\ T_1 \end{bmatrix} = \mathbf{M} \begin{bmatrix} q_2 \\ T_2 \end{bmatrix} \quad (4.22)$$

where

$$\mathbf{M} = \begin{bmatrix} \cosh(\gamma L) & k\gamma \sinh(\gamma L) \\ \frac{\sinh(\gamma L)}{k\gamma} & \cosh(\gamma L) \end{bmatrix} \quad (4.23)$$

$$\gamma = (1 + i) \sqrt{\frac{\pi \rho c}{Pk}} = \sqrt{2} e^{i\pi/4} \sqrt{\frac{\pi \rho c}{Pk}}$$

$L$  = thickness of the wall

$k$  = thermal conductivity

The X, Y, and Z admittances of the wall in Figure 4.11 are

$$X_1 = \frac{q_1}{T_1} \quad (4.24)$$

$$Y = \frac{q_1}{T_2} = \frac{q_2}{T_1} \quad (4.25)$$

$$Z_2 = \frac{q_2}{T_2} \quad (4.26)$$

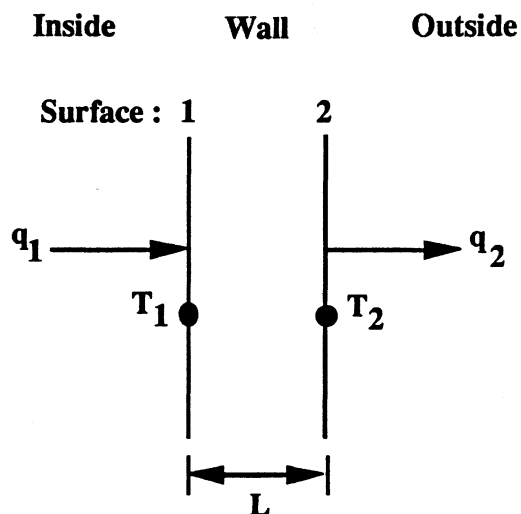


Figure 4.11 Surface 1&amp;2

Rearranging (4.22) and solving for  $X_1$  (4.24) gives

$$X_1 = \frac{q_2/T_2 + a g \tanh(\gamma L)}{1 + \frac{q_2/T_2 \tanh(\gamma L)}{a g}} \quad (4.27)$$

Where

$$a = \sqrt{\frac{2\pi\rho ck}{P}} \quad (4.28)$$

$$g = \frac{1}{\sqrt{2}}(1 + i) = e^{i\pi/4} \quad (4.29)$$

Likewise  $Z_2$  (4.26) is

$$Z_2 = \frac{q_1/T_1 + a g \tanh(\gamma L)}{1 + \frac{q_1/T_1 \tanh(\gamma L)}{a g}} \quad (4.30)$$

The  $X$  and  $Z$  admittance equations are identical for a single homogeneous layer.

### 4.5.1 Boundary Conditions

Each equation for thermal admittance has two unknowns - temperature ( $T$ ) and heat flux ( $q$ ). To solve the thermal equations either one of two boundary conditions are needed; a zero temperature boundary ( $T = 0$ ), or an adiabatic boundary ( $q = 0$ ).

**Zero Temperature** A zero temperature boundary does not actually mean that the boundary surface temperature is zero. Using the superposition principle, a periodic boundary temperature ( $T_b$ ) can be expressed as the sum of the average outside temperature ( $T_{sb}$ ) and the sinusoid ( $T_{db}$ ). The sinusoid has a mean value of zero so the boundary can be given as the sum of the zero temperature boundary ( $T_{zb}$ ), the average outside temperature ( $T_{sb}$ ), and the sinusoid ( $T_{db}$ )

$$T_b = T_{zb} + T_{sb} + T_{db} \quad (4.31)$$

where

$$T_{zb} = 0 \quad (4.32)$$

Setting  $T_2$  in Equation (4.22) equal to zero and solving for  $X_1$  (4.24) gives

$$X_1 = \frac{a g}{\tanh(\gamma L)} \quad (4.33)$$

Let the elements of the transfer matrix ( $M$ ) be denoted by  $m$  so that

$$M = \begin{bmatrix} m_{11} & m_{12} \\ m_{21} & m_{22} \end{bmatrix} \quad (4.34)$$

Then solving for  $Y$  (4.23) with  $T_2$  in Equation (4.22) equal to zero gives

$$Y = \frac{q_2}{T_1} = \frac{1}{m_{21}} \quad (4.35)$$

**Adiabatic Boundary** An adiabatic boundary is a good approximation when one side of the wall is well-insulated. An adiabatic boundary is also used for symmetric interior walls. A symmetric interior wall subject to the same ambient temperature on both sides will have no heat flux across the wall center-line [10]. This occurs because the temperature profile in the wall is also symmetric. At the center-line of the wall the slope of the temperature profile ( $dT/dx$ ) will be zero. Since conduction in a wall is equal to  $-k dT/dx$ , the heat flux at the center-line is zero.

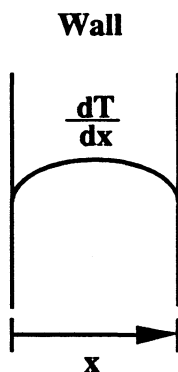


Figure 4.12 Symmetric Wall

Setting  $q_2$  in Equation (4.27) equal to zero and solving for  $X$  gives

$$X_1 = a g \tanh(\gamma L) \quad (4.36)$$

Since  $q_2$  is zero the  $Y$  admittance is zero.

$$Y = \frac{q_2}{T_1} = 0 \quad (4.37)$$

**Thickness** The parameter ( $\tau$ ) describes the non-dimensional thermal thickness of a wall. Thermal thickness ( $\tau$ ) is the ratio of wall storage capacity ( $\rho c L \omega$ ) to wall conductance ( $k/L$ ).

$$\tau = L \sqrt{\frac{\pi \rho c}{Pk}} = \sqrt{\frac{\rho c L \omega}{2k/L}} \quad (4.38)$$

where  $\tau$  is related to other wall parameters by

$$\gamma L = (1+i) \tau = \sqrt{2} g \tau \quad (4.39)$$

$$k \gamma = a g = \sqrt{2} k \tau g \quad (4.40)$$

For a wall with an adiabatic boundary, Equation (4.36) can be expressed as

$$X = a g \tanh(\gamma L) = a g \tanh(\sqrt{2} g \tau) \quad (4.41)$$

Dividing by (a) gives a non dimensional admittance (S)

$$S = \frac{X}{a} = g \tanh(\sqrt{2} g \tau) \quad (4.42)$$

Figure 4.13 shows the effect of thickness on the wall. The magnitude of the

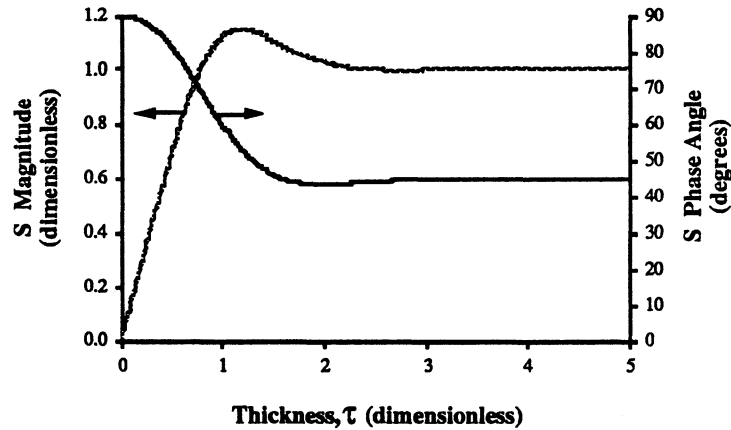


Figure 4.13 Admittance vs. Thickness

admittance increases to a maximum and then decreases slightly as the thickness of the wall increases. The wall thickness at the maximum admittance is given by [9]

$$L = 1.18 \sqrt{\frac{P k}{\pi \rho c}} \quad (4.43)$$

#### 4.5.2 Lumped Capacitance

The assumption of lumped capacitance is valid if the temperature of the wall ( $T_w$ ) is uniform. In transient heat transfer problems the Biot number is used to test this assumption. This assumption will also be true if the the temperature of the wall is uniform and close to the ambient temperature ( $T_\infty$ ). For periodic heat transfer, the product of the Biot and Fourier number can be used to check the validity of a lumped capacitance approximation.

Let

$$T_\infty = T_w = \frac{\Delta T}{2} \sin(\omega t) \quad (4.44)$$

Then

$$\frac{dT_w}{dt} = \frac{\omega \Delta T}{2} \cos(\omega t) \quad (4.45)$$

An energy balance at both (2) wall surfaces results in

$$h 2 A (T_\infty - T_w) = \rho c V \frac{dT_w}{dt} \quad (4.46)$$

Substituting (4.45) into (4.46) and rearranging yields

$$T_\infty - T_w = \frac{\rho c L \omega}{2 h} \frac{\Delta T}{2} \cos(\omega t) \quad (4.47)$$

where

$V$  = the volume of the wall

$A$  = the surface area on one side of the wall

$L$  = the thickness of the wall =  $\frac{V}{A}$

The assumption that

$$T_w \cong T_\infty \quad (4.48)$$

will hold if the right hand side of Equation (4.47) is nearly zero. This will be true if

$$\frac{\rho c L \omega}{2 h} \cong 0 \quad (4.49)$$

This term is equal to the inverse product of the Biot number and Fourier number

$$\frac{1}{Bi Fo} = \frac{k}{h L} \frac{\rho c L^2 \omega}{2 k} = \frac{\rho c L \omega}{2 h} \quad (4.50)$$

The Bi Fo number is the ratio of wall storage capacity to surface convective heat flux. Walls that have low storage capacity (light weight, thin walls) are often reasonably approximated as a lumped capacitance. Large values of the Bi Fo number indicate that lumped capacitance is a good approximation [11].

The admittance of a lumped capacitance is

$$X = \frac{q_w}{T_w} \quad (4.51)$$

From (4.45) and (4.46)

$$q_w = \rho c L \omega \frac{\Delta T}{2} \cos(\omega t) = \rho c L \omega \frac{\Delta T}{2} \sin(\omega t + \pi/2) \quad (4.52)$$

and from (4.44) and (4.48)

$$T_w = \frac{\Delta T}{2} \sin(\omega t) \quad (4.53)$$

Substituting 4.52 and 4.53 into 4.51 gives

$$\begin{aligned} X &= \frac{\rho c L \omega \sin(\omega t + \pi/2)}{\sin(\omega t)} = \rho c L \omega \frac{e^{i(\omega t + \pi/2)}}{e^{i\omega t}} \\ &= \rho c L \omega e^{i\pi/2} \end{aligned} \quad (4.54)$$

The result (4.54) indicates that the heat flux leads the temperature by  $\pi/2$  radians or 90 degrees. This is analogous to an electric capacitor where current leads voltage by 90 degrees. This result can also be seen in Figure 4.13. For thin walls ( $\tau \rightarrow 0$ ) the phase approaches 90 degrees. As the phase approaches 90 degrees the wall behaves more like a lumped capacitance.

## 4.6 ADMITTANCE OF LAYERED WALLS

The equations for thermal admittance can be applied to layered walls. To demonstrate this procedure, admittance values will be calculated for the interior walls of the Independent Life Insurance Building (ILIB). Since the ILIB has a glass curtain wall, the thermal mass of the exterior will be neglected.

### 4.6.1 Resistive Layer

To calculate admittances based on room temperature, the surface of the wall must be coupled to the room air. The room air adds a layer of resistance ( $R_1$ ), where  $R_1$  is the

combined surface convective and radiative resistance found in ASHRAE [12] tables.

Consider the two layer wall in Figure 4.14, the equations for the resistive layer are:

$$q_1 = q_2 = \frac{(T_1 - T_2)}{R_1} \quad (4.55)$$

$$T_1 = q_2 R_1 + T_2 \quad (4.56)$$

In matrix form

$$\begin{bmatrix} q_1 \\ T_1 \end{bmatrix} = M_1 \begin{bmatrix} q_2 \\ T_2 \end{bmatrix} \quad (4.57)$$

where

$$M_1 = \begin{bmatrix} 1 & 0 \\ R_1 & 1 \end{bmatrix} \quad (4.58)$$

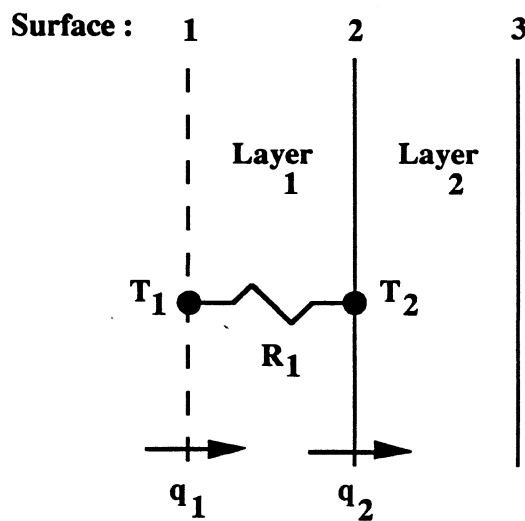


Figure 4.14 Resistive Layer

**Wall + Resistance** These equations can also be applied to a layer that has negligible thermal capacity such as an airspace inside a wall or a layer of insulation. Since the admittance of a purely resistive layer has no imaginary component its phase angle will be zero. Calculation of  $X$  admittance for a wall with a resistive layer is given in Equation (4.32). Note that the inverse of admittance is impedance. The inverse of Equation (4.59) is equivalent to the addition of resistance and impedance in electric circuits.

$$X_1 = \frac{1}{R_1 + \frac{1}{X_2}} \quad (4.59)$$

where

$X_1$  = admittance of layer 1

$X_2$  = admittance of layer 2

$\frac{1}{X_1}$  = impedance of layer 1

$\frac{1}{X_2}$  = impedance of layer 2

**Boundary Conditions** The matrix equation for a resistive layer with a zero temperature ( $T_2 = 0$ ) boundary is

$$\begin{bmatrix} q_1 \\ T_1 \end{bmatrix} = \begin{bmatrix} 1 & 0 \\ R_1 & 1 \end{bmatrix} \begin{bmatrix} q_2 \\ 0 \end{bmatrix} \quad (4.60)$$

Solving for admittance ( $X_1$ ) produces

$$X_1 = \frac{q_1}{T_1} = \frac{1}{R_1} \quad (4.61)$$

For an adiabatic boundary ( $q_2 = 0$ ), the admittance of a resistive layer is

$$\begin{bmatrix} q_1 \\ T_1 \end{bmatrix} = \begin{bmatrix} 1 & 0 \\ R_1 & 1 \end{bmatrix} \begin{bmatrix} 0 \\ T_2 \end{bmatrix} \quad (4.62)$$

and the admittance ( $X_1$ ) becomes

$$X_1 = \frac{q_1}{T_1} = \frac{0}{T_1} = 0 \quad (4.63)$$

#### 4.6.2 X AND Z ADMITTANCE

Thermal admittance equations for a single layer can be applied sequentially to calculate the admittance of walls with multiple layers. To demonstrate this procedure the admittance of the floor on the 9th story of the ILIB will be calculated. Admittance values are calculated for the diurnal frequency ( $P = 24$  hours). A diagram of the floor is shown in Figure 4.15.

The carpet and fireproofing are assumed to have no thermal capacitance. The resistance of the carpet ( $R_C$ ) and inside surface ( $R_i$ ) can be combined into an inside resistance ( $R_1$ ). The resistance of the fireproofing ( $R_{fp}$ ) and outside surface ( $R_o$ ) can also be combined into an outside resistance ( $R_3$ ).

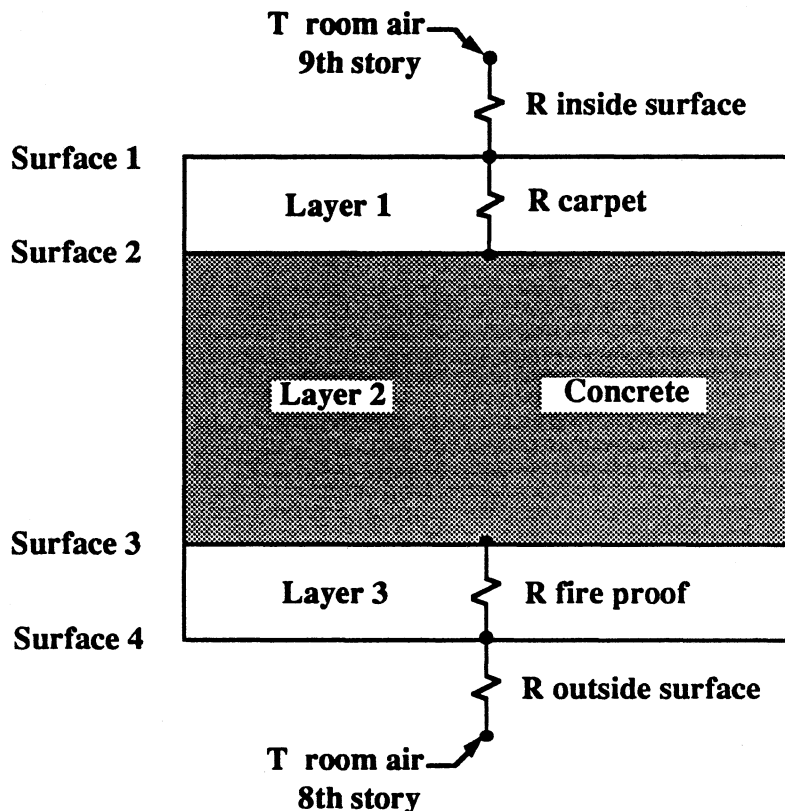


Figure 4.15 9th Floor Admittance

$$R_1 = R_c + R_i = 0.77 + 0.77 = 1.54 \left[ \frac{\text{hr ft}^2 \text{ F}}{\text{Btu}} \right] \quad (4.64)$$

$$R_3 = R_{fp} + R_o = 2.50 + 0.77 = 3.27 \left[ \frac{\text{hr ft}^2 \text{ F}}{\text{Btu}} \right] \quad (4.65)$$

Values for the resistance of the carpet are taken from table 3.4. Resistances for the fireproofing, inside surface, and outside surface are given in Section 3.2. The properties of the concrete layer are derived in Section 3.2. The values for the concrete are

$$L = 4.75 \text{ inches} = 0.396 \text{ ft} \quad (4.66)$$

$$\rho = 110 \quad \left[ \frac{\text{lb}}{\text{ft}^3} \right] \quad (4.67)$$

$$c = 0.22 \quad \left[ \frac{\text{Btu}}{\text{lb F}} \right] \quad (4.68)$$

$$k = 0.45 \quad \left[ \frac{\text{Btu}}{\text{hr ft F}} \right] \quad (4.69)$$

$$R_2 = \frac{L}{k} = 1.14 \quad \left[ \frac{\text{hr ft}^2 \text{ F}}{\text{Btu}} \right] \quad (4.70)$$

The overall resistance of the floor is then

$$R = R_1 + R_2 + R_3 = 5.95 \quad \left[ \frac{\text{hr ft}^2 \text{ F}}{\text{Btu}} \right] \quad (4.71)$$

and

$$U = \frac{1}{R} = 0.17 \quad \left[ \frac{\text{Btu}}{\text{hr ft}^2 \text{ F}} \right] \quad (4.72)$$

**X Admittance** The X admittance is calculated starting at the outside surface. Using the result given in Equation (4.62) for a zero temperature boundary with a resistive layer, the admittance at surface 3 is

$$X_3 = \frac{q_3}{T_3} = \frac{1}{R_3} \quad (4.73)$$

Proceeding to the concrete layer Equation (4.9) gives the admittance at surface 2

$$X_2 = \frac{q_3/T_3 + a g \tanh(\gamma L)}{1 + q_3/T_3 \frac{\tanh(\gamma L)}{a g}} = \frac{X_3 + a g \tanh(\gamma L)}{1 + X_3 \frac{\tanh(\gamma L)}{a g}} \quad (4.74)$$

The admittance at the inside surface and the final result for X is given by Equation (4.59) for a resistive layer

$$X_1 = \frac{1}{R_1 + \frac{1}{X_2}} \quad (4.75)$$

**Z Admittance** The Z admittance is calculated in the same manner starting from the inside surface. Using the result given in Equation (4.62) for a zero temperature boundary with a resistive layer, the admittance at surface 2 is

$$Z_2 = \frac{q_2}{T_2} = \frac{1}{R_1} \quad (4.76)$$

Proceeding to the next layer Equation (4.10) gives the admittance at surface 3

$$Z_3 = \frac{q_2/T_2 + a g \tanh(\gamma L)}{1 + q_2/T_2 \frac{\tanh(\gamma L)}{a g}} = \frac{Z_2 + a g \tanh(\gamma L)}{1 + Z_2 \frac{\tanh(\gamma L)}{a g}} \quad (4.77)$$

The admittance at the outside surface and the final result for Z is given by Equation (4.59) for a resistive layer

$$Z_4 = \frac{1}{R_3 + \frac{1}{Z_3}} \quad (4.78)$$

Numerical results for the X and Z calculations are given in Table 4.3. The resulting X and Z values for the wall are

$$X = 0.522 \left[ \frac{\text{Btu}}{\text{hr ft}^2 \text{ F}} \right] \angle 14.0^\circ \quad (4.79)$$

$$Z = 0.273 \left[ \frac{\text{Btu}}{\text{hr ft}^2 \text{ F}} \right] \angle 7.5^\circ \quad (4.80)$$

Values of  $\tanh(\gamma L)$  can be tabulated for values of  $\tau$  [9]. Calculations for X and Z may be computed with a hand calculator capable of handling vectors.

Layer	X Admittance		Z Admittance		a	$\tau$	R
	Mag	Phase	Mag	Phase			
1	0.522	$\angle 14.0$	0.649	$\angle 0.0$			1.54
2	1.776	$\angle 55.5$	1.679	$\angle 53.4$	1.69	1.05	
3	0.306	$\angle 0.0$	0.273	$\angle 7.5$			3.27

Table 4.3 X and Z Admittance Values

#### 4.6.3 Y ADMITTANCE

Calculation of the Y admittance involves the multiplication of the transfer matrices. Each layer is represented by its transfer matrix so that

$$\begin{bmatrix} q_1 \\ T_1 \end{bmatrix} = M \begin{bmatrix} q_4 \\ T_4 \end{bmatrix} \quad (4.81)$$

where

$$M = M_1 M_2 M_3 \quad (4.82)$$

Starting from the inside, the transfer matrix for layer 1 is given by Equation (4.58):

$$M_1 = \begin{bmatrix} 1 & 0 \\ R_1 & 1 \end{bmatrix} \quad (4.83)$$

Equation (4.3) for the the concrete (layer 2) gives

$$M = \begin{bmatrix} \cosh(\gamma L) & k\gamma \sinh(\gamma L) \\ \frac{\sinh(\gamma L)}{k\gamma} & \cosh(\gamma L) \end{bmatrix} \quad (4.84)$$

The transfer matrix for Layer 3 has the same form as the first layer

$$M_3 = \begin{bmatrix} 1 & 0 \\ R_3 & 1 \end{bmatrix} \quad (4.85)$$

The result is given by Equation (4.14)

$$Y = \frac{q_2}{T_1} = \frac{1}{m_{21}} = 0.057 \frac{\text{Btu}}{\text{hr ft}^2 \text{ F}} \angle -90.0^\circ \quad (4.86)$$

The small magnitude of Y is a result of the high resistance to heat flux across the floor.

Matrix multiplication is more difficult to perform by hand than the X and Z calculations. To assist with these calculations a FORTRAN program for calculating X, Y and Z admittance is given in the Appendix

#### 4.6.4 Symmetric Interior Wall

Admittance calculations are easier when the interior wall is symmetric. Figure 4.16 illustrates a symmetric interior wall in the ILIB. The center of the wall is adiabatic since the wall is symmetric and is exposed to the same temperature on both sides.

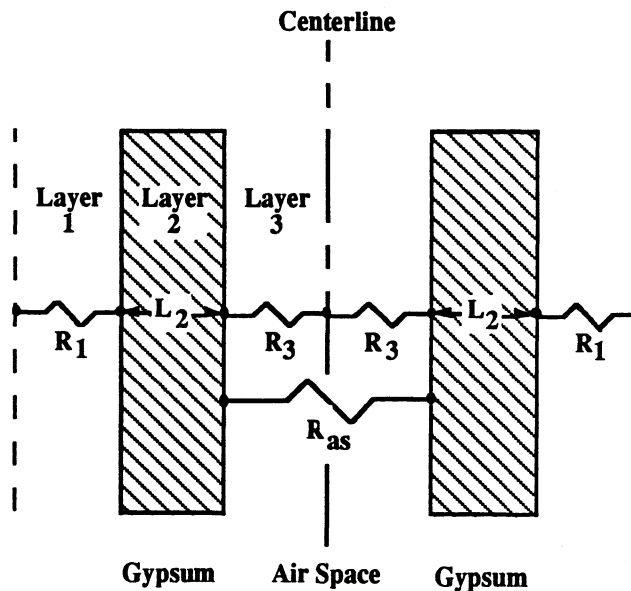


Figure 4.16 Symmetric Internal Wall

The Y admittance is zero since no heat is transferred across the center of the wall (Equation 4.16). The resistance of the airspace ( $R_{as}$ ) and the surface resistance ( $R_1$ ) are found in ASHRAE [12] tables.

$$R_1 = 0.68 \left[ \frac{\text{hr ft}^2 \text{ F}}{\text{Btu}} \right] \quad (4.87)$$

$$R_{as} = 1.01 \left[ \frac{\text{hr ft}^2 \text{ F}}{\text{Btu}} \right] \quad (4.88)$$

$$R_3 = \frac{R_{as}}{2} = 0.505 \left[ \frac{\text{hr ft}^2 \text{ F}}{\text{Btu}} \right] \quad (4.89)$$

Material properties for the gypsum are also found in ASHRAE [12] tables

$$\rho = 50 \left[ \frac{\text{lb}}{\text{ft}^3} \right] \quad (4.90)$$

$$c = 0.26 \left[ \frac{\text{Btu}}{\text{lb F}} \right] \quad (4.91)$$

$$k = 0.09 \left[ \frac{\text{Btu}}{\text{hr ft F}} \right] \quad (4.50)$$

Beginning at the center of the wall the X admittance for an air layer with an adiabatic boundary is given by Equation (4.37)

$$X_3 = \frac{q_3}{T_3} = \frac{0}{T_3} = 0 \quad (4.51)$$

Proceeding to the gypsum layer the admittance at surface 2 is given by Equation (4.27)

$$X_2 = \frac{q_3/T_3 + a g \tanh(\gamma L)}{1 + q_3/T_3 \frac{\tanh(\gamma L)}{a g}} = \frac{X_3 + a g \tanh(\gamma L)}{1 + X_3 \frac{\tanh(\gamma L)}{a g}} = a g \tanh(\gamma L) \quad (4.52)$$

where

$$L = 1/2 \text{ inch} = 0.042 \text{ feet}$$

Finally the admittance at surface 1 of the resistive layer is given by Equation (4.59)

$$X_1 = \frac{1}{R_1 + \frac{1}{X_2}} \quad (4.53)$$

The total admittance for both surfaces of the interior wall is twice the admittance for one surface

$$X_w = 2 X_1 \quad (4.54)$$

Numerical values for the X admittance calculation are given in Table (4.4). The resulting X admittance value is

$$X_w = 0.282 \left[ \frac{\text{Btu}}{\text{hr ft}^2 \text{ F}} \right] \angle 83.3^\circ \quad (4.55)$$

Layer	X Admittance		a	$\tau$	R
	Mag	Phase			
1	0.141	$\angle 83.3$			0.680
2	0.142	$\angle 88.8$	0.561	0.179	
3	0.0	$\angle 0.0$			0.505

**Table 4.4 X Admittance Values**

Table 4.5 lists the and calculated admittances for the 9th story of the ILIB. The paper and furniture are assumed to be lumped capacitances. Material properties of the components are listed in the Appendix.

Component	X (Btu/hr-ft <sup>2</sup> -F)	Y (Btu/hr-ft <sup>2</sup> -F)	Z (Btu/hr-ft <sup>2</sup> -F)
Floor	0.522 $\angle$ 14.0°	0.057 $\angle$ -90.0°	0.273 $\angle$ 7.5°
Ceiling	0.276 $\angle$ 7.6°	0.058 $\angle$ -90.0°	0.530 $\angle$ 14.2°
Walls	0.282 $\angle$ 83.3°		
Partitions	0.212 $\angle$ 85.2°		
Core Concrete	0.383 $\angle$ 10.6°	0.114 $\angle$ -86.9°	0.870 $\angle$ 23.3°
Steel Supports	0.414 $\angle$ 47.1°		
Steel Risers	0.458 $\angle$ 9.1°		
Metal Furniture	0.080 $\angle$ 90°		
Paper	0.405 $\angle$ 90°		

Table 4.5 ILIB Admittance Values

#### 4.7 CALCULATED ADMITTANCE VS MEASURED FLOOR HEAT FLUX.

Comparisons were made between calculated admittances and measured values of the floor heat flux. For a given sinusoidal temperature the heat flux can be predicted from admittance calculations. These comparisons will show how the heat flux can be approximated using only the diurnal and zero frequencies.

### 4.7.1 Discrete Fourier Transform

A discrete Fourier transform (DFT) was applied to the 9th floor temperature and heat flux data from the second experiment. The DFT transforms discrete experimental values in the time domain to the frequency domain. From the transform significant frequencies in the data can be identified. The DFT was performed using a IMSL [13] subroutine. The FORTRAN program which calls the IMSL subroutine is listed in the Appendix.

Figure 4.17 lists the results of the DFT in plots of magnitude versus frequency. Values are shown for the measured 9th floor heat flux ( $q_f$ ), 8th story temperature ( $T_8$ ), and 9th story temperature ( $T_9$ ). In each plot the magnitude at the diurnal frequency (24 hour period) is prominent. The contribution of other frequencies to the Fourier series is negligible since their magnitude is small compared to the diurnal and zero frequency terms. The values of the steady state and diurnal components from the DFT are

$$q_f = -0.558 + 2.05 \angle 94.6^\circ \left[ \frac{\text{Btu}}{\text{hr ft}^2} \right] \quad (4.56)$$

$$T_8 = T_{8s} + T_{8d} = 71.7 + 1.86 \angle 47.2^\circ \text{ [F]} \quad (4.57)$$

$$T_9 = T_{9s} + T_{9d} = 67.8 + 3.40 \angle 74.8^\circ \text{ [F]} \quad (4.58)$$

$q_f$  is the heat flux measured by the computer monitoring station.  $T_8$  is the average of the north and south zone temperatures on the 8th story.  $T_9$  is the air temperature measured by the computer monitoring station.

### 4.7.2 Heat Flux

The use of only two prominent frequencies (diurnal and steady state) simplifies the admittance calculations significantly. If more frequencies were added the admittance calculations would become cumbersome to perform by hand. The merit of admittance calculations is their ability to describe the main effects with a few fundamental

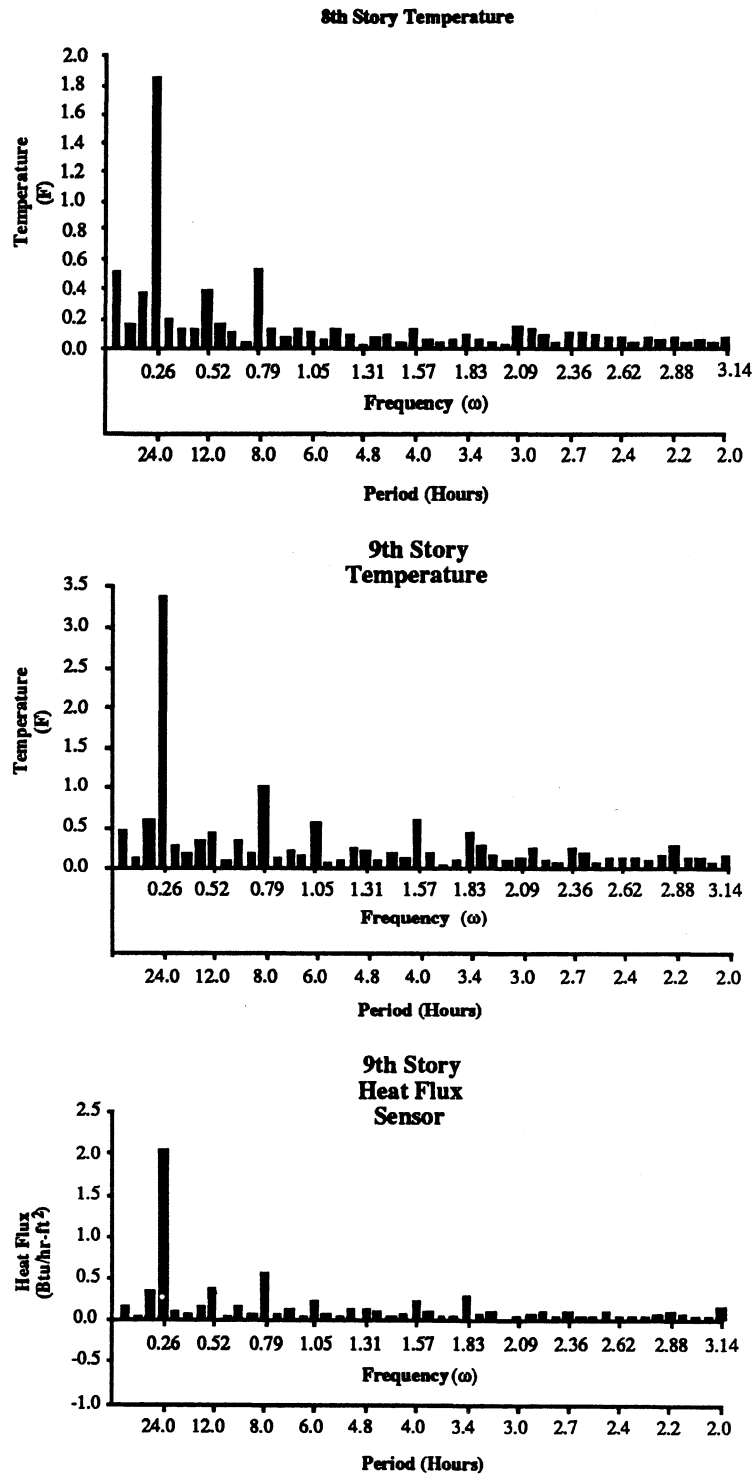


Figure 4.17 DFT Temperature and Heat Flux

frequencies. In this example heat flux will be calculated from admittance calculations and compared to the DFT values (4.56) above. The admittance equation for the 9th floor heat flux is

$$\begin{aligned}
 q_f &= U(T_9 - T_8) + XT_9 - YT_8 \\
 &= 0.17[67.8 - 71.7] \\
 &+ [0.522 \angle 14.0^\circ][3.40 \angle 74.8^\circ] - [0.057 \angle -90.0^\circ][1.86 \angle 47.2^\circ] \\
 &= -0.663 + [1.78 \angle 88.8^\circ] - [0.11 \angle -42.8^\circ] \\
 &= -0.663 + [1.85 \angle 91.3^\circ]
 \end{aligned} \tag{4.59}$$

Figure 4.18 shows that the calculated heat flux is close to the Fourier transform of the measured heat flux.

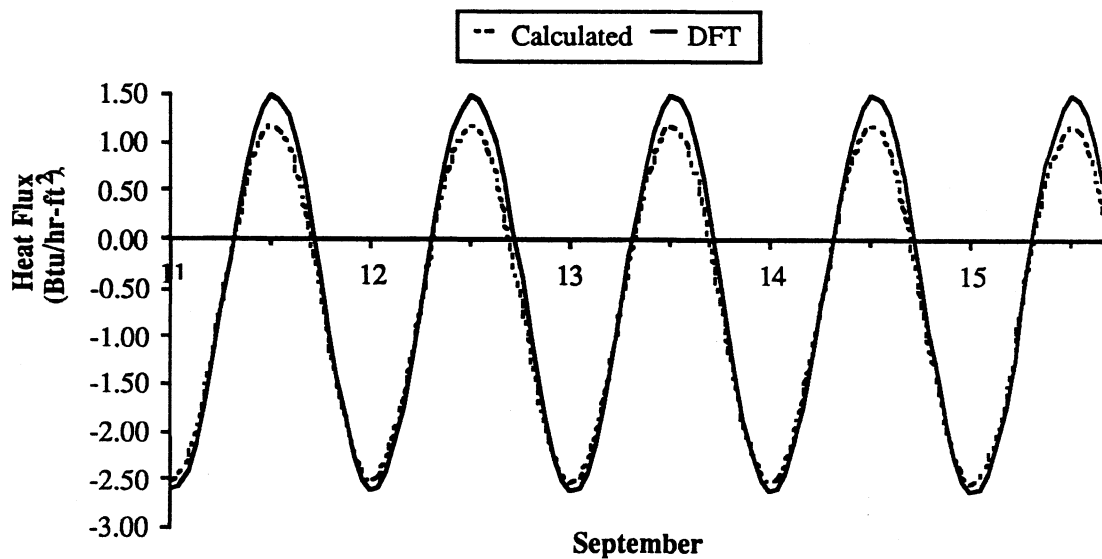


Figure 4.18 Calculated Heat Flux vs. the DFT of the Heat Flux

Figure 4.17 displays the next largest component of the fourier transform at a period of 8 hours. Equation (4.59) can be expanded to include the frequency with an 8 hour period. The heat flux is then calculated from the admittance equation including the 8 hour period

$$\begin{aligned}
 q_f &= U(T_9 - T_8) + [XT_9 - YT_8]_{P=8} + [XT_9 - YT_8]_{P=24} \\
 &= 0.17[67.8 - 71.7] \\
 &+ [0.559 \angle 7.3^\circ][1.0 \angle -136.4^\circ] - [0.017 \angle -137.5^\circ][0.529 \angle -171.6^\circ] \\
 &+ [0.522 \angle 14.0^\circ][3.40 \angle 74.8^\circ] - [0.057 \angle -90.0^\circ][1.86 \angle 47.2^\circ] \\
 &= -0.663 + [0.57 \angle -129.1^\circ]_{P=8} + [1.85 \angle 91.3^\circ]_{P=24} \quad (4.60)
 \end{aligned}$$

Figure 4.19 compares the sum the steady state, 24 hour, and 8 hour components of the

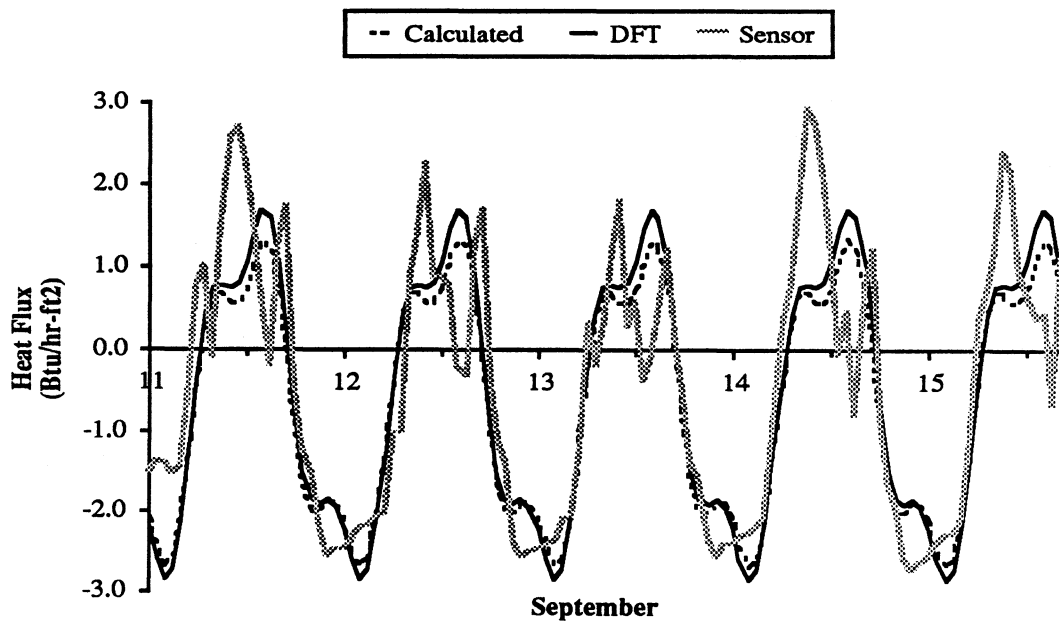


Figure 4.19 Calculated Heat Flux vs. the DFT of the Heat Flux

DFT to the calculated heat flux (4.60), and measured heat flux (Section 3.2.1). Additional frequencies make the calculated values closer to the measured values but also add to the complexity of the calculations.

#### 4.8 DIURNAL HEAT CAPACITY

The diurnal heat capacity [9] of a wall is the amount of thermal energy stored ( $\Delta Q$ ) over half of a 24 hour cycle. Diurnal heat capacity (dhc) is the amount of energy stored and then released over a 24 hour cycle per unit temperature difference ( $\Delta T$ ). The amount of energy stored, due to heat flux into the thermal mass, will reduce the amount of energy required for cooling.

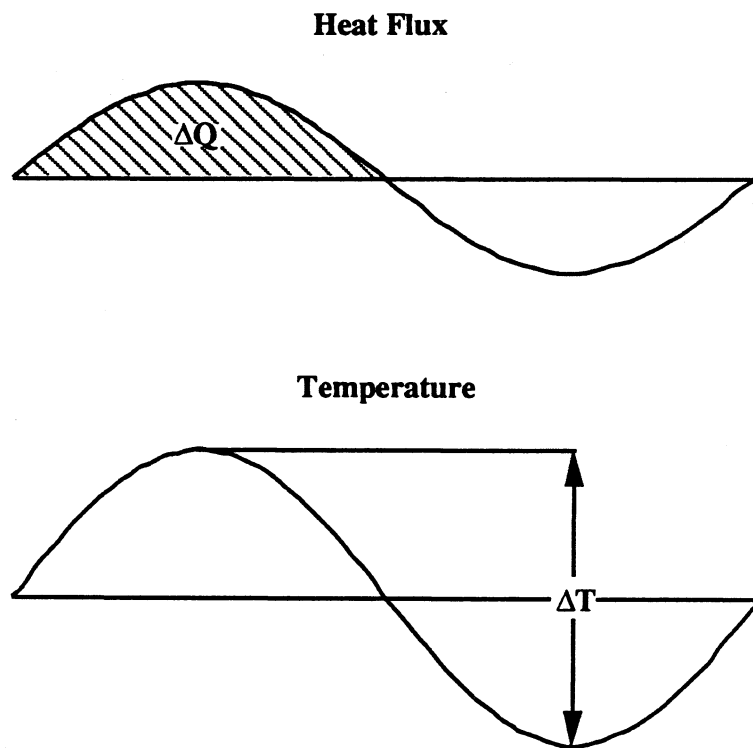


Figure 4.20 Diurnal Heat Capacity

Diurnal heat capacity is derived by integrating the heat flux ( $q$ ) over a half cycle.

Consider an interior wall exposed to a sinusoidal temperature ( $T$ ) on both sides

$$q = (X - Y)T \quad (4.61)$$

where

$$T(t) = \frac{\Delta T}{2} \sin(\omega t) \quad (4.62)$$

Then the thermal energy stored ( $\Delta Q$ ) is

$$\begin{aligned} \Delta Q &= \int_0^{12} q dt = \int_0^{12} (X - Y)T dt = (X - Y) \frac{\Delta T}{2} \int_0^{12} \sin(\omega t) dt \\ &= (X - Y) \frac{\Delta T}{2\omega} \int_0^{12} \sin(\omega t) \omega dt = (X - Y) \frac{\Delta T}{2\omega} [\cos(\omega t)]_0^{12} \\ &= (X - Y) \frac{\Delta T}{2\omega} [2] = (X - Y) \frac{\Delta T}{\omega} \end{aligned} \quad (4.63)$$

And the diurnal heat capacity of wall  $n$  ( $dhc_n$ ) is

$$dhc_n = \frac{\Delta Q}{\Delta T} = \frac{(X - Y)}{\omega} = \frac{24}{2\pi} (X - Y) = 3.82 (X - Y) \quad (4.64)$$

The  $dhc$  is the diurnal admittance divided by the diurnal frequency. The diurnal heat capacity (DHC) of a building or zone is

$$DHC = \sum_{n=1}^N A_n dhc_n \quad (4.65)$$

where

$N$  = total number of walls

$A_n$  = area of wall surface  $n$

$dhc_n$  = diurnal heat capacity of wall  $n$

The method for calculating DHC values is similar to the way UA values are calculated for a building. Table 4.6 lists the  $dhc$  and DHC for the 9th story of the ILIB.

Component	$dhc_n$ (Btu/ft <sup>2</sup> -F)	$DHC_n$ (Btu/F)
Floor	2.06 $\angle$ 19.9 <sup>o</sup>	29,870 $\angle$ 19.9 <sup>o</sup>
Ceiling	1.09 $\angle$ 18.9 <sup>o</sup>	15,805 $\angle$ 18.9 <sup>o</sup>
Walls	1.08 $\angle$ 83.3 <sup>o</sup>	5,380 $\angle$ 83.3 <sup>o</sup>
Partitions	0.81 $\angle$ 85.2 <sup>o</sup>	8,098 $\angle$ 85.2 <sup>o</sup>
Core Concrete	1.58 $\angle$ 26.4 <sup>o</sup>	356 $\angle$ 26.4 <sup>o</sup>
Steel Supports	1.58 $\angle$ 47.7 <sup>o</sup>	751 $\angle$ 47.7 <sup>o</sup>
Steel Risers	1.75 $\angle$ 9.1 <sup>o</sup>	194 $\angle$ 9.1 <sup>o</sup>
Metal Furniture	0.31 $\angle$ 90 <sup>o</sup>	3,646 $\angle$ 90 <sup>o</sup>
Paper	1.55 $\angle$ 90 <sup>o</sup>	15,731 $\angle$ 90 <sup>o</sup>
<b>Total</b>		<b>66,641 <math>\angle</math> 47.1<sup>o</sup></b>

**Table 4.6 Diurnal Heat Capacity**

Figure 4.21 shows the percent DHC for each component. The total value of DHC in Table 4.6 is the amount of energy that can be stored and then released over a 24 hour period per unit temperature difference ( $\Delta T$ ). Heat flux into the thermal mass will

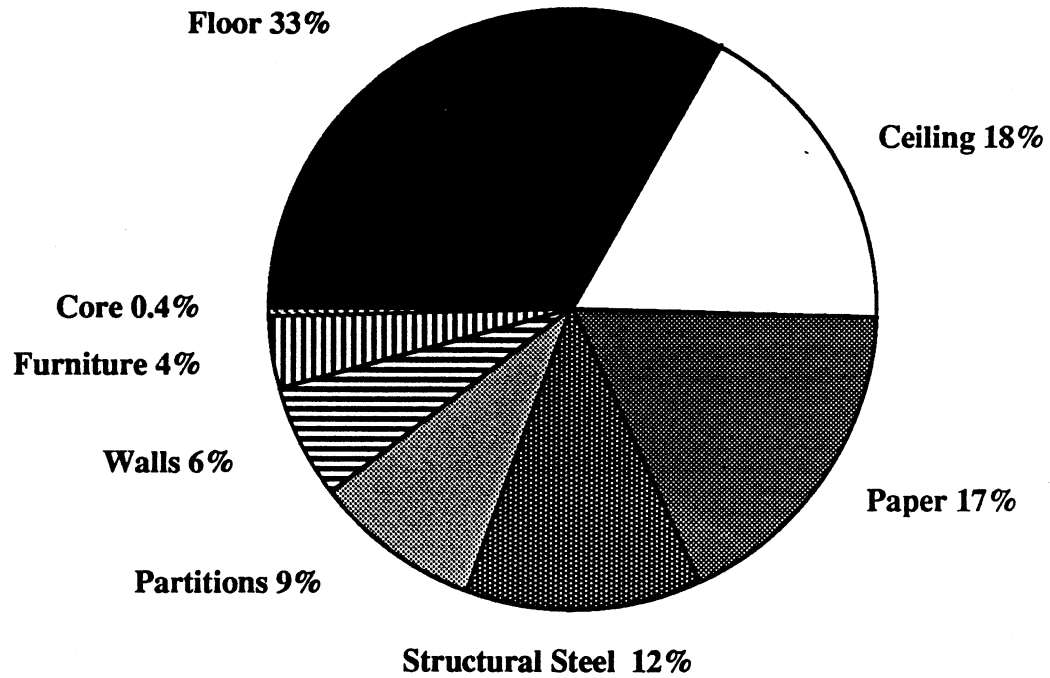


Figure 4.21 Diurnal Heat Capacity

increase the energy stored in the thermal mass and decrease the cooling load. The amount of thermal storage is

$$\Delta Q = \Delta T \text{ DHC} \quad (4.66)$$

The total measured reduction in cooling load ( $\Delta E$ ) is the amount of energy supplied to the 15th story ( $E_{15}$ ) less the amount of energy ( $E_9$ ) supplied to the 9th story ( $E_9$ ) during the daytime where

$$E_9 - E_{15} > 0 \quad (4.67)$$

An energy balance on a building story gives

$$E = Q_{cplg} + Q_{surf} + Q_{conv} + Q_{inf} + Q_{sens} \quad (4.68)$$

where

$Q_{cplg}$  = gains due to coupling with adjacent stories

$Q_{surf}$  = convective gains from surfaces

$Q_{conv}$  = internal convective gains

$Q_{inf}$  = gains from infiltration

$Q_{sens}$  = net sensible gain

During the daytime occupied period both the 9th story and 15th story are controlled to maintain a temperature of approximately 73 degrees.  $Q_{cplg}$ ,  $Q_{conv}$ ,  $Q_{inf}$ , and  $Q_{sens}$  are assumed to be approximately the same during the day for the 9th and 15th stories. Since the 9th story was cooled at night (pre-cooling) while the 15th story was not, the total reduction in cooling load ( $\Delta E$ ) should equal the amount of energy removed from the thermal mass.

$$\Delta E = \int (E_{15} - E_9)^+ = \Delta Q \quad (4.69)$$

Table 4.7 compares the calculated thermal storage capacity ( $\Delta Q$ ) to the measured reduction in cooling ( $\Delta E$ ) from the second experiment. The thermal storage is calculated using the total DHC value in Table 4.5.  $\Delta T$  is the difference between the maximum and minimum zone temperature on the 9th story for each day.

$$\Delta T = [T_{9max} - T_{9min}]_{24 \text{ hours}} \quad (4.70)$$

The average values of  $\Delta E$  and  $\Delta Q$  are within 4%. Daily values of  $\Delta E$  and  $\Delta Q$  vary somewhat more than their average values. Some variation may be attributable to interactions between stories and systematic differences between the 9th and 15th story. Comparisons of daily values may have been improved if the peak to peak temperature difference was more periodic (less variation from one day to the next). Still, the DHC method provides a good prediction of the average reduction in cooling for the week.

	$\Delta T$ (F)	$\Delta Q$ (Btu)	$\Delta E$ (Btu)
Monday	13.7	912,981	1,020,956
Tuesday	13.6	906,317	502,250
Wednesday	7.4	493,143	442,850
Thursday	7.4	493,143	665,371
Friday	8.6	573,113	882,572
Average	10.14	675,739	702,800

**Table 4.8 Temperature Difference and Thermal Storage**

DHC calculations were not compared to the first experiment since the opening of the perimeter supply air dampers allowed an additional amount of unmeasured cooling onto the 9th story. This unmeasured cooling makes the value of  $\Delta E$  from the first experiment unreliable.

#### 4.9 EFFECTIVENESS

Total heat capacity (thc) is the amount of thermal energy stored or released for a uniform change in temperature of the material.

$$\text{thc} = \rho c L \quad (4.71)$$

The thc is the maximum capacity of a material for thermal storage. A material with a high Biot number (thick walls) subject to a change in surface temperature [14] will not have a uniform temperature and its capacity for thermal storage will be reduced. It is

useful to introduce a thermal effectiveness parameter ( $\eta$ ) which relates the diurnal heat capacity to the maximum thermal capacity.

$$\eta_n = \frac{dhc_n}{thc_n} \quad (4.72)$$

Also

$$\eta = \frac{DHC}{THC} \quad (4.73)$$

where

$$THC = \sum_{n=1}^N A_n thc_n \quad (4.74)$$

$N$  = total number of surfaces

$A_n$  = area of surface  $n$

$thc_n$  = total heat capacity of surface  $n$

If the material is modeled as a lumped capacitance then the  $thc$  is equal to the  $dhc$

$$dhc = \frac{\rho c L \omega}{\omega} = \rho c L = thc \quad (4.75)$$

and

$$\eta = \frac{dhc}{thc} = 100\% \quad (4.76)$$

The effectiveness of components in the 9 story of the ILIB are given in Table 4.9. Note that the partition wall has an effectiveness of nearly 100% and its phase angle is almost 90 degrees. This means that the partition wall could be modeled as a lumped capacitance.

Components such as the concrete block and structural steel are isolated from the room air reducing their effectiveness for thermal storage. The steel is encased in fire proofing above a suspended ceiling and behind gypsum walls. The concrete block in the core of the building is located behind gypsum walls.

Component	THC (Btu/F)	DHC (Btu/F)	Effectiveness DHC/THC
Floor	137,504	29,870	21.7%
Ceiling	137,504	15,805	11.5%
Walls	5,417	5,380	99.3%
Partitions	8,125	8,098	99.7%
Core Concrete	2,475	356	14.4%
Steel Supports	12,180	751	6.1%
Steel Risers	14,716	194	1.3%
Metal Furniture	3,646	3,646	100.0%
Paper	15,731	15,731	100.0%
Total	337,298	66,641	19.8%

**Table 4.9 Thermal Effectiveness**

The effectiveness of the floor is low due to a high resistance between the concrete surface and the room air. If the diurnal heat capacity of the floor is recalculated without the carpet resistance then

$$dhc = 3.33 \angle 28.9^{\circ} \quad (4.77)$$

$$DHC = 48,285 \angle 28.9^{\circ} \quad (4.78)$$

$$\eta = 35.1\% \quad (4.79)$$

Removing the carpet increased the effectiveness of the floor by 13 percent. This example demonstrates that diurnal heat capacity is sensitive to changes in surface resistance [11].

#### **4.10 CHAPTER SUMMARY**

Admittance and diurnal heat capacity calculations are similar in form to the familiar U value calculations. The U value is equivalent to the steady state (zero frequency) admittance value.

Admittance and diurnal heat capacity methods provide an instructive and intuitive way to assess the contribution of each building component to the buildings thermal mass. These methods can be used to predict the reduction in cooling load due to thermal energy storage in a building. Comparisons with the experiments show good agreement between calculated and measured values of heat flux and energy storage.

---

## REFERENCES 4

---

1. Shurcliff, W. A., *Frequency Method of Analyzing a Building's Dynamic Thermal Performance*, 19 Appleton Street, Cambridge, Massachusetts, 1985.
2. Palmiter, L., and J. Hanford, "An Introduction to Frequency Methods For Building Thermal Analysis," Conference Proceedings, 11th National Passive Solar Conference, American Solar Energy Society, 1986.
3. *Energy Calculations and Data*, The Masonry Energy Information Series, Concrete Masonry Association of California and Nevada, Citrus Heights, California, 1986.
4. Ogata, K., *Modern Control Engineering*, Prentice-Hall, Inc., 1970.
5. Chapara, C. C., *Numerical Methods for Engineers*, Second Edition, McGraw-Hill, New York, 1988.
6. Davies, M. G., "The Thermal Admittance of Layered Walls," *Building Science*, Volume 8, pp. 207-220, Pergamon Press, 1973.
7. Subbarao, K., and J. V. Anderson, "A Graphical Method for Passive Building Energy Analysis," *ASME Transactions*, Volume 105, May 1983.
8. Duffie, J. A., and W. A. Beckman, *Solar Engineering of Thermal Processes*, John Wiley & Sons, New York, 1980.
9. Balcomb, J. D., *Heat Storage and Distribution Inside Passive Solar Buildings*, Report LA-9694-MS, Los Alamos National Laboratory, 1983.
10. Myers, G. E., *Analytical Methods in Conduction Heat Transfer*, Genium Publishing Corp., 1987.
11. Akbari, H., Samano, D., Mertol, A., Bauman, F., and R. Kammerud "The Effect of Variations in Convection Coefficients on Thermal Energy Storage in Buildings, Part I - Interior Partition Walls," *Energy and Buildings*, Volume 9, pp. 195-211, Lawrence Berkeley Laboratory, 1986.
12. *ASHRAE Handbook, Fundamentals Volume*, American Society of Heating, Refrigerating, and Air Conditioning Engineers, Atlanta, Georgia, 1989.
13. *IMSL Math Library*, FORTRAN Subroutines for Mathematical Applications, Version 1.0, IMSL, Houston, Texas, 1987.
14. Incropera, F. P., and D. P. DeWitt, *Introduction to Heat Transfer*, John Wiley & Sons, New York, 1985.

## *CHAPTER 5*

---

# **VENTILATION COOLING**

---

Ventilation cooling is the use of cool outdoor air to supplement or replace conventional vapor compression refrigeration. In commercial buildings, internal gains may cause a need for cooling even though outdoor air temperatures are relatively cool. Ventilation cooling could provide a way to pre-cool the building at a lower cost than by mechanical refrigeration. Savings will occur if the cost to operate a ventilation fan is less than the cost of conventional refrigeration to provide the same amount of cooling.

The economizer cycle and pre-cooling are two types of ventilation cooling commonly referred to in the literature. The economizer cycle [1] uses cool outdoor air during occupied day-time periods to assist or replace conventional refrigeration. A controller compares either outdoor air temperature or enthalpy to a set value. When the outdoor air temperature or enthalpy is below the set value the outdoor air damper is opened allowing more outdoor air into the building. Pre-cooling is the use of cool outdoor air to pre-cool a building during unoccupied night-time or weekend periods. Pre-cooling reduces the temperature of the thermal mass in the building. This cool thermal mass then reduces the amount of cooling required during the day-time.

### **5.1 SIMULATION**

Simulations in TRNSYS [2] were performed to investigate the potential for using outdoor air to cool the ILIB. TRNSYS contains a library of modules which model HVAC components. The flexible nature of TRNSYS allows these modules to be arranged or modified to simulate an HVAC system. Modules are linked together in a "simulation deck". The TRNSYS simulation deck is listed in the Appendix.

The TRNSYS Type 56 multi-zone model was used to compute cooling loads for a typical ILIB zone. TYPE 56 uses the transfer function method to compute heat transfer through building components. Cooling loads were calculated using energy rate control. Under energy rate control auxiliary cooling loads are equal to the net gains from the building zone. Cooling loads from the building zone were used to make the analysis independent of HVAC equipment selection.

To represent the ILIB a single story was modeled. One story of a multi-story building is sufficient if there is no net heat transfer between stories, and each story has similar construction, use, and internal loads. The load of a typical story can then be extrapolated to all stories. Since each story of a commercial office building is approximately the same, a typical story can be used to represent the building. Figure 5.1 is a schematic of the building zone model.

A separate module was written to provide either temperature or enthalpy control. TRNSYS allows new modules written in FORTRAN to be added to the simulation model. The controller compares either outdoor temperature or enthalpy to a set value. The controller then turns the ventilation on if the outdoor value is below the set value. The controller module is listed in the Appendix.

Since weather data for Jacksonville were not available, Typical Meteorological Year (TMY) [3] weather data for Miami were used in the simulations. The combination of warm temperatures and high humidity make this climate less desirable for ventilation cooling. Nevertheless, during the winter, cooler outdoor temperatures could provide some potential for ventilation cooling. Figure 5.2 shows the number of hours below a given temperature during a month in Miami. For example, in January there are 386 hours where the outside temperature is below 70°F.

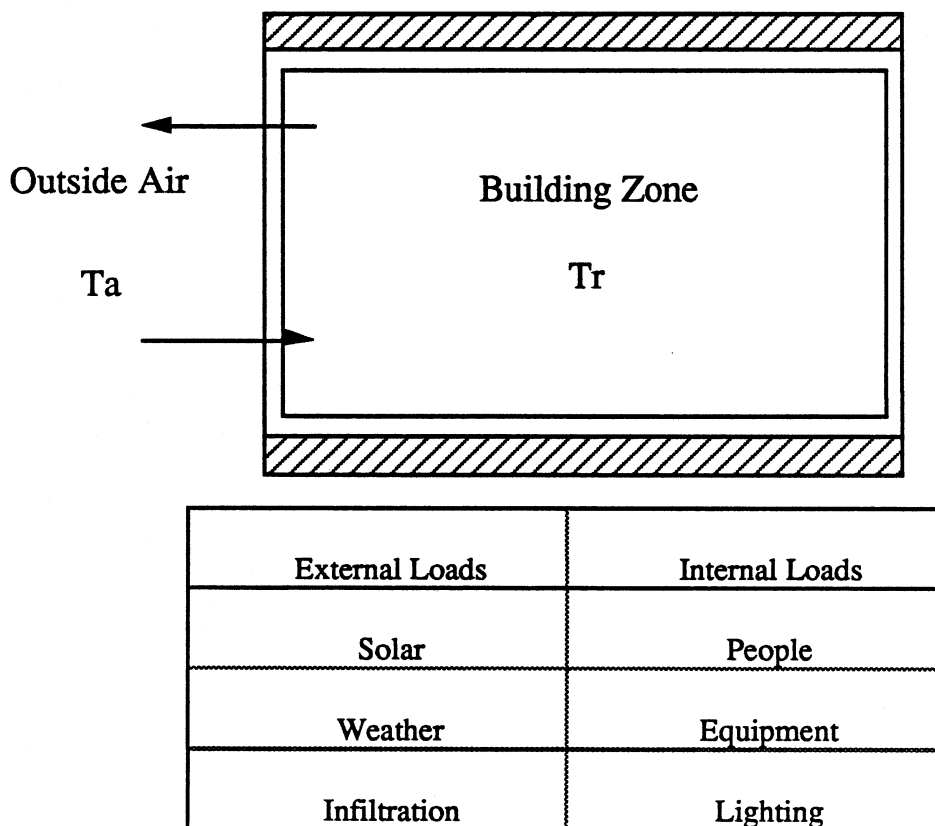


**Figure 5.1 Building Zone Model**

## 5.2 BUILDING DESCRIPTION

Several schedules were set up to simulate internal loads. These schedules are listed in Table 5.1. The TRNSYS building input description (BID) is listed in the appendix. The zone air temperature was controlled to maintain a temperature of  $\leq 72^{\circ}\text{F}$  and 50% relative humidity during the day-time occupied period (Monday to Friday 6am to 6pm). This corresponds to an enthalpy of 26.4 Btu/lb and is within the comfort region defined by ASHRAE [4]. During the weekend and night-time unoccupied periods the zone temperature and humidity are allowed to "float".

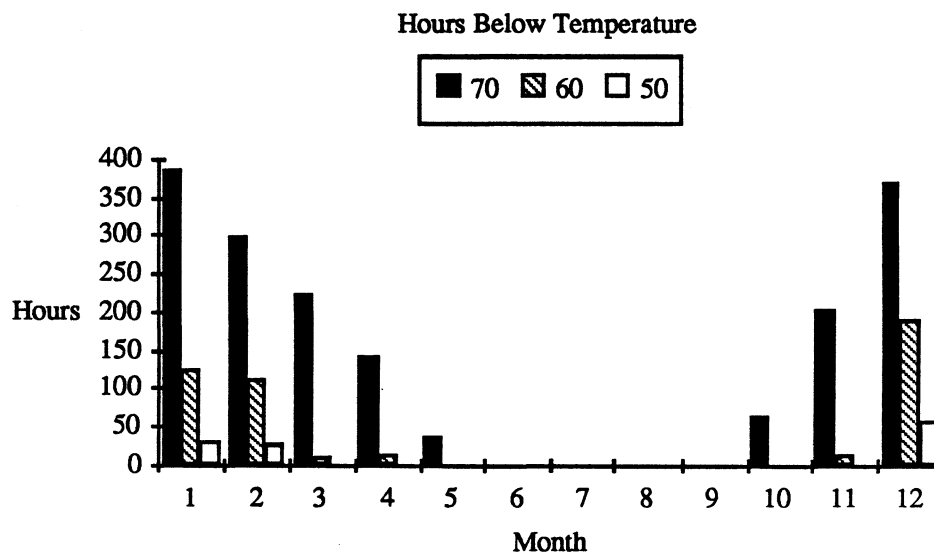


**Figure 5.2 Hours Below Temperature**

The TYPE 56 zone model uses an effective air mass multiplier [2] to simulate moisture capacitance. This multiplier was set to a value of 1 which includes the moisture of the room air only. Simulations with higher values of the multiplier increased latent loads but did not change the overall results.

The ventilation controller set points were 70°F for temperature control and 26 Btu/lb for enthalpy control. The ventilation controller can also be scheduled so that ventilation would occur during a set time period. Ventilation flow rates varied from of 3 to 5 air changes per hour during the experiments. The ventilation flow rate was set to 4 air changes per hour in the simulations. The infiltration flow rate was set to 0.5 air changes per hour.

	Total Load	Week		Weekend	
		Time	% Load	Time	%Load
Occupancy	13,260 (Btu/hr)	7am - 5pm	100%	7am - 5pm	10%
Lighting	22,080 (Watts)	6am - 9pm	100%	7am - 5pm	20%
Equipment	10,762 (Watts)	7am - 5pm	100%		60%

**Table 5.1 Internal Loads & Schedules**

### 5.3 SIMULATION RESULTS

Simulations were performed with and without ventilation cooling. Simulations with ventilation cooling allowed outdoor ventilation to occur any time the outdoor air temperature or enthalpy was below a set value. This allowed ventilation to occur during both day-time occupied periods, and night-time unoccupied periods. During the day-time the ventilation cooling could overlap with the auxiliary cooling.

Simulations with ventilation cooling were compared to simulations with no ventilation cooling (base cooling load). Figure 5.3 compares the total sensible and latent loads for ventilation cooling under temperature and enthalpy control to the base sensible and latent loads. The results show cooling load reductions during the winter season.

The percent reduction in cooling load is

$$\text{Cooling Reduction (\%)} = \frac{\text{Base Cooling Load} - \text{Ventilation Cooling Load}}{\text{Base Cooling Load}} * 100\% \quad (5.1)$$

The percent cooling reduction under temperature control was 4.75% . The percent cooling reduction under enthalpy control was 4.90% .

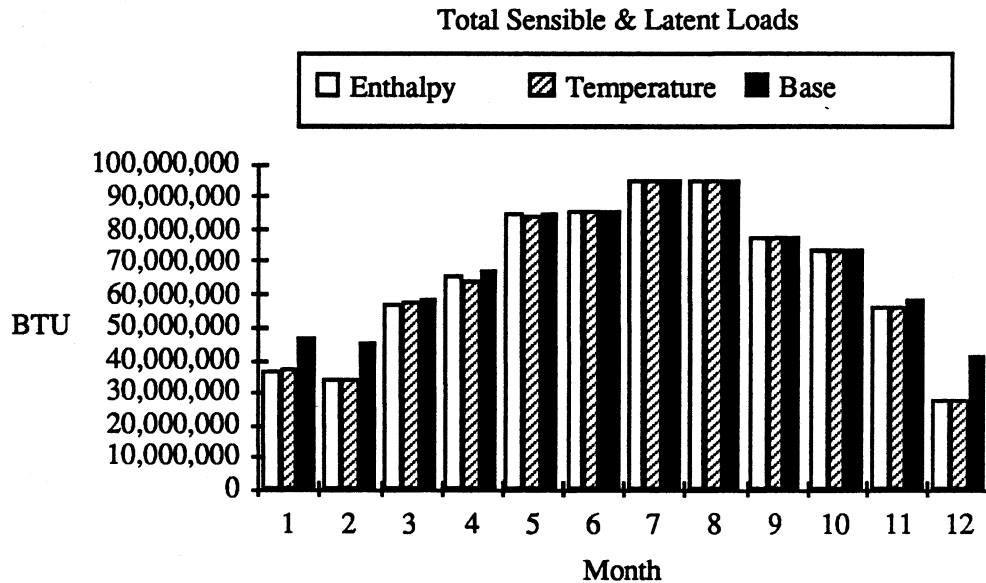


**Figure 5.3 Total Sensible and Latent Loads**

Figure 5.4 shows the latent component of the cooling load. Under enthalpy control the latent load is less than the latent load under temperature control. This illustrates how ventilation under temperature control may increase latent cooling loads. However, temperature control is less difficult to instrument and maintain than enthalpy control.

To simulate pre-cooling, a time schedule was added to allow ventilation cooling from 7pm to 5am. The addition of a schedule eliminates any ventilation during the occupied period, and the ventilation cooling does not overlap with the auxiliary cooling. With a scheduled pre-cooling period, the cooling load reduction under temperature control was 1.27%. Reduction in cooling load under enthalpy control was 0.77%. Scheduling decreased the net reduction in cooling load under both temperature and enthalpy control.

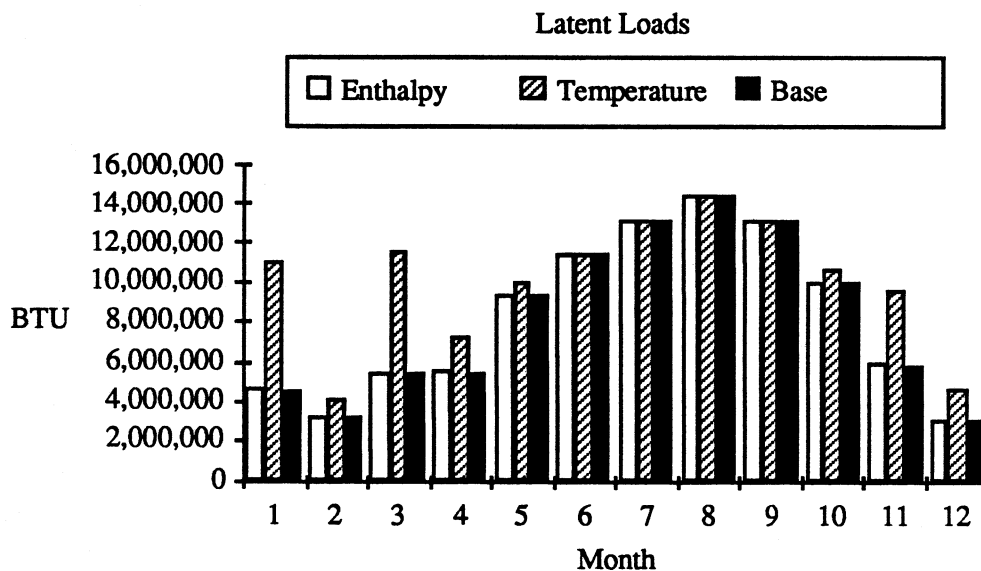


**Figure 5.4 Latent Loads**

To compare the different ventilation cooling strategies, two additional ratios (cooling effectiveness, and electrical effectiveness) will be defined. Cooling effectiveness is the cooling load reduction divided by the ventilation cooling input

$$\text{Cooling Effectiveness} = \frac{\text{Base Cooling Load} - \text{Ventilation Cooling Load}}{\text{Ventilation Cooling Input}} \quad (5.2)$$

where

$$\text{Ventilation Cooling Input} = \dot{m} c_p (T_r - T_a) \quad (5.3)$$

$\dot{m}$  = mass flow-rate of air

$c_p$  = specific heat of air

$T_r$  = room air temperature

$T_a$  = outside air temperature

This ratio compares the total amount of ventilation cooling delivered to the building to the resulting reduction in the auxiliary cooling load.

Electrical effectiveness is the reduction in the electrical energy required for cooling divided by the electrical energy required for the ventilation fan. The reduction in the electrical energy required for cooling is

Auxiliary Cooling Reduction (KWH)

$$= \frac{(\text{Base Cooling Load} - \text{Ventilation Cooling Load})}{\text{COP} * 3413} \quad (5.4)$$

where the average coefficient of performance (COP) is assumed to be 3.0. The electrical power required to drive the fan is approximated [6] by

$$\text{Fan Input (KWH)} = \frac{\text{Air Change Rate} * \text{Volume} * \text{Total Pressure} * \text{Fan Hours}}{\text{Fan Efficiency} * 511370} \quad (5.5)$$

where

$$\begin{aligned} \text{Air Change Rate} &= 4.0 \text{ (air changes/hour)} \\ \text{Volume} &= 119,000 \text{ Ft}^3 \text{ (building volume)} \\ \text{Total Pressure} &= 2 \text{ inches of water ("Wg.)} \\ \text{Fan Efficiency} &= 60\% \text{ (combined fan \& motor efficiency)} \\ \text{Fan Hours} &= \text{total number of ventilation hours} \end{aligned}$$

The electrical effectiveness ratio is then

$$\text{Electrical Effectiveness} = \frac{\text{Auxillary Cooling Reduction (KWH)}}{\text{Fan Input (KWH)}} \quad (5.6)$$

This ratio relates the reduction in the electrical energy required for cooling, to the increase in electrical energy required to operate the ventilation fan. For electrical rates that do not vary by time of day, this is the ratio of savings to costs. Table 5.2 shows the calculated percent cooling reduction, cooling effectiveness, and electrical effectiveness for each simulation.

Annual Cooling Load Reduction (%)		
Control	No Schedule	Scheduled
Temperature	4.75%	1.27%
Enthalpy	4.90%	0.77%

Cooling Effectiveness		
Control	No Schedule	Scheduled
Temperature	0.40	0.52
Enthalpy	0.62	0.52

Electrical Effectiveness		
Control	No Schedule	Scheduled
Temperature	0.72	0.38
Enthalpy	1.36	0.47

**Table 5.2 Simulation Summary**

The simulations without a ventilation schedule yielded the greatest reduction in annual cooling loads. Enthalpy control appears to be more effective than temperature control according to the higher values of cooling and electrical effectiveness.

#### **5.4 SUMMARY**

Some potential for ventilation cooling of the ILIB exists even in the warm humid climate of Miami. Results from the simulations show reductions in cooling load due to ventilation cooling. Enthalpy control was shown to be a more effective strategy than temperature control for ventilation cooling.

---

## REFERENCES 5

---

1. Mitchell, J. W., *Energy Engineering*, John Wiley & Sons, New York, 1983.
2. Klein, S. A., et al., *TRNSYS: A Transient Simulation Program*, University of Wisconsin-Madison, Engineering Experiment Station Report 38-12, Version 12.2, 1988.
3. *SOLMET Manual*, US National Climatic Center, Asheville, N.C., Vols. 1 and 2, 1978.
4. *ASHRAE Handbook, Fundamentals Volume*, American Society of Heating, Refrigerating, and Air Conditioning Engineers, Atlanta, Georgia, 1989.
5. *Typical Meteorological Year Weather Data*, National Oceanic and Atmospheric Administration, Asheville, North Carolina, 1979.
6. *Industrial Ventilation, A Manual of Recommended Practice*, 18th Edition, American Conference of Governmental Industrial Hygienists, Lansing, Michigan, 1984.

## CHAPTER 6

---

# CONCLUSIONS

---

The objective of this research project was to investigate the effect of building thermal mass on cooling loads. The interaction of the HVAC system with the building's thermal mass was studied through the analysis of data from experiments performed at the ILIB. Results from these experiments show the effect of pre-cooling on thermal comfort, heat flux, and energy use. Diurnal heat capacity calculations were shown to give a reasonable estimate of the thermal storage capabilities of the ILIB. Simulations based on the ILIB investigate the use of outdoor air ventilation as a source of pre-cooling.

### 6.1 RESULTS

Experimental data from two experiments at the ILIB show actual measured effects of pre-cooling. Few experimental studies are available that show the effect of pre-cooling on peak cooling loads.

#### Thermal Comfort

Pre-cooling can have a detrimental effect on thermal comfort. Strategies for pre-cooling need to allow a sufficient warm-up period for the building occupants. Warm up time was calculated using an estimated temperature rate

$$\text{Warm Up Time (Hours)} = \frac{(\text{Target Temperature} - \text{Zone Temperature})}{\text{Temperature Rate}} \quad (6.1)$$

The temperature rate appears to have a linear relation to indoor temperature and a quadratic relationship with outdoor temperature.

### Heat Flux

Measurements of heat flux at the floor surface were taken to determine the response of the building thermal mass to pre-cooling. The results show the effect of pre-cooling on the charging and discharging of the thermal mass. From the floor heat flux the carpet resistance and the surface convective resistance could be calculated.

Resistance $\left[\frac{\text{hr-ft}^2\text{-F}}{\text{Btu}}\right]$	First Experiment	Second Experiment
Carpet	1.02	0.77
Surface	1.02	1.59
Total	2.04	2.36

**Table 6.1 Carpet and Surface Resistance**

### Energy Use

The effect of pre-cooling on energy use was measured by taking the difference between energy supplied to the 9th and 15th stories. Reductions in cooling load were shown to occur shortly after the end of the pre-cooling period. The amount of weekend pre-cooling was reduced in the second experiment. Additional pre-cooling over the weekend was shown to be ineffective in reducing cooling loads. The results are shown in Table 6.2.

First Experiment	Week - 5 Days Monday to Friday	Experiment - 7 Days Friday to Friday
9 Energy / 15 Energy	1.36	2.04
Discharge / Charge	42%	19%

Second Experiment	Week - 5 Days Monday to Friday	Experiment - 7 Days Friday to Friday
9 Energy / 15 Energy	1.34	1.61
Discharge / Charge	40%	26%

**Table 6.2 Energy Parameters - First & Second Experiment**

### **Diurnal Heat Capacity**

Diurnal heat capacity calculations provide a way to predict the effective thermal storage capabilities of a building. For a given diurnal temperature difference, the amount of energy that can be stored and released in a building can be predicted. A thermal effectiveness parameter shows how much of the total heat capacity is available for diurnal energy storage. The overall effectiveness for a typical story of the ILIB is 20%.

DHC is a simplified and intuitive method that can evaluate the transient effects of thermal storage. More complex calculations such as finite difference methods and transfer function methods are better suited for computer simulations. Diurnal heat capacity calculations can also be used as a design method to optimize the amount and location of the thermal mass.

### **Ventilation Cooling**

Simulation results indicate that some potential exists for ventilation cooling of the ILIB. Annual cooling load reductions of 4.9% were achieved with enthalpy control. Enthalpy control was shown to be more effective than temperature control in reducing latent loads.

### **Pre-Cooling Guidelines**

Based on the experimental results the following pre-cooling strategy is recommended:

- o Include a warm-up period before the beginning of occupancy. Warm-up time can be calculated from estimates of the temperature rate.
- o Avoid long term (weekend) charging periods. Charging and discharging periods should occur within a 24 hour cycle.
- o During occupancy, keep zone temperatures at the lower limit of the comfort range until the beginning of the peak period.

---

## BIBLIOGRAPHY

---

Akbari, H., Samano, D., Mertol, A., Bauman, F., and R. Kammerud "The Effect of Variations in Convection Coefficients on Thermal Energy Storage in Buildings, Part I - Interior Partition Walls," *Energy and Buildings*, Volume 9, pp. 195-211, Lawrence Berkeley Laboratory, 1986.

Akbari, H., Samano, D., Mertol, A., Bauman, F., and R. Kammerud "The Effect of Variations in Convection Coefficients on Thermal Energy Storage in Buildings, Part II - Exterior Massive Walls and Simulations," *Energy and Buildings*, Volume 10, pp. 29-47, Lawrence Berkeley Laboratory, 1987.

*ASHRAE Handbook, Fundamentals Volume*, American Society of Heating, Refrigerating, and Air Conditioning Engineers, Atlanta, Georgia, 1989.

Athienitis, A. K., "A Predictive Control Algorithm for Massive Buildings," *ASHRAE Transactions*, Volume 94, Part 2, 1988.

Balcomb, J. D., *Heat Storage and Distribution Inside Passive Solar Buildings*, Report LA-9694-MS, Los Alamos National Laboratory, 1983.

Chapara, C. C., *Numerical Methods for Engineers*, Second Edition, McGraw-Hill, New York, 1988.

Childs, K. W., Courville, G. E., and E. L. Bales, "Thermal Mass Assessment; An Explanation of the Mechanisms by Which Building Mass Influences Heating and Cooling Energy Requirements," Oak Ridge National Laboratory, Oak Ridge, Tennessee, September, 1983.

Davies, M. G., "The Thermal Admittance of Layered Walls," *Building Science*, Volume 8, pp. 207-220, Pergamon Press, 1973.

Duffie, J. A., and W. A. Beckman, *Solar Engineering of Thermal Processes*, John Wiley & Sons, New York, 1980.

*Energy Calculations and Data*, The Masonry Energy Information Series, Concrete Masonry Association of California and Nevada, Citrus Heights, California, 1986.

Fanger, P. O., *Thermal Comfort Analysis and Applications in Environmental Engineering*, McGraw-Hill, New York, 1972.

Gurjral, P. S., Clark, R. J. and D. J. Burch, "An Evaluation of Thermal Energy Conservation Schemes for an Experimental Masonry Building," NBS Building Science Series 137, National Bureau of Standards, Department of Commerce, July, 1982.

Hackner, R. J., "HVAC System Dynamics and Energy Use in Existing Buildings," M.S. Thesis, University of Wisconsin-Madison, 1984.

Halabi, O. A. F., "Moisture Storage in Buildings," M.S. Thesis, University of Wisconsin-Madison, 1990.

Holman, J. P., *Experimental Methods for Engineers*, Third Edition, McGraw-Hill, New York, 1978.

*IMSL Math Library*, FORTRAN Subroutines for Mathematical Applications, Version 1.0, IMSL, Houston, Texas, 1987.

Incropera, F. P., and D. P. DeWitt, *Introduction to Heat Transfer*, John Wiley & Sons, New York, 1985.

*Industrial Ventilation, A Manual of Recommended Practice*, 18th Edition, American Conference of Governmental Industrial Hygienists, Lansing, Michigan, 1984.

Kammerud, R., Ceballos, E., Curtis, B., Place, W., and B. Anderson, "Ventilation Cooling of Residential Buildings," *ASHRAE Transactions*, Volume 90, Part 1B, 1984.

Kimura, K., *Scientific Basis of Air Conditioning*, Applied Science Publishers, London, 1977.

Klein, S. A., et al., *TRNSYS: A Transient Simulation Program*, University of Wisconsin-Madison, Engineering Experiment Station Report 38-12, Version 12.2, 1988.

Madsen, J. M., "Modeling Heat Transfer in Rooms using Transfer Function Methods," M.S. Thesis, University of Wisconsin-Madison, 1982.

*Manual of Steel Construction*, Eighth Edition, American Institute of Steel Construction, Chicago, Illinois, 1980.

Mitchell, J. W., and W. A. Beckman, "Theoretical Limits for Storage of Energy in Buildings," *Solar Energy*, Volume 42, Number 2, pp. 113-120, 1989.

Mitchell, J. W., *Energy Engineering*, John Wiley & Sons, New York, 1983.

Muncey, R. W. R., *Heat Transfer Calculations for Buildings*, Applied Science Publishers, London, 1979.

Myers, G. E., *Analytical Methods in Conduction Heat Transfer*, Genium Publishing Corp., 1987.

Myers, G. E., Class Notes for ME 764, Department of Mechanical Engineering, University of Wisconsin-Madison, 1988.

Ogata, K., *Modern Control Engineering*, Prentice-Hall, Inc., 1970.

Palmiter, L., and J. Hanford, "An Introduction to Frequency Methods For Building Thermal Analysis," Conference Proceedings, 11th National Passive Solar Conference, American Solar Energy Society, 1986.

Pawelski, M. J., "Development of Transfer Function Load Models and Their Use in Modeling the CSU Solar House I," M.S. Thesis, University of Wisconsin-Madison, 1976.

Seem, J. E., Armstrong, P. R., and C. E. Hancock, "Algorithms for Predicting Recovery Time from Night Setback," *ASHRAE Transactions*, Volume 96, Part 2, 1989.

Shapiro, M. M., Yager, A. J., and T. H. Ngan, "Test Hut Validation of a Microcomputer Predictive HVAC Control," *ASHRAE Technical Data Bulletin*, Building Operation Dynamics, Volume 4, Number 2, pp. 14-33, 1988.

Shurcliff, W. A., *Frequency Method of Analyzing a Building's Dynamic Thermal Performance*, 19 Appleton Street, Cambridge, Massachusetts, 1985.

Smith, S. J., *Circuits, Devices, and Systems*, Third Edition, John Wiley & Sons, 1976.

*SOLMET Manual*, US National Climatic Center, Ashville, N.C., Vols. 1 and 2, 1978.

Subbarao, K., and J. V. Anderson, "A Graphical Method for Passive Building Energy Analysis," *ASME Transactions*, Volume 105, May 1983.

---

**APPENDIX**

---

<b>A</b>	<b>SENSORS - PRODUCT INFORMATION</b>	<b>112</b>
<b>B</b>	<b>FINITE DIFFERENCE PROGRAM</b>	<b>113</b>
<b>C</b>	<b>ADMITTANCE PROGRAM</b>	<b>119</b>
<b>D</b>	<b>COMPONENT MATERIAL PROPERTIES</b>	<b>127</b>
<b>E</b>	<b>DISCRETE FOURIER TRANSFORM</b>	<b>128</b>
<b>F</b>	<b>TRNSYS SIMULATION DECK</b>	<b>132</b>
<b>G</b>	<b>TRNSYS BUILDING INPUT DESCRIPTION</b>	<b>137</b>

---

**APPENDIX A**


---

**SENSORS - PRODUCT INFORMATION**

ITEM	MODEL	LOCATION
Energy Management & Control System (EMCS)	Barber Colman ECON VI	ILIB Control Room
Velocity Sensor	Staefa FKA-V1	ILIB Supply and Return Air Ducts
Temperature Sensor	Staefa TS-5931	ILIB Supply and Return Air Ducts
Computer Monitoring Station	Apple IIE with Strawberry Tree Analog Connection II	ILIB 9th Story
Heat Flux Sensor	International Thermal Measurement, Model A-1	ILIB 9th Floor
Meter	Solomat MPM 500e with 355 RH and 129MS	Hand Held
Probe	355 RH Temperature and Humidity	Hand Held
Probe	129 MS Velocity, Hot Wire Anemometer	Hand Held
Meter	Fluke Model 21 Multimeter with 00T	Hand Held
Probe	00T-807 1502 Temperature Sensor	Hand Held

---

**APPENDIX B**


---

**FINITE DIFFERENCE PROGRAM**

```
*****
This finite difference program computes boundary heat flux from measured temperatures.
The temperatures are read from a file TEMP.DAT. Boundary resistances are calculated
using the computed heat flux. This program is adapted from a program written by G.E.
Meyers, ME764, 1988.
*****
```

**PROGRAM FDMFLOOR**

- \* Convection at Node 1,
- \* Specified Temperature at Node N

```
COMMON C(50,10),S(50,10),R(50),T(50),Y(50)
COMMON N,IBW,TIME,DTIME,NUMAX
DATA IOUT/11/,NROW/50/,NCOL/10/
OPEN (UNIT=IOUT,FILE='FLROUT',STATUS='NEW')
```

- \* Add Input For Surface Temperature

- \*1 Experiment 1
- \*1 OPEN (UNIT=TIN,FILE='TEMP1.DAT',STATUS='OLD')
- \*2 Experiment 2
- OPEN (UNIT=TIN,FILE='TEMP2.DAT',STATUS='OLD')

```
REWIND TIN
READ (TIN,700)
```

```
CALL INPUT
```

- \* Save Boundary Conductance

```
CONDUCT = S(N,1)
```

- \* Set Tolerance For R & H Value Calculation

```
WRITE(6,*) 'TOLERANCE'
READ(5,*) TOL
```

```
QBOUND = 0.0
```

- \* Set Initial Values

```
RVALUE = 0.0
```

RAVG = 0.0  
 RSUM = 0.0  
 IAVG = 0

HVALUE = 0.0  
 HAVG = 0.0  
 HSUM = 0.0  
 JAVG = 0

DAY = 0.0

\* Set Initial Fluid Temp (TOLD)

TOLD = 70.0

\*1 Experiment 1

\*1 NUSTART = 25

\*1 NUEND = 312

\*2 Experiment 2

\*2 Week&Weekend: 7 Days Sat - Fri

NUSTART = 4

NUEND = 168

\*2 Experiment 2

\*2 Week: Mon 12 to Fri 12

\* NUSTART = 64

\* NUEND = 160

ZERO = 0.0

QPLUS = 0.0

QMINUS = 0.0

WRITE (IOUT,601)

DT2 = DTIME/2.0

\* Multiply R \* T(N) = Boundary Temp

\* Initial R Vector

\* Modify R For Specified Temp

DO 20 I=1,N

R(I) = R(I)\*DTIME\*T(N)

SAVE = C(I,1)

DO 10 J=1,IBW

C(I,J) = S(I,J)\*DT2

S(I,J) = -C(I,J)

10 CONTINUE

C(I,1) = SAVE + C(I,1)

S(I,1) = SAVE + S(I,1)

20 CONTINUE

```
CALL DBAND(NROW,NCOL,N,IBW,C,NOGO)
IF (NOGO.EQ.1) GO TO 99
WRITE (IOUT,602)
WRITE (IOUT,603)
WRITE (IOUT,604) (I, I=1,N)
```

\* Modify R For Convection

$$R(1) = R(1)*TOLD/T(N)$$

\* Specified Temperature at Node N

\* Convection At Node 1

\* Read Floor, Carpet, Room, and Return Air Temperatures

```
DO 40 NU=1,NUMAX
```

```
READ (TIN,701) TSURF, TCARP, TAIR, TRAIR
```

\* Modify R For Specified Surface Temp

```
DO 30 I = 1, N
  R(I) = R(I) * (TSURF / T(N))
30 CONTINUE
```

\* Modify R For Convection

$$R(1) = R(1) * (TRAIR*T(N)) / (TSURF*TOLD)$$

```
CALL YAXPB(NROW,NCOL,N,IBW,S,R,T,Y)
CALL SBAND(NROW,NCOL,N,IBW,C,Y,T)
```

```
T(N) = TSURF
TOLD = TRAIR
```

\* Compute Boundary Heat Flux and R Value

\* Specific Example Q (Btu/Hr-ft<sup>2</sup>), R (Hr-Ft-F/Btu)

\* NUSTART Set To Remove Initial Transient

```
IF (NU .GE. NUSTART .AND. NU .LE. NUEND) THEN
  QBOUND = CONDUCT*(T(N) - T(N-1))
```

\* Data BTU/ft<sup>2</sup>-Dtime

\* Integrate BTU/ft<sup>2</sup>

```
QTOT = QBOUND*DTIME + QTOT
IF (QBOUND .GT. ZERO) THEN
  QPLUS = QBOUND*DTIME + QPLUS
ELSE
  QMINUS = QBOUND*DTIME + QMINUS
```

```

ENDIF

IF (ABS(QBOUND) .GE. TOL) THEN
  IF(ABS(TCARP-TSURF) .GE. TOL) THEN
    RCarp = ABS( (TCARP - TSURF)/QBOUND )
    RAVG = RCarp + RAVG
    RSUM = RCarp**2 + RSUM
    IAVG = IAVG + 1
  ENDIF

  IF (ABS(TAIR-TCARP) .GE. TOL) THEN
    Rsurf = ABS( (TAIR - TCARP)/QBOUND )
    HAVG = Rsurf + HAVG
    HSUM = Rsurf**2 + HSUM
    JAVG = JAVG + 1
  ENDIF
ENDIF

WRITE (IOUT,605) NU, DAY, TIME, QBOUND, RCarp, RSurf,
&      (T(I), I=1,N)

ENDIF

TIME = TIME + DTIME
IF (TIME .GE. 24.0) THEN
  TIME = 0.0
  DAY = DAY + 1.0
ENDIF

40  CONTINUE

* Compute average and standard deviation

RAVG = RAVG/REAL(IAVG)
HAVG = HAVG/REAL(JAVG)

RSUM = (RSUM/REAL(IAVG) - RAVG**2.0)**0.5
HSUM = (HSUM/REAL(JAVG) - HAVG**2.0)**0.5

WRITE (IOUT,606) RAVG, HAVG
WRITE (IOUT,607) IAVG, JAVG
WRITE (IOUT,608) RSUM, HSUM
WRITE (IOUT,609) QTOT, QMINUS, QPLUS, TOL

GO TO 999
99  CONTINUE
    WRITE (IOUT,610)
601  FORMAT (/, 'CRANK-NICOLSON APPROXIMATION')
602  FORMAT (/, 'TRANSIENT TEMPERATURES')
603  FORMAT (/, 2X, 'NU', 3X, 'DAY', 3X, 'TIME', 3X, 'QBOUND', 2X, 'RCarp',
&          2X, 'RSurf', 2X, 'TEMPERATURE')

```

```

604  FORMAT (35X,10I7)
605  FORMAT (I4, 10F7.2)
606  FORMAT (/,16X,'RCarp= ',F8.2,5X,'RSurf= ',F8.2)
607  FORMAT (5X,'OBSERVATIONS:',4X,I8,12X,I8)
608  FORMAT (5X,'STD DEVIATION:',4X,F8.2,12X,F8.2)
609  FORMAT (5X,'QTOT=',F8.2,2X,'QMINUS=',F8.2,2X,'QPLUS=',F8.2,
&      2X,'TOLERANCE =',F8.2)

610  FORMAT (' ',DBAND FAILED. LOOK FOR INPUT ERRORS.)

700  FORMAT ( 1(/) )
*1  Format For TEMP1 Data File Experiment 1
*1   701  FORMAT (30X, F5.2, 4X, F5.2, 4X, F5.2, 4X, F5.2)
*2  Format For TEMP2 Data File Experiment 2
701  FORMAT (16X, F5.2, 3X, F5.2, 3X, F5.2, 3X, F5.2)

999  CONTINUE
      STOP
      END

```

\*\*\*\*\*

```

      SUBROUTINE INPUT
      COMMON C(50,10),S(50,10),R(50),T(50),Y(50)
      COMMON N,IBW,TIME,DTIME,NUMAX
      CHARACTER TITLE*80
      REAL HVALUE

      DATA IIN/10/,IOUT/11/
*1  Experiment 1
*1   OPEN (UNIT=IIN,FILE='FLRIN1',STATUS='OLD')
*2  Experiment 2
      OPEN (UNIT=IIN,FILE='FLRIN2',STATUS='OLD')

*  Input Value For Convection in Return Air Plenum

      WRITE(6,*) 'H Value For Return Air'
      READ (5,*) HVALUE

      READ (IIN,501) TITLE
      WRITE (IOUT,601) TITLE
      READ (IIN,*) N,IBW
      WRITE (IOUT,602) N,IBW
C**Read main-diagonal entries in C matrix
      WRITE (IOUT,603)
      READ (IIN,*) (C(I,1),I=1,N)
      WRITE (IOUT,604) (C(I,1),I=1,N)
C**Read entries in S matrix, economy-banded form
      WRITE (IOUT,605)
      DO 10 I=1,N

```

```

      READ (IIN,*) (S(I,J),J=1,IBW)
10  CONTINUE

```

\* Modify For Convection At Return Air Plenum

```

      S(1,1) = S(1,1) + HVALUE

      DO 20 I=1,N
        WRITE (IOUT,604) (S(I,J),J=1,IBW)
20  CONTINUE

```

C\*\*Read entries in r vector

```

      WRITE (IOUT,606)
      READ (IIN,*) (R(I),I=1,N)

```

\* Modify R For Convection At Return Air Plenum

```

      R(1) = R(1) + HVALUE

      WRITE (IOUT,604) (R(I),I=1,N)

      WRITE (IOUT,609) R(1)

```

C\*\*Read time-stepping parameters

```

      READ (IIN,*) TIME,DTIME,NUMAX
      WRITE (IOUT,607) TIME,DTIME,NUMAX

```

C\*\*Read initial temperature distribution

```

      WRITE (IOUT,608)
      READ (IIN,*) (T(I),I=1,N)
      WRITE (IOUT,604) (T(I),I=1,N)

```

```

501  FORMAT (A80)
601  FORMAT (/,A80)
602  FORMAT (/,' N =',I3,5X,'IBW =',I3)
603  FORMAT (/,' MAIN-DIAGONAL ENTRIES IN C MATRIX',/)
604  FORMAT (10E12.4)
605  FORMAT (/,' ENTRIES IN S MATRIX, ECONOMY-BANDED STORAGE',/)
606  FORMAT (/,' ENTRIES IN R VECTOR',/)
607  FORMAT (/,' TIME =',E11.4,5X,'DTIME =',E11.4,5X,'NUMAX =',I4)
608  FORMAT (/,' INITIAL TEMPERATURE DISTRIBUTION')

609  FORMAT (/,' BOUNDARY H VALUE =',F6.2)

```

```

      RETURN
      END

```

---

**APPENDIX C**


---

**ADMITTANCE PROGRAM**

```
*****
This program calculates the X, Y, and Z admittance for a multi-layered wall. The wall
has (NL) number of layers and (NL+1) Surfaces. If the wall is convectively coupled to an
air temperature then the inside surface (layer 1) will have resistance R(1). The boundary
condition can be adiabatic, convective, or fixed temperature. Convective boundary layers
are given a outside surface resistance R(NL+1). X Admittance is calculated at the inside
surface. Y Admittance is calculated from the inside to outside surface. Z Admittance is
calculated at the outside surface.
*****
```

**PROGRAM ADMITTANCE**

```
PARAMETER (N = 20, N1 = N+1, ND = N*4)
PARAMETER (NIN = 5, NOUT = 6, NDAT = 15)
```

```
& COMPLEX M(N1,2,2), MULT(2,2), TM(2,2), X(N1), Y, Z(N), G,
& ARG, HYPTAN(N), HYPCOS, HYP SIN, SUM
```

```
& REAL A(N), R(N1), T(N), Ri, Ro, P, L, RHO, SPHT, COND,
& smallX, smallY, DHC, PHASE, MAG, ZERO, PI
```

```
CHARACTER YN*1
```

```
***** Subroutine Vector Converts Rectangular to Polar Coordinates
```

**EXTERNAL VECTOR**

```
***** Initialize To Zero. If Boundary Condition Adiabatic,
***** R(NL+1) Remains = 0, and Matrix M(NL+1) Elements = 0.
```

```
DATA (((M(I,J,K), K=1,2), J=1,2), I=1,N)/ND*0.0/
DATA (R(I), I=1,N1)/N1*0.0/
```

```
***** Output Data File
```

```
OPEN (UNIT=NDAT, FILE = 'ADMIT', STATUS= 'NEW')
```

```
***** Constants
```

```
G = (1.0/SQRT(2.0)) * (1.0, 1.0)
PI = ACOS(-1.0)
ZERO = 1.0E-4
```

```

***** Set Period (Diurnal = 24 Hours)

      WRITE(NOUT,*) 'PERIOD (HOURS)'
      READ (NIN,*) P

***** Number of Layers

      WRITE(NOUT,*) 'Number of Layers'
      READ (NIN,2003) NL

***** Outside Surface Boundary Condition: Adiabatic or Convective

      WRITE(NOUT,*) 'Enter Layer Properties From Outside to Inside'
      WRITE(NOUT,*) 'Outside Surface Adiabatic? y/n'
100   READ (NIN,2005) YN

***** If Adiabatic Then Add A Boundary Layer X(NL+1)=0.0
***** Leave Matrix Elements = 0.0
***** Y = Z = 0.0 for Adiabatic Boundary.

      IF (YN .EQ. 'y' .OR. YN .EQ. 'Y') THEN
          NL = NL+1
          X(NL) = (0.0,0.0)
          GOTO 200

      ELSEIF (YN .NE. 'n' .AND. YN .NE. 'N') THEN
          WRITE(NOUT,*) 'Enter yes or no'
          GOTO 100
      ENDIF

***** If Boundary Not Adiabatic Then Resistance or Material

130   WRITE(NOUT,*) 'Outside Layer Resistance Only? y/n'
      READ (NIN,2005) YN

      IF (YN .EQ. 'y' .OR. YN .EQ. 'Y') THEN
          WRITE(NOUT,*) 'Resistance (Hr-Ft2-F/BTU)'
150   READ (NIN,*) R(NL)
          IF (R(NL) .LE. ZERO) THEN
              WRITE(NOUT,*) 'Enter a R Value Greater Than Zero'
              GOTO 150
          ENDIF

***** Resistance Boundary with Fixed Temperature = 0 at Surface NL+1
***** Set Values For Resistive Boundary
***** X Admittance Vector: X(Surface)
***** M Transfer Matrix: M(Surface, Row, Column)

          X(NL) = 1/R(NL)
          M(NL,2,1) = R(NL)
          M(NL,1,1) = (1.0,0.0)

```

```

M(NL,2,2) = (1.0,0.0)
M(NL,1,2) = (0.0,0.0)

```

```

WRITE(NDAT,3007) NL
WRITE(NDAT,*) M(NL,1,1), M(NL,1,2)
WRITE(NDAT,*) M(NL,2,1), M(NL,2,2)

```

```

GOTO 200

```

```

ELSEIF (YN .NE. 'n' .AND. YN .NE. 'N') THEN
  WRITE(NOUT,*) 'Enter yes or no'
  GOTO 130
ENDIF

```

```

***** Read Material Properties For Material Layer
***** Material Boundary with Fixed Temperature = 0 at Surface NL+1

```

```

WRITE(NOUT,*) 'Thickness (Inches)'
READ (NIN,*) L
L = L/12.0

```

```

WRITE(NOUT,*) 'Density (LBm/FT3)'
READ (NIN,*) RHO

```

```

WRITE(NOUT,*) 'Specific Heat (BTU/LBm-F)'
READ (NIN,*) SPHT

```

```

WRITE(NOUT,*) 'Conductivity (BTU/Ft-F-Hr)'
READ (NIN,*) COND

```

```

***** Calculate Parameters

```

```

A(NL) = (2.0*PI*COND*RHO*SPHT/P)**0.5
T(NL) = L*(PI*RHO*SPHT/(P*COND))**0.5
ARG   = T(NL)*G*(2.0**0.5)

```

```

***** Hyperbolic Tangent (small Z) of the Argument (ARG).
***** Hyperbolic Tangent, Cosine, and Sine Evaluated Using
***** Euler Identities.

```

```

HYPTAN(NL) = (EXP(2*ARG)-1.0)/(EXP(2*ARG)+1.0)
HYPCOS    = 0.5*(EXP(ARG) + EXP(-1.0*ARG))
HYPSIN    = 0.5*(EXP(ARG) - EXP(-1.0*ARG))

```

```

***** Admittance and Transfer Matrix for Material Boundary

```

```

X(NL) = A(NL)*G/HYPTAN(NL)

```

```

M(NL,1,1) = HYPCOS
M(NL,2,1) = HYPSIN/(A(NL)*G)
M(NL,1,2) = HYPSIN*(A(NL)*G)

```

```
M(NL,2,2) = HYPCOS
```

```
WRITE(NDAT,3007) NL
WRITE(NDAT,*) M(NL,1,1), M(NL,1,2)
WRITE(NDAT,*) M(NL,2,1), M(NL,2,2)
```

```
***** Print Boundary Layer Admittance
```

```
200 CONTINUE
```

```
CALL VECTOR(X(NL), XMAG, XPHASE)
```

```
WRITE(NDAT,3003)
WRITE(NDAT,3004)
WRITE(NDAT,3005) NL, XMAG, XPHASE, A(NL), T(NL), R(NL)
```

```
***** Main Program Loop: Calculate X and Y Admittance
```

```
***** Start at Surface NL (Outside)
```

```
***** Proceed to Surface 1 (Inside)
```

```
DO 500 I = NL-1,1,-1
  WRITE(NOUT,*) 'LAYER', I
```

```
***** Resistive Layer Calculation
```

```
300 WRITE(NOUT,*) 'Resistance Only? y/n'
   READ (NIN,2005) YN

   IF (YN .EQ. 'y' .OR. YN .EQ. 'Y') THEN
     WRITE(NOUT,*) 'Resistance (Hr-Ft2-F/BTU)'
350   READ (NIN,*) R(I)
     IF (R(I) .LE. ZERO) THEN
       WRITE(NOUT,*) 'Enter a R Value Greater Than Zero'
       GOTO 350
     ENDIF
```

```
***** Admittance and Transfer Matrix For Resistive Layer
```

```
X(I) = X(I+1)/(1.0 + R(I)*X(I+1))
```

```
M(I,2,1) = R(I)
M(I,1,1) = (1.0,0.0)
M(I,2,2) = (1.0,0.0)
M(I,1,2) = (0.0,0.0)
```

```
WRITE(NDAT,3007) I
WRITE(NDAT,*) M(I,1,1), M(I,1,2)
WRITE(NDAT,*) M(I,2,1), M(I,2,2)
```

```
CALL VECTOR(X(I), XMAG, XPHASE)
```

```

XDHC = XMAG*P/(PI*2.0)

WRITE(NDAT,3003)
WRITE(NDAT,3004)
WRITE(NDAT,3005) I, XMAG, XPHASE, ZERO, ZERO, R(I)

GOTO 500

ELSEIF (YN .NE. 'n' .AND. YN .NE. 'N') THEN
  WRITE(NOUT,*) 'Enter yes or no'
  GOTO 300
ENDIF

```

\*\*\*\*\* Read Material Properties For Non Resistive Layer

```

WRITE(NOUT,*) 'Thickness (Inches)'
READ (NIN,*) L
L = L/12.0

WRITE(NOUT,*) 'Density (LBm/FT3)'
READ (NIN,*) RHO

WRITE(NOUT,*) 'Specific Heat (BTU/LBm-F)'
READ (NIN,*) SPHT

WRITE(NOUT,*) 'Conductivity (BTU/Ft-F-Hr)'
READ (NIN,*) COND

```

\*\*\*\*\* Calculate Parameters

```

A(I) = (2.0*PI*COND*RHO*SPHT/P)**0.5
T(I) = L*(PI*RHO*SPHT/(P*COND))**0.5
ARG = T(I)*G*(2.0**0.5)

```

\*\*\*\*\* Hyperbolic Tangent (small Z) of the Argument (ARG).  
 \*\*\*\*\* Hyperbolic Tangent, Cosine, and Sine Evaluated Using  
 \*\*\*\*\* Euler Identities.

```

HYPTAN(I) = (EXP(2*ARG)-1.0)/(EXP(2*ARG)+1.0)
HYPCOS   = 0.5*(EXP(ARG) + EXP(-1.0*ARG))
HYPSIN   = 0.5*(EXP(ARG) - EXP(-1.0*ARG))

```

\*\*\*\*\* Admittance and Transfer Matrix for Material Layers

```

& X(I) = (X(I+1) + A(I)*HYPTAN(I)*G) /
  (1 + X(I+1)*HYPTAN(I)/(A(I)*G))

```

```

M(I,1,1) = HYPCOS
M(I,2,1) = HYPSIN/(A(I)*G)
M(I,1,2) = HYPSIN*(A(I)*G)
M(I,2,2) = HYPCOS

```

```

WRITE(NDAT,3007) I
WRITE(NDAT,*) M(I,1,1), M(I,1,2)
WRITE(NDAT,*) M(I,2,1), M(I,2,2)

CALL VECTOR(X(I), XMAG, XPHASE)

XDHC = XMAG*P/(PI*2.0)

WRITE(NDAT,3003)
WRITE(NDAT,3004)
WRITE(NDAT,3005) I, XMAG, XPHASE, A(I), T(I), ZERO

500 CONTINUE

***** Multiply NL Transfer Matrices
***** Initialize Transfer Matrix For First Multiplication
***** M1*M2 Set TM = M1

      DO 550 I=1,2
        DO 530 J=1,2
          TM(I,J) = M(1,I,J)
530     CONTINUE
550     CONTINUE

      DO 900 L = 2,NL

***** Multiply Transfer Matrices M(I)*TM

          DO 800 I=1,2
            DO 700 J=1,2
              MULT(I,J) = (0.0,0.0)
              DO 600 K=1,2
                SUM = TM(I,K)*M(L,K,J)
                MULT(I,J) = MULT(I,J) + SUM
600             CONTINUE
700             CONTINUE
800             CONTINUE

***** Next Transfer Matrix = MULT

          DO 850 I=1,2
            DO 830 J=1,2
              TM(I,J) = MULT(I,J)
830             CONTINUE
850             CONTINUE

900 CONTINUE

***** If Boundary Adiabatic Then Z = Y = 0
***** Check Boundary Layer

```

```

IF (R(NL) .LT. ZERO) THEN
  IF (REAL(X(NL)).LT.ZERO.AND.AIMAG(X(NL)).LT.ZERO) THEN
    Z(NL) = (0.0,0.0)
    Y      = (0.0,0.0)
    GOTO 990
  ENDIF
ENDIF
ENDIF

```

```

***** X and Y Admittance From Transfer Matrix
***** X Admittance = TM(1,1)/TM(2,1)
***** Y Admittance = 1.0/TM(2,1)
***** Print Transfer Matrix

```

```

WRITE(NDAT,4001)
WRITE(NDAT,*) TM(1,1), TM(1,2)
WRITE(NDAT,*) TM(2,1), TM(2,2)
WRITE(NDAT,4003)

```

```

***** Print Y Admittance

```

```

Y = 1.0/TM(2,1)
CALL VECTOR(Y, YMAG, YPHASE)
YDHC = YMAG*P/(2.0*PI)
WRITE(NDAT,4005) YMAG, YPHASE

```

```

***** Calculate Z Admittance From Stored Property Values
***** Check First Layer = Boundary For Z Admittance
***** Boundary Layer Resistance or Material?

```

```

IF (R(1) .GT. ZERO) THEN
  Z(1) = 1/R(1)
ELSE
  Z(1) = A(1)*G/HYPTAN(1)
ENDIF

```

```

***** Print Z Admittance For Boundary Layer

```

```

CALL VECTOR(Z(1), ZMAG, ZPHASE)
ZDHC = ZMAG*P/(2.0*PI)
WRITE(NDAT,5001)
WRITE(NDAT,3004)
WRITE(NDAT,3005) 1,ZMAG,ZPHASE,A(1),T(1),R(1)

```

```

DO 990 I=1,NL-1

```

```

***** Check For Material Or Resistive Layer

```

```

IF (R(I+1) .GT. ZERO) THEN
  Z(I+1) = Z(I)/(1.0 + R(I+1)*Z(I))
ELSE

```

```

&      Z(I+1) = ( Z(I) + A(I+1)*G*HYPTAN(I+1) ) /
          ( 1.0 + Z(I) * HYPTAN(I+1)/(A(I+1)*G) )
      ENDIF

```

\*\*\*\*\* Print Z Admittance For Each Layer

```

      CALL VECTOR(Z(I+1), ZMAG, ZPHASE)
      ZDHC = ZMAG*P/(2.0*PI)
      WRITE(NDAT,5001)
      WRITE(NDAT,3004)
      WRITE(NDAT,3005) I+1,ZMAG,ZPHASE,
&      A(I+1),T(I+1),R(I+1)

```

990 CONTINUE

\*\*\*\*\* Print Final Results

```

      WRITE(NOUT,6001)
      WRITE(NOUT,6003)
      WRITE(NOUT,6005)
      WRITE(NOUT,6007) XMAG, XPHASE, YMAG, YPHASE, ZMAG, ZPHASE

```

```

      WRITE(NDAT,6001)
      WRITE(NDAT,6003)
      WRITE(NDAT,6005)
      WRITE(NDAT,6007) XMAG, XPHASE, YMAG, YPHASE, ZMAG, ZPHASE

```

\*\*\*\*\* Formatted Output

```

2003 FORMAT (I4)
2005 FORMAT (A1)
3003 FORMAT (/4X,'Layer',5X,'X Admittance',
&      8X,'A',6X,'T',6X,'R')
3004 FORMAT (12X,2X,'MAG',4X,'PHASE')
3005 FORMAT (4X,I3,4X,F7.3,1X,F7.2,8X,
&      F5.3,2X,F5.3,2X,F5.3)
3007 FORMAT (/4X,'Matrix',I3)
4001 FORMAT (/4X,'Transfer Matrix')
4003 FORMAT (/6X,'Y Admittance',
&      /4X,2X'MAG',4X,'PHASE')
4005 FORMAT (4X,F7.3,1X,F7.2)
5001 FORMAT (/4X,'Layer',5X,'Z Admittance',
&      8X,'A',6X,'T',6X,'R')
6001 FORMAT (/8X,'ADMITTANCE')
6003 FORMAT (14X,'X',17X,'Y',17X,'Z')
6005 FORMAT (8X,3('MAG',6X,'PHASE',4X))
6007 FORMAT (1X,'ADMT:',3(F7.3,2X,F7.2,2X))
      STOP
      END

```

## APPENDIX D

### COMPONENT MATERIAL PROPERTIES

STORAGE	Quantity	Weight (lb)	Density (lb/ft <sup>3</sup> )	Sp Ht (Btu/lbF)	Conduct (Btu/hrftF)	Area (ft <sup>2</sup> )	Thick (ft)	Volume (ft <sup>3</sup> )	Capacity (Btu/F)	Capacity (Btu/F)
FLOOR	1	631620	110	0.22	0.451	14500.00	0.396	5225.00	137,504	137,504
CEILING	1	631620	110	0.22	0.451	14500.00	0.396	5225.00	137,504	137,504
WALLS 1/2"	2	10418	50	0.26	0.093	5000.00	0.042	208.33	5,417	5,417
PARTITION 3/8"	2	15625	50	0.26	0.097	10000.00	0.031	234.38	8,125	8,125
CORE										
Concrete Block	1	11250		0.22	0.600	225.00	0.667		2,475	2,475
STRUCTURAL STEEL										
Floor Supports	70	101496	489	0.12		5651.51	0.037			
W18x40	12	920	489	0.12			0.026		1,325	
W18x35	36	700	489	0.12			0.025		3,024	
W36x194	18	3492	489	0.12			0.064		7,543	
W36x150	4	600	489	0.12			0.052		288	12,180
Steel Risers	26	122634	489	0.12		1329.79	0.189			
W14x665	10	5985	489	0.12			0.236		7,182	
W14x605	4	5445	489	0.12			0.216		2,614	
W14x287	4	2583	489	0.12			0.108		1,240	
W14x426	8	3834	489	0.12			0.156		3,681	14,716
METAL						11928.34				
Desk	64	190	489	0.12	26.200	74.60	0.005	0.39	1,459	
Table	50	80	489	0.12	26.200	31.41	0.005	0.16	480	
File 2 Dr	77	60	489	0.12	26.200	23.56	0.005	0.12	554	
4 Dr	80	120	489	0.12	26.200	47.12	0.005	0.25	1,152	3,646
PAPER 8.5x11										
Desk	64	151	58	0.32	0.080	0.65	4.000	1.95	3,088	
Table	50	75	58	0.32	0.080	0.65	2.000	1.30	1,206	
File 2Dr	77	151	58	0.32	0.080	0.65	4.000	2.60	3,716	
4Dr	80	302	58	0.32	0.080	0.65	8.000	5.19	7,721	15,731
								TOTAL:	337,297	337,297

---

**APPENDIX E**


---

**DISCRETE FOURIER TRANSFORM**

```
*****
This program computes the discrete fourier transform of a data file. The data file is read
into a sequence (SEQ). The forward and inverse transform are then computed using an
IMSL subroutine.
*****
```

```
PROGRAM FFT
```

```
INTEGER IDIM
PARAMETER (IDIM=300)
```

```
INTEGER N, M, NINP, NOUT
REAL COEF(IDIM), C(IDIM), SEQ(IDIM), FREQ, X(IDIM),
&      R(IDIM), PHI, TOL
```

```
* IMSL LIBRARY FFT ROUTINES
```

```
EXTERNAL FFTRF, FFTRB
```

```
OPEN (UNIT = 10, FILE = 'SEQ.DAT', STATUS='OLD')
OPEN (UNIT = 15, FILE = 'FREQ.FWD', STATUS='NEW')
OPEN (UNIT = 20, FILE = 'FREQ.INV', STATUS='NEW')
REWIND 10
REWIND 15
REWIND 20
```

```
PI      = ACOS(-1.0)
TWOPI  = 2.0*PI
```

```
* Set Input & Output Unit Numbers)
```

```
CALL UMACH (1,NINP)
CALL UMACH (2,NOUT)
```

```
* Number of Data Points To Read
```

```
100  WRITE(NOUT,*) 'Number of Data Points?'
      READ (NINP,*) N
      IF (N+1 .GT. IDIM) THEN
          WRITE (NOUT,*) 'Too Large Try Again'
          GOTO 100
      ENDIF
```

```

WRITE(NOUT,*) 'Time Step of Data Points?'
READ (NINP,*) dT

```

\*\*\*\*\* Setup Dummy Variables To Match Data File

```

DO 200 I=1,N
  READ (10,*) DATE, TIME, UC, OC, SEQ(I)
  X(I) = SEQ(I)
200 CONTINUE

```

```

CALL FFTRF (N,SEQ,COEF)

```

\* Even or Odd Number of Data Points?

```

IREMAIN = JMOD(N,2)
IF (IREMAIN .EQ. 0) THEN

```

\*\*\*\*\* Even

```

  M=N/2+1
  COEF(N+1)=0.0
ELSE

```

\*\*\*\*\* Odd

```

  M=(N+1)/2
ENDIF

```

```

WRITE (15,1000)
WRITE (NOUT,1000)

```

```

WRITE (15,1003)
WRITE (NOUT,1003)

```

```

C(1) = COEF(1)/REAL(N)
R(1) = C(1)
PHI = 0.0
FREQ = 0.0

```

```

WRITE (15,1005) (1, R(1))
WRITE (NOUT,1005) (1, R(1))

```

```

DO 400 I=2,M

```

\* J = 2 (EVEN) = A COS

\* J = 1 (ODD) = B SIN

```

  DO 300 J = 1,2
    C(2*I-J) = COEF(2*I-J)*2.0/REAL(N)
300 CONTINUE

```

```

A = C(2*I-2)
B = C(2*I-1)*(-1.0)

```

```

* Find quadrant (sign) and check for division by zero
* before calculating phase angle (PHI)

```

```

ZERO = 0.001
R(I) = (A**2.0 + B**2.0)**0.5

```

```

***** Check for division by zero

```

```

IF (ABS(B) .LE. ZERO) THEN
  IF (A .GT. ZERO) THEN
    PHI = 90.0
  ELSEIF (A .LE. -1.0*ZERO) THEN
    PHI = -90.0
  ELSE
    PHI = 0.0
  ENDIF
ELSE
  PHI = (180/PI)*ATAN(A/B)
ENDIF

```

```

***** Check Quadrant

```

```

IF (A .GT. ZERO) THEN
  IF (B .LT. -1.0*ZERO) THEN
    PHI = PHI + 180
  ENDIF
ELSEIF (A .LT. -1.0*ZERO) THEN
  IF (B .LT. -1.0*ZERO) THEN
    PHI = PHI - 180
  ENDIF
ENDIF

```

```

FREQ = TWOPI*REAL(I-1)/REAL(N)
PERIOD = (1.0/FREQ)*TWOPI*dT

```

```

WRITE (15,1005) (I, R(I), PHI, FREQ, PERIOD)
WRITE (NOUT,1005) (I, R(I), PHI, FREQ, PERIOD)

```

```

400 CONTINUE

```

```

1000 FORMAT (1X,'FORWARD TRANSFORM')
1003 FORMAT (3X,'M INDEX',5X,'MAG',11X,'PHI',11X,'FREQ',10X,'PERIOD')
1005 FORMAT (1X, I5, 2X, F12.3, 2X, F12.3, 2X, F12.3, 2X, F12.3)

```

```

* Set Filter Tolerance

```

```

WRITE (NOUT,*) 'Set Tolerance'
READ (NINP,*) TOL

```

```
IF ( ABS(R(1)) .LT. TOL) THEN
  C(1) = 0.0
  COEF(1) = 0.0
ENDIF

DO 500 I=2,M
  IF( ABS(R(I)) .LT. TOL )THEN
    C(2*I-2) = 0.0
    C(2*I-1) = 0.0
    COEF(2*I-2) = 0.0
    COEF(2*I-1) = 0.0
  ENDIF
500 CONTINUE

CALL FFTRB (N, COEF, SEQ)

WRITE (20,1007) (TOL)
WRITE (20,1010)
WRITE (20,1015) (1, 1, C(1), SEQ(1)/REAL(N), X(1))

DO 700 I = 2,M
  DO 600 J = 2,1,-1
    K=2*I-J
    WRITE (20,1015) (K, I, C(K), SEQ(K)/REAL(N), X(K))
600 CONTINUE
700 CONTINUE
1007 FORMAT (1X,'INVERSE TRANSFORM',5X,'TOLERANCE =',1X,F10.3)
1010 FORMAT (5X,'N INDEX',1X,'M INDEX',6X,'COEF',10X,
&          'SEQ', 11X,'XVAL')
1015 FORMAT (3X, I5, 3X, I5, 2X, F12.3, 2X, F12.3, 2X, F12.3)

STOP
END
```

---

**APPENDIX F**


---

**TRNSYS SIMULATION DECK**

```
*****
*
*   INDEPENDENT INSURANCE BUILDING   *
*   FLOOR MODEL                       *
*   January 10, 1990                 *
*
*****
```

```
SIM 1 8760 0.5
WIDTH 132
```

```
*
*****
```

```
UNIT 9 TYPE 9 DATA READER
*****
```

```
* Convert to English Units
* 1 - DN Solar, 2 - Horz Solar, 3 - Dry Bulb, 4 - Humidity, 5 - Wind
PAR 19
5 1 -1 0.08816 0 -2 0.08816 0 3 0.18 32.0 4 0.0001 0 5 3.281 0 20 1
(9X,F4.0,1X,F4.0,1X,F4.0,1X,F6.0,1X,F2.0)
```

```
*
*****
UNIT 16 TYPE 16 RADIATION PROCESSOR
*****
```

```
*
PAR 7
* Erb Fix Day Lat Solc Shft IE
  3 1 182 25.78 428.00 -1
INP 12
* Ih T- T+ rho N S E W
  9,2 9,19 9,20 0,0 0,0 0,0 0,0 0,0 0,0 0,0 0,0 0,0 0,0
  0.0 0.0 0.0 0.2 90. -165. 90. 15. 90. -75. 90. 105.
```

```
*
*****
UNIT 20 TYPE 33 PSYCHROMETRICS OUTSIDE AIR
*****
```

```
*
PAR 2
* Dry Bulb & Humidity Ratio
  4 2
INP 2
* Tosa Wosa
  9,3 9,4
  80.0 0.01
```

\*  
 \*\*\*\*\*  
 UNIT 22 TYPE 33 PSYCHROMETRICS ROOM AIR  
 \*\*\*\*\*

\*  
 PAR 2  
 \* Dry Bulb & Humidity Ratio

4 2  
 INP 2  
 \* Tr Wr  
 46,1 46,8  
 72.0 0.008

\*  
 \*\*\*\*\*  
 UNIT 24 TYPE 14 FORCING FUNCTION  
 \*\*\*\*\*

\*  
 PAR 12  
 \* NIGHT VENTILATION 8PM TO 6AM  
 0 1 8 1 8 0 18 0 18 1 24 1

\*  
 \*\*\*\*\*  
 UNIT 40 TYPE 40 CONTROL  
 \*\*\*\*\*

\*  
 PAR 1  
 \* Mode 1 = Temp 2 = Enthalpy

1  
 INP 5  
 \* Tosa Tra Hosa Hra TimeVent  
 9,3 0,0 20,3 0,0 24,1  
 70.0 70.0 40.0 26.0 1.0

\*  
 \*\*\*\*\*  
 UNIT 46 TYPE 56 OFFICE  
 \*\*\*\*\*

\*  
 PAR 2  
 \* L U L U  
 21 22

INP 8  
 \* Tmp w Ih N S E W Flow  
 9,3 9,4 16,4 16,6 16,11 16,14 16,17 40,1  
 0.0 0.0 0.0 0.0 0.0 0.0 0.0 0.0

\*  
 \*\*\*\*\*  
 UNIT 26 TYPE 28 OUTPUT FOR TEMPERATURE  
 \*\*\*\*\*

PAR 15  
 1 96 144 10 2  
 0 -4 0 -4 0 -4 0 -4 0 -4

INP 5  
 9,3 46,1 46,18 46,17 46,16  
 LABELS 5  
 TOSA TPERM TFLR TROOF TWALL  
 \*  
 \*\*\*\*\*  
 UNIT 28 TYPE 28 OUTPUT FOR CONTROL  
 \*\*\*\*\*  
 PAR 17  
 1 96 144 12 2  
 0 -4 0 -4 0 -4 0 -4 0 -4  
 INP 6  
 40,1 46,5 9,3 20,3 46,1 22,3  
 LABELS 6  
 CTL Qvent Tosa Hosa Troom Hroom  
 \*  
 \*\*\*\*\*  
 UNIT 29 TYPE 28 OUTPUT FOR ENERGY BALANCE  
 \*\*\*\*\*  
 PAR 17  
 \* Monthly Totals  
 -1 1 8760 14 2  
 0 -4 0 -4 0 -4 0 -4 0 -4  
 INP 6  
 \* Qsens Qsurf Qvent QConv Qinf Qlat  
 46,2 46,3 46,5 46,7 46,4 46,10  
 LABELS 6  
 QSENS QSURF QVENT QCONV QINF QLAT  
 \*  
 \*\*\*\*\*  
 UNIT 30 TYPE 28 OUTPUT FOR ENERGY BALANCE  
 \*\*\*\*\*  
 PAR 17  
 \* Monthly Totals  
 -1 1 8760 14 2  
 \* Qsens Qs+ Qs- Qlat Fan Hours  
 0 -3 8 -4 0 7 8 -4 0 -4 0 -4  
 INP 4  
 \* Qsens QHeat QCool Qlat Fan Hours  
 46,2 46,2 46,10 40,1  
 LABELS 5  
 QSENS Q+ Q- QLat Fan  
 \*  
 END

\*\*\*\*\*

THIS ROUTINE MODELS A ENTHALPY CONTROLLER FOR NIGHT COOLING.

\*\*\*\*\*

SUBROUTINE TYPE40(TIME,XIN,OUT,T,DTDT,PAR,INFO)

\* Dimension Arrays To # Inputs, Outputs & Parameters

DIMENSION XIN(5),OUT(1),PAR(1),INFO(10)  
 REAL TR, TOSA, HR, TVENT, HOSA, FLOW  
 INTEGER MODE  
 EXTERNAL TYPECK

\*\*\* FIRST CALL OF THE SIMULATION

IF(INFO(7).EQ.-1)THEN  
   NI = 5           ! Number of Inputs  
   NP = 1          ! Number of Parameters  
   ND = 0          ! Number of Derivatives  
   INFO(6) = 1     ! Number of Outputs  
   INFO(9) = 1     ! Initialize  
   CALL TYPECK(1,INFO,NI,NP,ND)  
   OUT(1) = 0.0    ! Initialize  
 ENDIF

\*\*\* SET PARAMETERS

\*\*\* 1 = Temperature Control, 2 = Enthalpy Control

MODE = PAR(1)

\*\*\* SET INPUTS

TOSA = XIN(1)     ! Outside Air Temperature  
 TR = XIN(2)      ! Room Air Temperature  
 HOSA = XIN(3)    ! Outside Air Enthalpy  
 HR = XIN(4)      ! Room Air Enthalpy  
 TVENT= XIN(5)    ! Ventilation Time Schedule

C\*\*\* SET OUTPUTS

OUT(1) = 0.0

\*\*\* MODE 1: Set Flow = 0 Unless Outside Temp Lower Than Room Temp

IF (MODE .EQ. 1) THEN  
 IF (TOSA .GE. TR) RETURN  
 OUT(1) = 1.0\*TVENT

\*\*\* MODE 2: Set Flow = 0 Unless Outside Enthalpy Lower Than Room Enthalpy

```
ELSEIF (MODE .EQ. 2) THEN  
  IF (HOSA .GE. HR) RETURN  
  OUT(1) = 1.0*TVENT
```

```
ENDIF
```

```
RETURN  
END
```

---

**APPENDIX G**


---

**TRNSYS BUILDING INPUT DESCRIPTION**

\*INPUT DATA FOR INDEPENDENT INSURANCE

\*OFFICE 9th FLOOR MODEL

\*ENGLISH UNITS

\*

\*December 28, 1989

\*

\*\*\*\*\*

PROPERTIES

\*\*\*\*\*

\*

DENSITY =0.075 : CAPACITY =0.241 : HVAPOR =1055.0  
 SIGMA =1.7122E-09 : RTEMP =527.67

\*

\*\*\*\*\*

TYPES

\*\*\*\*\*

\*

\*-----LAYERS

\*

\* THICKNESS (FT)

\* CONDUCTIVITY (BTU/HR-FT-F)

\* CAPACITY (BTU/LBm-F)

\* DENSITY (LBm/FT\*\*3)

\* RESISTANCE (HR-FT\*\*2-F/BTU)

\*

\* Values From ASHRAE Fundamentals 1981

\*

LAYER CONCRETE

\* Interpolated Values, Average Thickness 4.75 Inch

\*

THICKNESS = 0.396 : CONDUCTIVITY = 0.45  
 CAPACITY = 0.22 : DENSITY = 110.0

\*

LAYER FIREPROOF

\* Modeled as resistance

\*

RESISTANCE = 2.5

\*

LAYER CARPET

\* Table 3.1A Carpet and Rubber Pad

\* Experiment 2 R=0.77

\*

RESISTANCE = 0.77

\*  
 \* LAYER CORNERS  
 \* Model as 4 Inch Concrete  
 \*  
 \* THICKNESS = 0.33 : CONDUCTIVITY = 0.45  
 \* CAPACITY = 0.22 : DENSITY = 110.0  
 \*  
 \* LAYER GYPWALL  
 \* Interior Walls - 1/2 Inch Thick Gypsum  
 \*  
 \* THICKNESS = 0.0417 : CONDUCTIVITY = 0.093  
 \* CAPACITY = 0.26 : DENSITY = 50.0  
 \*  
 \* LAYER GYPART  
 \* Interior Partition - 3/8 Inch Thick Gypsum  
 \*  
 \* THICKNESS = 0.0312 : CONDUCTIVITY = 0.097  
 \* CAPACITY = 0.26 : DENSITY = 50.0  
 \*  
 \* LAYER HOLLOW  
 \* Interior Walls - Non Reflective Airspace 2.5 Inch  
 \*  
 \* RESISTANCE = 1.02  
 \*  
 \*  
 \*-----INPUTS  
 \*  
 \* Input Ventilation Flow Rate From Controller  
 \*  
 \* INPUTS FLOW  
 \*  
 \*-----WALLS  
 \*  
 \* CONVECTION (H) (BTU/HR-FT\*\*2-F)  
 \* ASHRAE HFRONT = 1.46 Inside Still Air  
 \* HBACK = 4.00 Outside 7 MPH Wind  
 \*  
 \* WALL OUTSIDE  
 \* LAYERS = GYPWALL, HOLLOW, CORNERS  
 \* ABS-FRONT = 0.8 : ABS-BACK = 0.8  
 \* HFRONT = 1.46 : HBACK = 4.00  
 \* WALL INSIDE  
 \* LAYERS = GYPWALL, HOLLOW, GYPWALL  
 \* ABS-FRONT = 0.8 : ABS-BACK = 0.8  
 \* HFRONT = 1.46 : HBACK = 1.46  
 \* WALL PARTITION  
 \* LAYERS = GYPART, HOLLOW, GYPART  
 \* ABS-FRONT = 0.8 : ABS-BACK = 0.8  
 \* HFRONT = 1.46 : HBACK = 1.46  
 \* WALL FLOOR  
 \* LAYERS = CARPET, CONCRETE, FIREPROOF

ABS-FRONT = 0.8 : ABS-BACK = 0.8  
 HFRONT = 1.35 : HBACK = 1.35  
 WALL ROOF  
 LAYERS = FIREPROOF, CONCRETE, CARPET  
 ABS-FRONT = 0.8 : ABS-BACK = 0.8  
 HFRONT = 1.35 : HBACK = 1.35

\*  
\*-----WINDOWS

\*  
\* Curtain Wall Modeled As Glass Adjusted For Framing  
\* ASHRAE HOUTSIDE = 1.46 Inside Still Air  
\* HINSIDE = 4.00 Outside 7.5 MPH Wind

WINDOW DOUBLE  
 UGLASS = 0.972 : HINSIDE = 1.46 : HOUTSIDE = 4.00  
 ABSORBTANCE = 0.580 : REFLECTANCE = 0.356

\*  
\*-----GAINS

\*  
\* Add Gains and Schedules  
\* Computer Equipment PC's  
\* BTU/Hr

#### GAIN PEOPLE

\* Table 4.5, 26.24 - 255 BTU/Hr Sensible, 255 BTU/Hr Latent  
\* Gain / Person Convective 68% Radiative 32%  
CONVECTIVE = 173.0 : RADIATIVE = 82.0 : HUMIDITY = 0.0024

#### GAIN LIGHTS

\* Estimated at 92 Watts/Fixture \* 3.413 = 314.0 Btu/Hr-Fixture  
\* Convective 15% Radiative 85%  
CONVECTIVE = 47.0 : RADIATIVE = 267.0 : HUMIDITY = 0.0

#### GAIN EQUIPMENT

\* Typewriters, Computers, Printers, Copiers  
\* Total Load 10,762 Watts \* 3.413 = 36,730 Btu/Hr  
\* Convective 20% Radiative 80%  
CONVECTIVE = 7246.0 : RADIATIVE = 29384.0 : HUMIDITY = 0.0

\*  
\*-----SCHEDULES

\*  
\* Weekday & Weekend Schedules

\* Occupancy

#### SCHEDULE OCCWKD

HOURS = 0, 7, 17

VALUES = 0.0, 1.0, 0.0

#### SCHEDULE OCCWKE

HOURS = 0, 7, 17

VALUES = 0.0 0.1 0.0

#### SCHEDULE OCCUPY

DAYS = 1,6  
 HOURLY = OCCWKD,OCCWKE

\* Lighting

SCHEDULE LITEWKD  
 HOURS = 0, 6, 21  
 VALUES = 0.1, 1.0, 0.1  
 SCHEDULE LITEWKE  
 HOURS = 0, 6, 21  
 VALUES = 0.1 0.2 0.1  
 SCHEDULE LIGHT  
 DAYS = 1,6  
 HOURLY = LITEWKD, LITEWKE

\* Day Cooling & Heating

SCHEDULE COOLWKD  
 HOURS = 0, 6, 18  
 VALUES = 0.0 1.0 0.0  
 SCHEDULE COOLWKE  
 HOURS = 0, 6, 18  
 VALUES = 0.0 0.0 0.0  
 SCHEDULE AMCOOL  
 DAYS = 1,6  
 HOURLY = COOLWKD, COOLWKE

\* Humidity Limit

SCHEDULE LATWKD  
 HOURS = 0, 6, 18  
 VALUES = 1.0 0.0085 1.0  
 SCHEDULE LATWKE  
 HOURS = 0, 6, 18  
 VALUES = 1.0 1.0 1.0  
 SCHEDULE LATENT  
 DAYS = 1,6  
 HOURLY = LATWKD, LATWKE

\* Equipment

SCHEDULE EQPWKD  
 HOURS = 0, 7, 17  
 VALUES = 0.6, 1.0, 0.6  
 SCHEDULE EQPWKE  
 HOURS = 0, 7, 17  
 VALUES = 0.6 0.6 0.6  
 SCHEDULE EQUIP  
 DAYS = 1,6  
 HOURLY = EQPWKD, EQPWKE

\*  
 \*-----INFILTRATION  
 \*

INFILTRATION LEAK  
 AIRCHANGE = 0.5

```

*
*-----VENTILATION
*
VENTILATION PMVENT
  TEMPERATURE= OUTSIDE
  AIRCHANGE = INPUT FLOW
  HUMIDITY = OUTSIDE
*
*-----HEATING & COOLING
*
COOLING CHILL
  ON = 72.0
  POWER = SCHEDULE 800000.0*AMCOOL
  HUMIDITY = SCHEDULE 1.0*LATENT
HEATING HOT
  ON = 68.0
  POWER = SCHEDULE 800000.0*AMCOOL
  HUMIDITY = SCHEDULE 0.0*LATENT
*
*-----ORIENTATIONS
*
ORIENTATIONS HORIZONTAL NORTH SOUTH EAST WEST
*
*-----ZONES
*
ZONES FLOOR9
*
*****
BUILDING
*****
*
* ASSUMPTIONS:
* Identical boundary floor and ceiling
*
ZONE FLOOR9

WINDOW = DOUBLE
  AREA = 1440.0 : ORIENTATION = NORTH : TRANSMITTANCE = 0.064
WINDOW = DOUBLE
  AREA = 810.0 : ORIENTATION = EAST : TRANSMITTANCE = 0.064
WINDOW = DOUBLE
  AREA = 1440.0 : ORIENTATION = SOUTH : TRANSMITTANCE = 0.064
WINDOW = DOUBLE
  AREA = 810.0 : ORIENTATION = WEST : TRANSMITTANCE = 0.064

WALL = OUTSIDE
  AREA = 108.0 : EXTERNAL : ORIENTATION = NORTH
WALL = OUTSIDE
  AREA = 108.0 : EXTERNAL : ORIENTATION = EAST
WALL = OUTSIDE
  AREA = 108.0 : EXTERNAL : ORIENTATION = SOUTH

```

WALL = OUTSIDE  
AREA = 108.0 : EXTERNAL : ORIENTATION = WEST

WALL = INSIDE  
AREA = 5000.0 : INTERNAL  
WALL = PARTITION  
AREA = 10000.0 : INTERNAL  
WALL = ROOF  
AREA = 14500.0 : INTERNAL  
WALL = FLOOR  
AREA = 14500.0 : INTERNAL

REGIME

GAIN = PEOPLE : SCALE = SCHEDULE 52.0\*OCCUPY  
GAIN = LIGHTS : SCALE = SCHEDULE 240.0\*LIGHT  
GAIN = EQUIPMENT : SCALE = SCHEDULE EQUIP  
INFILTRATION = LEAK  
VENTILATION = PMVENT  
COOLING = CHILL  
HEATING = HOT  
CAPACITANCE = 1.0 : VOLUME = 119000.0  
TINITIAL = 70.0 : WINITIAL = 0.008  
WCAPR = 1.0

\*

\*\*\*\*\*

OUTPUTS

\*\*\*\*\*

\*

TRANSFER : TIMEBASE = 0.5  
ZONES = FLOOR9  
NTYPES = 1, 2, 3, 4, 5, 6, 7, 9, 10, 11, 17, 19, 21

\*

END